

Forschungszentrum Karlsruhe
Technik und Umwelt

Wissenschaftliche Berichte
FZKA 5564

**State-of-the-Art of
High Power Gyro-Devices
and Free Electron Masers
1994**

M. Thumm

Institut für Technische Physik
Projekt Kernfusion

April 1995

Forschungszentrum Karlsruhe
Technik und Umwelt
Wissenschaftliche Berichte
FZKA 5564

**STATE-OF-THE-ART OF HIGH POWER GYRO-DEVICES
AND FREE ELECTRON MASERS
1994**

M. Thumm

Institut für Technische Physik
Projekt Kernfusion

Forschungszentrum Karlsruhe GmbH, Karlsruhe
1995

**Als Manuskript gedruckt
Für diesen Bericht behalten wir uns alle Rechte vor**

**Forschungszentrum Karlsruhe GmbH
Postfach 3640, 76021 Karlsruhe
ISSN 0947-8620**

**STATE-OF-THE-ART OF HIGH POWER GYRO-DEVICES
AND FREE ELECTRON MASERS
1994**

Abstract

At present, gyrotron oscillators are mainly used as high power millimeter wave sources for electron cyclotron resonance heating (ECRH) and diagnostics of magnetically confined plasmas for generation of energy by controlled thermonuclear fusion. 140 GHz gyrotrons with output power $P_{\text{out}} = 0.54 \text{ MW}$, pulse length $\tau = 3.0 \text{ s}$ and efficiency $\eta = 42 \%$ are commercially available. Total efficiencies around 50 % have been achieved using single-stage depressed collectors. Diagnostic gyrotrons deliver $P_{\text{out}} = 40 \text{ kW}$ with $\tau = 40 \mu\text{s}$ at frequencies up to 650 GHz ($\eta \geq 4 \%$). Recently, gyrotron oscillators have also been successfully used in material processing and plasma chemistry. Such technological applications require gyrotrons with the following parameters: $f \geq 24 \text{ GHz}$, $P_{\text{out}} = 10\text{-}50 \text{ kW}$, CW, $\eta \geq 30 \%$. This paper reports on achievements and problems related to the development of very high power mm-wave gyrotrons for long pulse or CW operation and describes the microwave technological peculiarities of the different development steps. In addition, this work gives a short overview of the present development of gyrotrons for technological applications, relativistic gyrotrons, quasi-optical gyrotrons, cyclotron autoresonance masers (CARMs), gyro klystrons, gyro-TWT amplifiers, gyrotwystron amplifiers, gyro-BWO's, peniotrons and free electron masers (FEMs). The most impressive FEM output parameters are: $P_{\text{out}} = 2 \text{ GW}$, $\tau = 20 \text{ ns}$, $\eta = 13 \%$ at 140 GHz (LLNL) and $P_{\text{out}} = 15 \text{ kW}$, $\tau = 20 \mu\text{s}$, $\eta = 5 \%$ in the range from 120 to 900 GHz (UCSB).

**ENTWICKLUNGSSTAND VON HOCHLEISTUNGS-GYRO-RÖHREN
UND FREI-ELEKTRONEN-MASERN
1994**

Übersicht

Gyrotronoszillatoren werden derzeit vorwiegend als Hochleistungsmillimeterwellenquellen für die Elektron-Zyklotron-Resonanzheizung (ECRH) und Diagnostik von magnetisch eingeschlossenen Plasmen zur Erforschung der Energiegewinnung durch kontrollierte Kernfusion eingesetzt. 140 GHz Gyrotrons mit einer Ausgangsleistung von $P_{\text{out}} = 0.54 \text{ MW}$ bei Pulslängen von $\tau = 3.0 \text{ s}$ und Wirkungsgraden von $\eta = 42\%$ sind kommerziell erhältlich. Durch den Einsatz von Kollektoren mit einstufiger Gegenspannung werden Gesamtwirkungsgrade um 50 % erreicht. Gyrotrons zur Plasmadiagnostik erreichen Frequenzen bis zu 650 GHz bei $P_{\text{out}} = 40 \text{ kW}$ und $\tau = 40 \mu\text{s}$ ($\eta \geq 4 \%$). In jüngster Zeit jedoch finden Gyrotronoszillatoren auch für technologische Prozesse und in der Plasmachemie erfolgreich Verwendung. Dabei werden Röhren mit folgenden Parametern eingesetzt: $f \geq 24 \text{ GHz}$, $P_{\text{out}} = 10\text{-}50 \text{ kW}$, CW, $\eta \geq 30 \%$. In diesem Beitrag wird auf den aktuellen Stand und die Probleme bei der Entwicklung von Hochleistungs-mm-Wellen-Gyrotrons für Langpuls- und Dauerstrichbetrieb sowie auf die mikrowellentechnischen Besonderheiten der einzelnen Entwicklungsphasen eingegangen. Außerdem wird auch kurz über den neuesten Stand der Entwicklung von Gyrotrons für technologische Anwendungen, relativistischen Gyrotrons, quasi-optischen Gyrotrons, Zyklotron-Autoresonanz-Masern (CARMs), Gyroklystrons, Gyro-TWT-Verstärkern, Gyrotwystron-Verstärker, Gyro-Rückwärtswellenoszillatoren (BWOs), Peniotrons und Frei-Elektronen-Maser (FEM) berichtet. FEM-Rekordausgangsparameter sind hier: $P_{\text{out}} = 2 \text{ GW}$, $\tau = 20 \text{ ns}$, $\eta = 13 \%$ bei 140 GHz (LLNL) und $P_{\text{out}} = 15 \text{ kW}$, $\tau = 20 \mu\text{s}$, $\eta = 5 \%$ im Bereich von 120 bis 900 GHz (UCSB).

Contents

1	Introduction	1
2	Classification of Fast-Wave Microwave Sources	2
3	Dispersion Diagrams of Fast Cyclotron Mode Interaction	3
	3.1 Gyrotron oscillator and gyroklystron amplifier	4
	3.2 Cyclotron autoresonance maser (CARM)	6
	3.3 Gyro-TWT (travelling wave tube) and gyrotwystron amplifier	8
	3.4 Gyro-BWO (backward wave oscillator)	9
	3.5 Overview on gyro-devices	10
4	Gyrotron Oscillators for Plasma Heating	11
5	Very High Frequency Gyrotron Oscillators	29
6	Gyrotrons for Technological Applications	32
7	Relativistic Gyrotrons	33
8	Quasi-Optical Gyrotrons	34
9	Cyclotron Autoresonance Masers (CARMs)	35
10	Gyroklystrons, Gyro-TWTs, Gyrotwystrons, Gyro-BWOs and other Gyro-Devices	36
11	Free Electron Masers (FEMs)	40
	11.1 Possibilities	40
	11.2 Accelerator options and key issues	42
	11.3 The FOM-Fusion-FEM	43
12	Comparison of Gyrotron and FEM for Nuclear Fusion	46
	Acknowledgments	47
	References	48

1 Introduction

The possible applications of gyrotron oscillators and other cyclotron-resonance maser (CRM) fast wave devices span a wide range of technologies. The plasma physics community has already taken advantage of recent advances in producing high power micro- and millimeter (mm) waves in the areas of RF plasma heating for magnetic confinement fusion studies, such as lower hybrid heating (1-8 GHz) and electron cyclotron resonance heating (28-140 GHz), plasma production for numerous different processes and plasma diagnostic measurements such as collective Thomson scattering or heat pulse propagation experiments. Other applications which await the development of novel high power sources include deep space and specialized satellite communication, high resolution Doppler radar, radar ranging and imaging in atmospheric and planetary science, drivers for next-generation high-gradient linear accelerators, nonlinear spectroscopy, material processing and plasma chemistry.

Most work on CRM devices has investigated the conventional gyrotron oscillator (gyromonotron) [1-4] in which the wave vector of the radiation in an open-ended, irregular cylindrical waveguide cavity is transverse to the direction of the applied magnetic field, resulting in radiation near the electron cyclotron frequency or at one of its harmonics. Long pulse and CW gyrotron oscillators delivering output powers of 100-400 kW at frequencies between 28 and 82.6 GHz have been used very successfully in thermonuclear fusion research for plasma ionization and start-up, electron cyclotron resonance heating (ECRH) and local current density profile control by noninductive electron cyclotron current drive (ECCD) at power levels up to 4 MW.

ECRH has become a well-established heating method for both tokamaks [5] and stellarators [6]. The confining magnetic fields in present day fusion devices are in the range of $B_0=1-3.5$ Tesla. As fusion machines become larger and operate at higher magnetic fields ($B \cong 5T$) and higher plasma densities in steady state, it is necessary to develop CW gyrotrons that operate at both higher frequencies and higher mm-wave output powers. The requirements of the projected tokamak experiment ITER (International Thermonuclear Experimental Reactor) and of the planned new stellarator (W7-X) at the Division of the Max-Planck-Institut für Plasmaphysik in Greifswald are between 10 and 50 MW at frequencies between 140 GHz and 170 GHz [7]. This suggests that mm-wave gyrotrons that generate output power of at least 1 MW, CW, per unit are required. Since efficient ECRH needs axisymmetric, narrow, pencil-like mm-wave beams with well defined polarization (linear or elliptical), single mode gyrotron emission is necessary in order to generate a TEM_{00} Gaussian beam mode. Single mode 110-170 GHz gyromonotrons capable of high average power 0.5 - 1 MW per tube, CW, are currently under development. There has been continuous progress towards higher frequency and power but the main issues are still the long pulse or CW operation and the appropriate mm-wave vacuum window. The availability of sources with fast frequency tunability would permit the use of a simple, non-steerable mirror antenna at the plasma torus for local current drive experiments [8]. Slow frequency tuning has been shown to be possible on quasi-optical Fabry-Perot cavity gyrotrons [9] as well as on cylindrical cavity gyrotrons with step tuning (different working modes) [10, 11].

This work reports on the status and future prospects of the development of gyrotron oscillators for ECRH but also refers to the development of pulsed very high frequency gyromonotrons for active plasma diagnostics [12].

Recently, gyrotron oscillators also are successfully utilized in materials processing (e.g. advanced ceramic sintering, surface hardening or dielectric coating of metals and alloys) as well as in plasma chemistry [13]. The use of gyrotrons for such technological applications appears to be of interest if one can realize a relatively simple, low cost device which is easy in service (such as a magnetron). Gyrotrons with low magnetic field (operated at the 2nd harmonic of the electron cyclotron frequency), low anode voltage, high efficiency and long lifetime are under development. The state-of-the-art in this area is also briefly reviewed here.

The next generation of high-energy physics accelerators and the next frontier in understanding of elementary particles is based on the super collider. For linear electron-positron colliders that will reach center-of-mass energies of about 1 TeV it is thought that sources at 17 to 35 GHz with $P_{\text{out}} = 300 \text{ MW}$, $\tau = 0.2 \mu\text{s}$ and characteristics that will allow approximately 1000 pulses per second will be necessary as drivers [14]. These must be phase-coherent devices, which can be either amplifiers or phase locked oscillators. Such generators are also required for super range high resolution radar and atmospheric sensing [15]. Therefore this report gives an overview of the present development status of relativistic gyrotrons, cyclotron autoresonance masers (CARM), gyrotron travelling wave tube amplifiers (Gyro-TWT), gyroklystrons and gyrotwistrons for such purposes as well as of free electron masers (FEM) and broadband gyrotron backward wave oscillators (Gyro-BWO) for use as drivers for FEM amplifiers.

The present status review is an updated and extended version of the KfK Report 5235 (October 1993) with the same title. Since the beginning of 1995 the name of the Kernforschungszentrum Karlsruhe (KfK) has been changed to Forschungszentrum Karlsruhe (FZK).

2 Classification of fast-wave microwave sources

Fast-wave devices in which the phase velocity v_{ph} of the electromagnetic wave is greater than the speed of light c , generate or amplify coherent electromagnetic radiation by stimulated emission of bremsstrahlung from a beam of relativistic electrons. The electrons radiate because they undergo oscillations transverse to the direction of beam motion by the action of an external force (field). For such waves the electric field is mainly transverse to the propagation direction.

The condition for coherent radiation is that the contribution from the electrons reinforces the original emitted radiation in the oscillator or the incident electromagnetic wave in the amplifier. This condition is satisfied if a bunching mechanism exists to create electron density variations of a size comparable to the wavelength of the imposed electromagnetic wave. To achieve such a mechanism, a resonance condition must be satisfied between the periodic motion of the electrons and the electromagnetic wave in the interaction region [15]

$$\omega - k_z v_z \cong s\Omega \quad , \quad s = 1, 2, \dots \quad (k_z v_z = \text{Doppler term}) \quad (1)$$

here ω and k_z are the electromagnetic wave frequency and characteristic axial wavenumber, respectively, v_z is the translational electron drift velocity, Ω is an effective frequency, which is associated with macroscopic oscillatory motion of the electrons, and s is the harmonic number.

In the electron cyclotron maser (ECM), electromagnetic energy is radiated by relativistic electrons gyrating along an external longitudinal magnetic field. In this case, the effective frequency Ω corresponds to the relativistic electron cyclotron frequency:

$$\Omega_c = \Omega_{c0}/\gamma \quad \text{with} \quad \Omega_{c0} = eB_0/m_0 \quad \text{and} \quad \gamma = [1 - (v/c)^2]^{-1/2} \quad (2)$$

where e and m_0 are the charge and rest mass of an electron, γ is the relativistic factor, and B_0 is the magnitude of the guide magnetic field. A group of relativistic electrons gyrating in a strong magnetic field will radiate coherently due to bunching caused by the relativistic mass dependence of their gyration frequency. Bunching is achieved because, as an electron loses energy, its relativistic mass decreases and it thus gyrates faster. The consequence is that a small amplitude wave's electric field, while extracting energy from the particles, causes them to become bunched in gyration phase and reinforces the existing wave electric field. The strength of the magnetic field determines the value of the radiation frequency.

In the case of a spatially periodic magnetic or electric field (undulator/wiggler), the transverse oscillation frequency Ω_b (bounce frequency) of the moving charges is proportional to the ratio of the electron beam velocity v_z to the wiggler field spatial period λ_w . Thus,

$$\Omega_b = k_w v_z \quad , \quad k_w = 2\pi/\lambda_w \quad (3)$$

The operating frequency of such devices, an example of which is the FEM [16,17], is determined by the condition that an electron in its rest frame "observes" both the radiation and the periodic external force at the same frequency. If the electron beam is highly relativistic, ($v_{ph} \cong v_z \cong c$) the radiation will have a much shorter wavelength than the external force in the laboratory frame ($\lambda \cong \lambda_w/2\gamma^2$ so that $\omega \cong 2\gamma^2 \Omega_b$). Therefore, FEMs are capable of generating electromagnetic waves of very short wavelength determined by the relativistic Doppler effect. The bunching of the electrons in FEMs is due to the perturbation of the beam electrons by the ponderomotive potential well which is caused by "beating" of the electromagnetic wave with the spatially periodic wiggler field. It is this bunching that enforces the coherence of the emitted radiation.

In the case of the ECMs and FEMs, unlike most conventional microwave sources and lasers, the radiation wavelength is not determined by the characteristic size of the interaction region. Such fast wave devices require no periodically rippled walls or dielectric loading and can instead use a simple hollow-pipe oversized waveguide as a circuit. These devices are capable of producing very high power radiation at cm-, mm-, and submillimeter wavelengths.

3 Dispersion diagrams of fast cyclotron mode interaction

The origin of the ECMs traces back to the late 1950s, when three investigators began to examine theoretically the generation of microwaves by the ECM interaction [1,18]: Richard Twiss in Australia [19], Jürgen Schneider in the U.S [20] and Andrei Gaponov in Russia [21]. In early experiments with devices of this type, there was some debate about the generation mechanism and the relative roles of fast-wave interactions mainly producing azimuthal electron bunching and slow-wave interactions mainly producing axial bunching [1,18]. The predominance of the fast-wave ECM resonance with its azimuthal bunching in producing microwaves was experimentally verified in the mid-1960s in the U.S. [22] (where the term "electron cyclotron maser" was apparently coined) and in Russia [23].

Many configurations can be used to produce coherent radiation based on the electron cyclotron maser instability. The departure point for designs based on a particular concept is the wave-particle interaction. Dispersion diagrams, also called ω - k_z plots or Brillouin diagrams [24,25], show the region of cyclotron interaction (maximum gain of the instability) between an electromagnetic mode and a fast electron cyclotron mode (fundamental or harmonic) as an intersection of the waveguide mode dispersion curve (hyperbola):

$$\omega^2 = k_z^2 c^2 + k_\perp^2 c^2 \quad (4)$$

with the beam-wave resonance line (straight) given by eq. (1). In the case of a device with cylindrical resonator the perpendicular wavenumber is given by $k_\perp = X_{mn} / R_0$ where X_{mn} is the n^{th} root of the corresponding Bessel function (TM_{mn} modes) or derivative (TE_{mn} modes) and R_0 is the waveguide radius. Phase velocity synchronism of the two waves is given in the intersection region. The interaction can result in a device that is either an oscillator or an amplifier. In the following subsections, the different ECM devices are classified according to their dispersion diagrams.

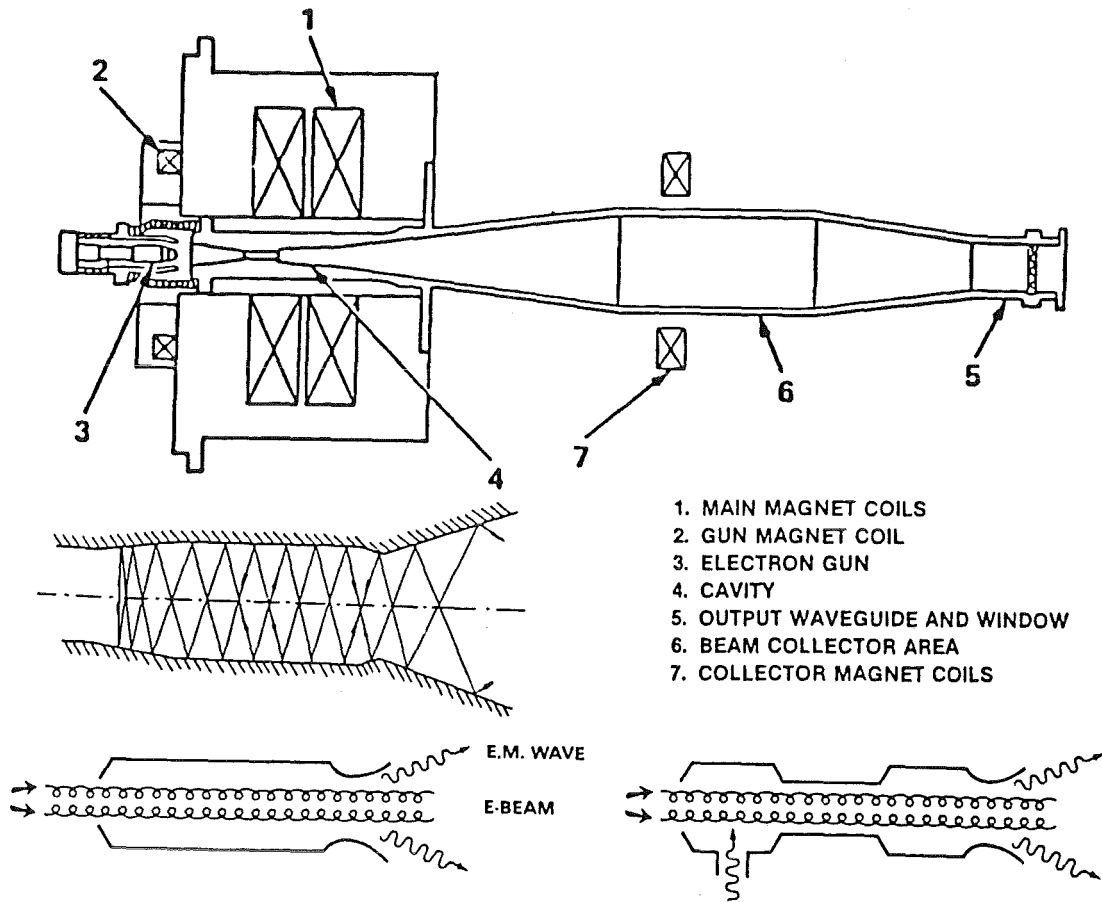
3.1 Gyrotron oscillator and gyrokystron amplifier

Gyrotron oscillators were the first ECMs to undergo major development. Increases in device power were the result of Russian developments from the early 1970s in magnetron injection guns, which produce electron beams with the necessary transverse energy (while minimizing the spread in transverse energies) and in tapered, open-ended waveguide cavities that maximize efficiency by tailoring the electric field distribution in the resonator [1-3].

Gyrotron oscillators and gyrokystrons are devices which usually utilize only weakly relativistic electron beams (<100 kV) with high transverse momentum (pitch angle $\alpha = v_\perp/v_z > 1$) [26]. The wavevector of the radiation in the cavity is transverse to the direction of the external magnetic field ($k_\perp \gg k_z$, and the Doppler shift is small) resulting according to eqs. (1) and (2) in radiation near the electron cyclotron frequency or at one of its harmonics:

$$\omega \cong s\Omega_c, \quad s = 1, 2, \dots \quad (5)$$

In the case of cylindrical cavity tubes (see Figs. 1 and 2) the operating mode is close to cutoff ($v_{\text{ph}} = \omega/k_z \gg c$) and the frequency mismatch $\omega - s\Omega_c$ is small but positive in order to achieve correct phasing, i.e. keeping electron bunches in the retarding phase [24-26]. The Doppler term $k_z v_z$ is of the order of the gain width and is small compared with the radiation frequency. The dispersion diagrams of fundamental and harmonic gyrotrons are illustrated in Figs. 3 and 4, respectively. The velocity of light line is determined by $\omega = ck_z$. For given values of γ and R_0 , a mode represented by X_{mn} and oscillating at frequency ω is only excited over a narrow range of B_0 . By variation of the magnetic field, a sequence of discrete modes can be excited. The frequency scaling is determined by the value of B_0/γ . Cyclotron harmonic operation reduces the required magnetic field for a given frequency by the factor s . The predicted efficiency for gyrotrons operating at higher harmonics ($s = 2$ and 3) are comparable with those operating at the fundamental frequency [1-3,24].



1. MAIN MAGNET COILS
2. GUN MAGNET COIL
3. ELECTRON GUN
4. CAVITY
5. OUTPUT WAVEGUIDE AND WINDOW
6. BEAM COLLECTOR AREA
7. COLLECTOR MAGNET COILS

Fig. 1: Schematic of VARIAN CW gyrotron oscillator [4] and scheme of irregular waveguide cavities of gyromonotron oscillator (left) and gyroklystron amplifier [24].

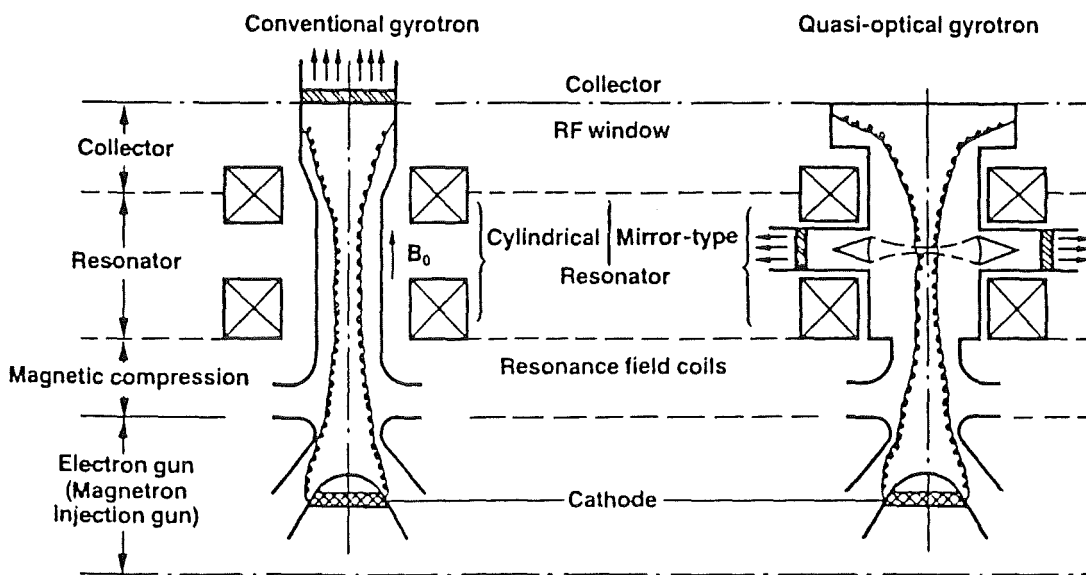


Fig. 2: Principle of a conventional gyrotron with cylindrical resonator and of a quasi-optical gyrotron with mirror resonator [9].

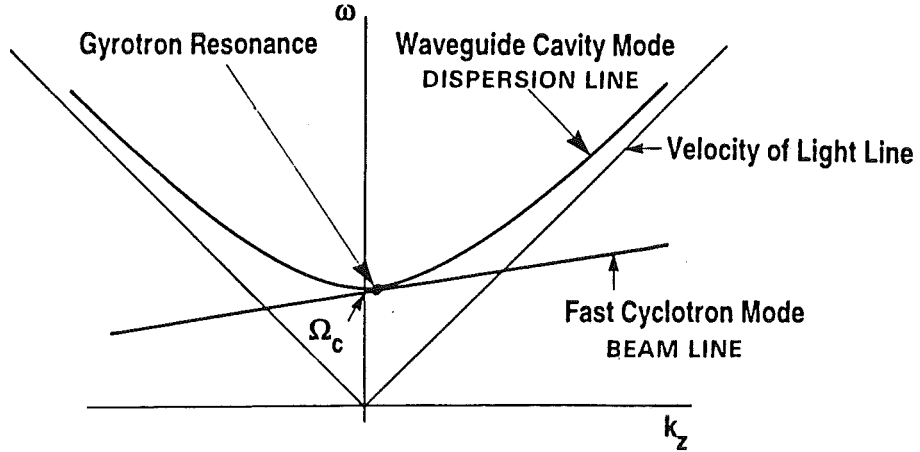


Fig. 3 Dispersion diagram of gyrotron oscillator (fundamental resonance)

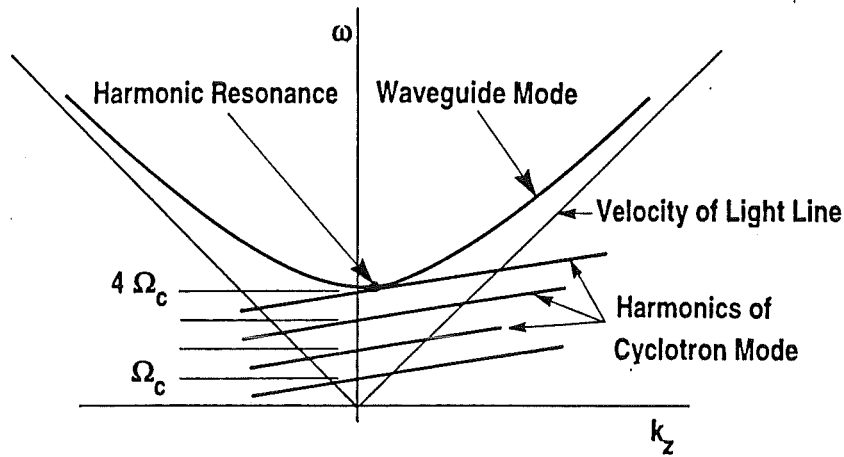


Fig. 4 Dispersion diagram of harmonic frequency gyrotron oscillator

3.2 Cyclotron autoresonance maser (CARM)

In a gyrotron with a highly relativistic beam ($\geq 1\text{MeV}$), an efficient interaction will lead to an average energy loss in the order of the initial electron energy. As a result, the change in the gyrofrequency is much greater than in the mildly relativistic case. It is therefore desirable to identify the condition under which such a highly relativistic electron beam remains in synchronism with the RF field. A possibility for achieving synchronism is to utilize the interaction of electrons with electromagnetic waves propagating with a phase velocity close to the speed of light in the direction of the magnetic field. In this case, the Doppler shift term $k_z v_z$ is large, and the appropriate resonance condition is

$$\omega \cong k_z v_z + s\Omega_c \quad (6)$$

If $v_{ph} \cong c$, the increase in cyclotron frequency due to extraction of beam energy (decrease of γ) nearly compensates the decrease in the Doppler shifted term. Therefore, if the resonance condition is initially fulfilled, it will continue to be satisfied during the interaction. This phenomenon is called autoresonance, and the cyclotron maser devices operating in the relativistic Doppler-shifted regime are called cyclotron autoresonance masers [16]. Fig. 5

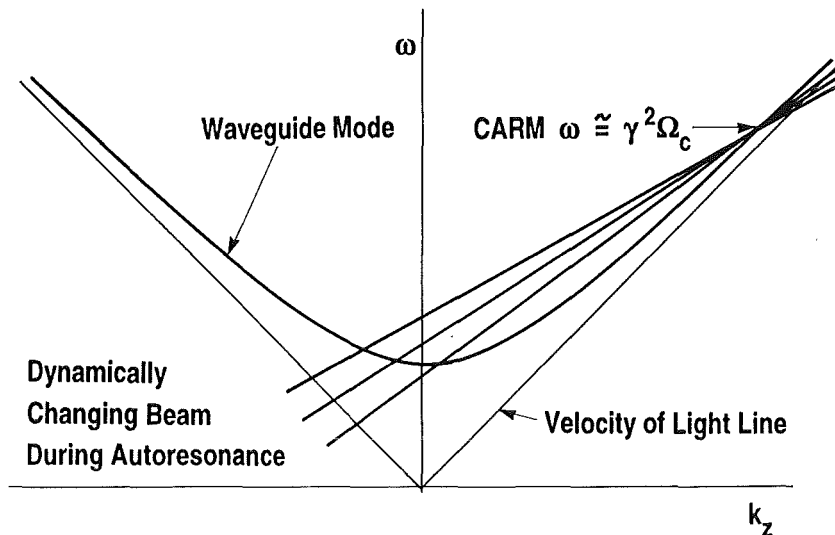


Fig. 5: Dispersion diagram of the cyclotron autoresonance maser (CARM).

shows how the Brillouin diagram of the fast cyclotron wave changes during the autoresonance interaction such that the working frequency ω remains constant even though both Ω_c and v_z are changing. The CARM interaction corresponds to the upper intersection and is based on the same instability mechanism as that of the gyrotron but operated far above cutoff. The instability is convective, so feedback, e.g. by a Bragg resonator (see Fig. 6) [16] is required for an oscillator and it is necessary to carefully discriminate against the other interactions corresponding to the lower frequency intersection in the dispersion diagram Fig. 5. The problem can be alleviated by employing the fundamental TE_{11} or (HE_{11} hybrid mode) and properly choosing system parameters to be within the stability limit. Compared to a gyrotron, there is a large Doppler frequency upshift of the output ($\omega \cong \gamma^2 \Omega_c$) permitting a considerably reduced magnetic field B_0 . Since the axial bunching mechanism can substantially offset the azimuthal bunching the total energy of the beam and not only the transverse component is available for RF conversion.

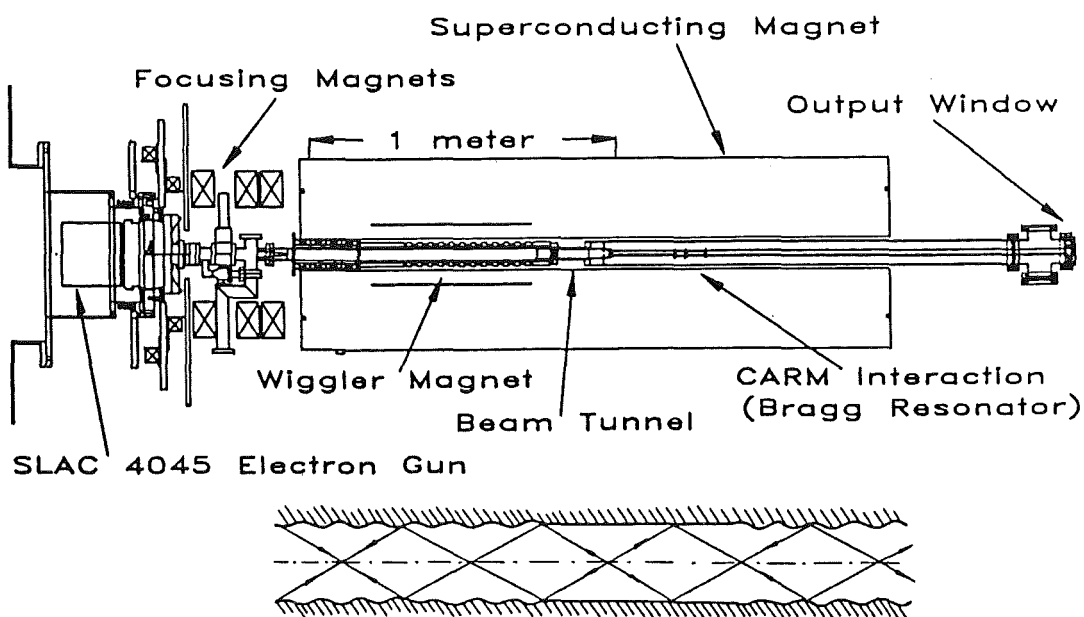


Fig. 6: Schematic of the long-pulse MIT CARM oscillator experiment [27] and scheme of a Bragg resonator [16].

In contrast to the gyrotron the CARM has an electron beam with low to moderate pitch angle ($\alpha < 0.7$). The efficiency of CARMs is extremely sensitive to spread in the parallel beam velocity. The velocity spread $\Delta v_z/v_z$ must be lower than 1% to achieve the full theoretically expected efficiency of 40%. [16,26].

3.3 Gyro-TWT (travelling wave tube) and gyrotwystron amplifier

From the theoretical point of view, the gyro-TWT differs from the CARM only in regimes of operation. The gyro-TWT utilizes a moderately relativistic electron beam to interact with a fast waveguide mode near the grazing intersection of the frequency versus wavenumber plot (see Fig. 7) where the resonance line is tangent to the electromagnetic mode. This produces high gain and efficiency because the phase velocities of the two modes are

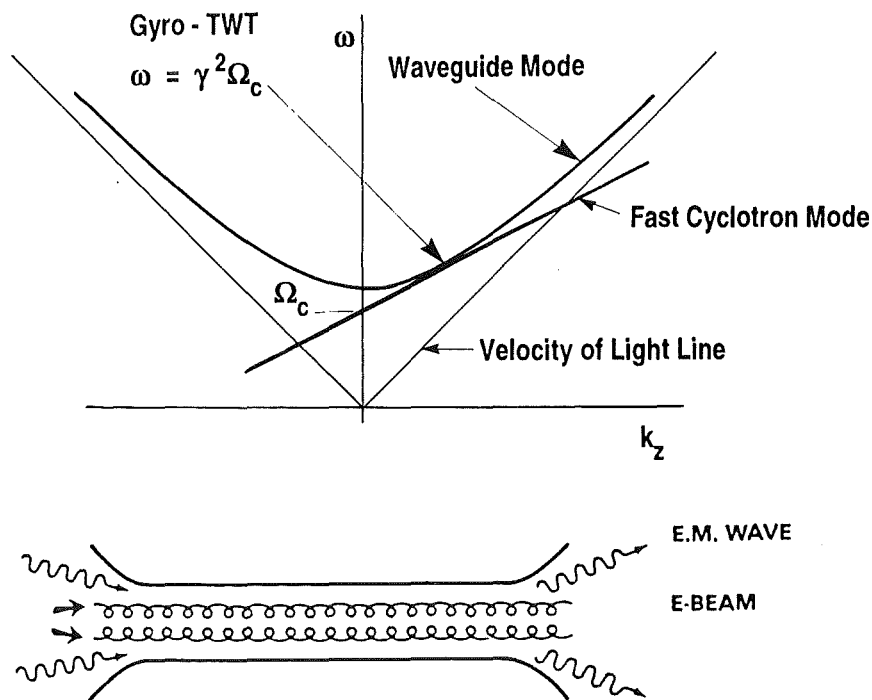


Fig. 7: Dispersion diagram and scheme of interaction circuit of Gyro-TWT amplifier.

nearly matched and the group velocity of the waveguide mode is nearly equal to v_z . In the gyro-TWT regime ($\omega/k_z \gg c$), the axial bunching mechanism is too weak to be of any significance. To benefit from autoresonance, the cutoff frequency should be reduced relative to the cyclotron frequency. The circuit employed in a gyro-TWT consists simply of an unloaded waveguide. Since no resonant structures are present, the gyro-TWT is potentially capable of much larger bandwidth than a gyrokystron and thus can be used as output amplifier in mm-wave radar communication systems. Recent devices employ tapered magnetic field and interaction circuit as well as two stages in order to optimize the beam-wave interaction along the waveguide [28].

The gyrotwystron [1], a hybrid device, is derived from the gyrokystron by extending the length of the drift section and replacing the output cavity with a slightly tapered waveguide section like in a gyro-TWT. The output waveguide section is excited by the beam of electrons that are bunched because of modulation in the input cavity.

3.4 Gyro-BWO (backward wave oscillator)

If the electron beam and/or magnetic field is adjusted so that the straight fast-wave beam line crosses the negative k_z -branch of the waveguide mode hyperbola (see Fig. 8) then an absolute instability (internal feedback) with a "backward wave" occurs. In the gyro-BWO the

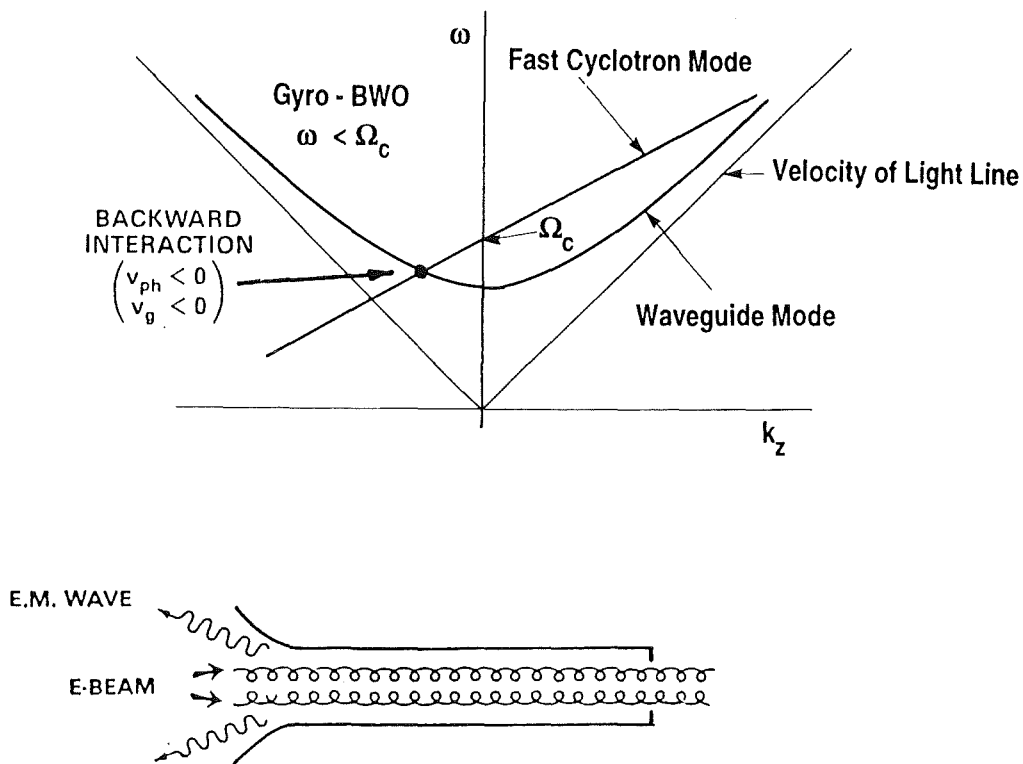


Fig. 8: Dispersion diagram and scheme of interaction circuit of Gyro-BWO.

frequency of operation is now governed by the slope of the line, which is a function of v_z , and thus of the beam acceleration voltage U_{beam} . Consequently, just as in the case of other BWOs (e.g. carcinotron), the frequency of oscillations can be continuously changed very fast over a broad range, using U_{beam} in place of B_0 . However, there is a Doppler down shift in frequency ($\Omega_c/2 < \omega < \Omega_c$), so that very high magnetic fields are required for high frequency operation.

3.5 Overview on gyro-devices

Bunching of electrons in the gyrotron oscillator discussed in section 3.1 has much in common with that in conventional "O-type" electron beam devices, namely, monotron, klystron, TWT, BWO and twystron [1]. In both cases the primary energy modulation of electrons gives rise to bunching (azimuthal or longitudinal) which is inertial. The bunching continues even after the primary modulation field is switched off (at the drift section of a klystron-type devices). This analogy suggests the correspondence between O-type devices and various types of gyro-devices. Table I presents the schematic drawings of devices of both classes and the orbital efficiencies calculated using a uniform approximation for the longitudinal structure of the RF field in the gyromonotron ($s=1$) [1]. For the gyroklystron, the calculation was made in the narrow-gap approximation of the RF field in the input and output cavities. The electrodynamic systems of the gyro-TWT and gyro-BWO, as well as the output section of the gyrotwystron, were assumed to have the form of a uniform waveguide. In all these cases the magnetic field is assumed to be homogeneous.

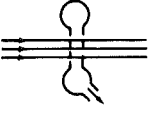
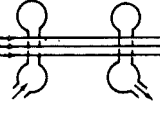
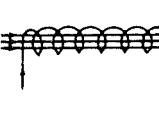
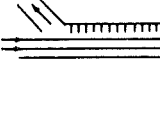
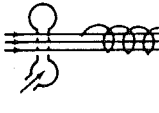
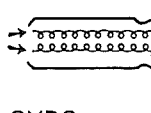
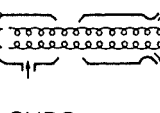
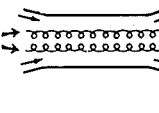
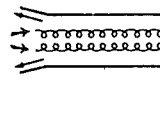
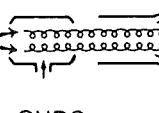
"O" TYPE DEVICE					
	MONOTRON	KLYSTRON	TWT	BWO	TWYSTRON
TYPE OF GYROTRON					
	GYRO-MONOTRON	GYRO-KLYSTRON	GYRO TWT	GYRO BWO	GYRO-TWYSTRON
RF FIELD STRUCTURE					
ORBITAL EFFICIENCY	0.42	0.34	0.7	0.2	0.6

Table I: Overview of gyro-devices and comparison with corresponding conventional O-type devices [1].

In Section 10, we will briefly consider two other source types similar to, but also fundamentally different in one way or another from, the ECMs. The large orbit gyrotron employs an axis-encircling electron beam in which the trajectory of each electron takes it around the axis of the cylindrical interaction region. Peniotron and gyropeniotron are driven by an interaction that is phased quite differently from the ECM interaction; in practice, the peniotron and ECM mechanisms compete [24-26].

4 Gyrotron oscillators for plasma heating

Long-pulse and CW gyrotrons utilizing open-ended cylindrical resonators which generate output powers of 100 - 400 kW per unit, at frequencies between 28 and 82.6 GHz, have been used very successfully for plasma formation, electron cyclotron resonance heating (ECRH) and local current density profile control by noninductive current drive (ECCD) in tokamaks [5] and stellarators [6]. Gyrotron complexes with total power of up to 4 MW are used [12]. Table II summarizes the capabilities and performance parameters of such gyrotrons together with the features of 8 GHz gyrotron oscillators for lower hybrid heating and current drive in tokamak plasmas. The confining toroidal magnetic fields in present day fusion machines are in the range of $B_0=1-3.5$ Tesla. As experimental devices become larger and operate at higher magnetic fields ($B=5T$) and higher plasma densities ($n_{e0}=1-2 \cdot 10^{20}/m^3$) in steady state, present and forthcoming ECH requirements call for gyrotron output powers of at least 1 MW, CW at frequencies ranging from 110-170 GHz [7] (the reference frequencies are 110 GHz, 140 GHz and 170 GHz). Since efficient ECRH and ECCD needs axisymmetric, narrow, pencil-like mm-wave beams with well defined polarization, single mode emission is necessary in order to generate a TEM_{00} Gaussian beam mode at the plasma torus launching antenna [7, 37].

Single mode mm-wave gyrotron oscillators capable of high average power, 0.5-1 MW per tube, in longpulse or CW operation, are currently under development in several scientific and industrial laboratories. The present state of the art is given in Table III. Some experimental results are shown in Figs. 9 and 10.

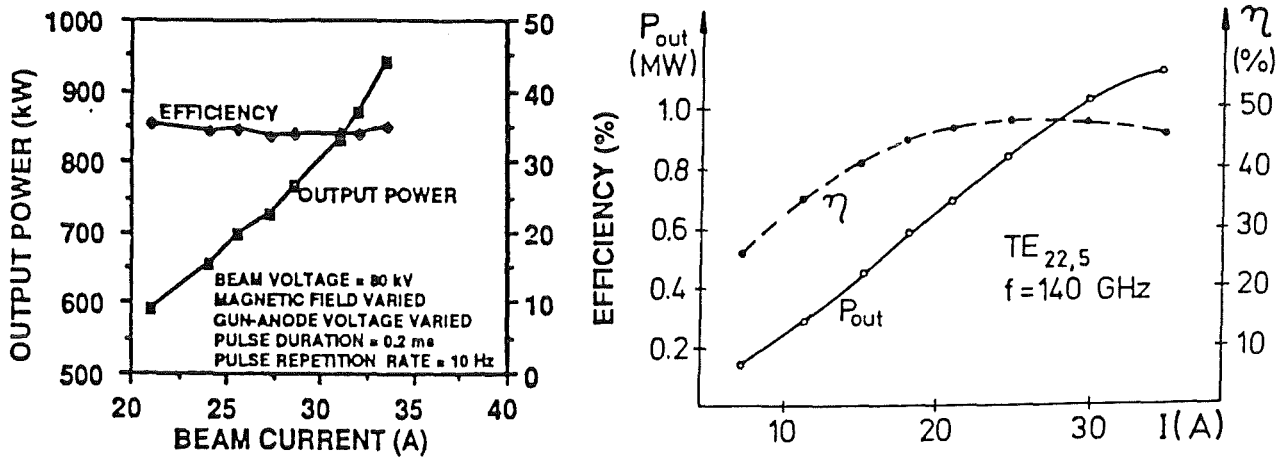


Fig. 9: Output power and efficiency versus beam current of 140 GHz gyrotrons, left: VARIAN [4], right: IAP [46].

Institution	Frequency [GHz]	Mode cavity	Mode output	Power [MW]	Efficiency [%]	Pulse length [s]		
ABB, Baden	[29]	8	TE ₀₁	TE ₀₁	0.35	35	0.5	
			39	TE ₀₂	TE ₀₂	0.25	42	0.1
HUGHES, Torrance	[24]	60	TE ₀₂	TE ₀₂	0.2	35	0.1	
IEAS, Beijing	[30]	34.3 (2 Ω_c)	TE _{02/03}	TE ₀₃	0.2	30	0.02	
			36.5 (2 Ω_c)	TE ₀₂	TE ₀₂	0.1	25	0.02
NRL, Washington D.C.	[24]	35	TE ₀₁	TE ₀₁	0.15	31	0.02	
PHILIPS, Hamburg	[31]	70	TE ₀₂	TE ₀₂	0.14	30	CW	
GYCOM (SALUT, IAP)		28	TE ₄₂	TEM ₀₀	0.5	30	0.1	
Nizhny Novgorod	[11,32]	37.5	TE ₆₂	TEM ₀₀	0.5	35	0.1	
			53.2	TE ₈₃	TEM ₀₀	0.52	42	0.1
			75	TE ₉₄	TEM ₀₀	0.5	37	0.1
			82.6	TE _{10,4}	TEM ₀₀	0.5	37	0.1
			82.6	TE _{15,4}	TEM ₀₀	0.5	37	1.0
			8	TE ₅₁	TE ₅₁	1.0	45	1.0
THOMSON TE, Velizy	[33]	35	TE ₀₂	TE ₀₂	0.2	43	0.15	
TOSHIBA, Nasushiobara	[34]	28	TE ₀₂	TE ₀₂	0.2	35.7	0.075	
41			TE ₀₂	TE ₀₂	0.2	31.3	0.1	
56			TE ₀₂	TE ₀₂	0.2	32.9	0.1	
		70	TE ₀₂	TE ₀₂	0.025	28.4	0.001	
VARIAN, Palo Alto	[4,35]	8	TE ₂₁	TE ₁₀	0.5	33	1.0	
			28	TE ₀₂	TE ₀₂	0.34	37	CW
						0.2	45	CW
			35	TE ₀₂	TE ₀₂	0.2	35	CW
			53.2, 56, 60	TE _{01/02}	TE ₀₂	0.23	37	CW
			70	TE _{01/02}	TE ₀₂	0.21	36	3
		84	TE _{15,2}	TE _{15,2/4}	0.5	28	0.1	
				0.89	28	0.001		
VARIAN, NIFS Palo Alto, Nagoya	[36]	84	TE _{15,3}	TEM ₀₀	0.35	28	0.0004	
				0.05	28	CW		

Table II: Performance parameters of gyrotron oscillators for electron cyclotron resonance heating (ECRH) (28-84 GHz) and lower hybrid heating (8 GHz) of plasmas in magnetic confinement fusion studies.

Institution	Frequency [GHz]	Mode		Power [MW]	Efficiency [%]	Pulse length [s]
		cavity	output			
FZK, PHILIPS, [38]	140.8	TE ₀₃	TE ₀₃	0.12	26	0.5
FZK, Karlsruhe [39,40]	132.6	TE _{9,4}	TE _{9,4}	0.42	21	0.005
	140.2	TE _{10,4}	TE _{10,4}	0.69	28	0.005
	140.2	TE _{10,4}	TEM ₀₀	0.60	27	0.012
				0.50	32	0.03
				0.50	48(DEPCOL)	0.03
	140.5	TE _{10,4}	TEM ₀₀	0.46	51(DEPCOL)	0.2
	147.4	TE _{11,4}	TE _{11,4}	0.35	19	0.005
	154.8	TE _{12,4}	TEM ₀₀	0.35	18	0.01
				0.35	27(DEPCOL)	0.005
MITSUBISHI, Amagasaki [41,42]	120	TE _{02/03}	TE ₀₃	0.16	25	0.06
	120	TE _{15,2}	TE _{15,2}	1.02	32.5	0.0001
				0.46	30	0.1
				0.25	30	0.21
GYCOM (SALUT, IAP)	110	TE _{15,4}	TEM ₀₀	0.5	33	0.5
Nizhny Novgorod [11,32]	140	TE _{22,6}	TEM ₀₀	0.85	36	0.4
				0.5	33	2.0
	158.5	TE _{24,7}	TEM ₀₀	0.7	30	0.7
THOMSON, Velizy [33]	100	TE ₃₄	TE ₃₄	0.19	30	0.07
	110	TE ₉₃	TE ₉₃	0.42	17.5	0.002
	110	TE ₆₄	TE ₆₄	0.34	19	0.01
				0.39	19.5	0.21
THOMSON, CRPP, FZK	118	TE _{22,6}	TEM ₀₀	0.51	31	0.002
TOSHIBA, JAERI	110	TE _{22,2}	TEM ₀₀	0.75	27.6	0.002
Nasushiobara, Naka [43,44]				0.61	30	0.05
				0.61	50(DEPCOL)	0.05
				0.42	48(DEPCOL)	3.3
				0.35	48(DEPCOL)	5.0
	110.1	TE _{22,6}	TE _{22,6}	0.62	30	0.0015
	120	TE ₀₃	TE ₀₃	0.17	25	0.01
	120	TE _{12,2}	TE _{12,2}	0.46	24	0.1
				0.25	24	0.22
	120	TE _{12,2}	TEM ₀₀	0.5	24	0.1
GYCOM (TORIY, IAP)	140	TE _{22,6}	TEM ₀₀	0.97	34	0.3
Moscow, N. Novgorod [45-47]				0.735	34	1.5
				0.535	42	3.0
VARIAN, Palo Alto [4,35,48]	106.4 (2 Ω_c)	TE _{02/03}	TE ₀₃	0.135	21	0.1
	106.4	TE _{12,2}	TE _{12,2}	0.4	30	0.1
	110	TE _{15,2}	TE _{15,2}	0.5	28	1.0
				0.3	28	2.0
	110	TE _{22,2}	TE _{22,2/4}	0.5	27	2.5
	110	TE _{22,6}	TEM ₀₀	0.55	27.5	0.0006
	140	TE _{02/03}	TE ₀₃	0.1	27	CW
	140	TE _{15,2}	TE _{15,2}	1.04	38	0.0005
				0.32	30	3.6
				0.26	28	5.0
				0.2 (0.4)	28	avg. (peak)

DEPCOL: Depressed Collector (single stage)

Table III: Present development status of high frequency gyrotron oscillators for ECRH and stability control in magnetic fusion devices ($f \geq 100$ GHz, $\tau \geq 0.5$ ms).

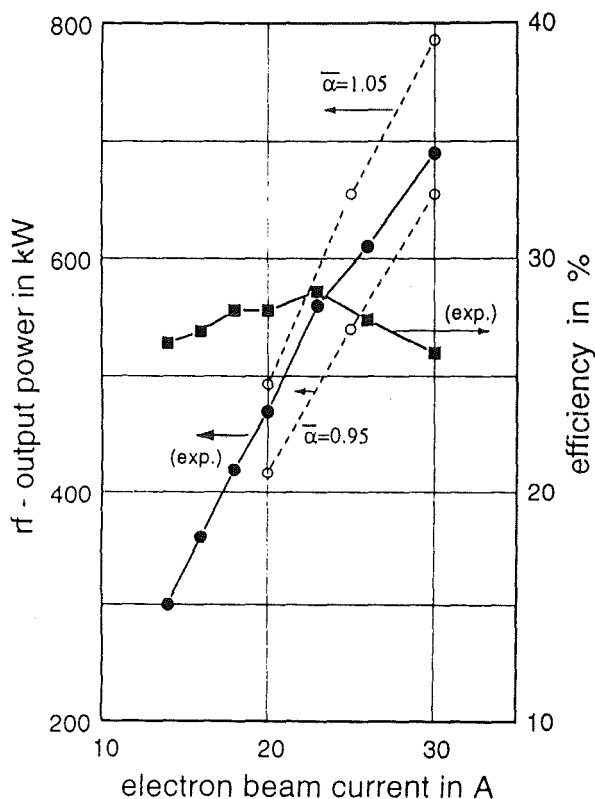


Fig. 10:

Output power and efficiency of the FZK 140 GHz $TE_{10,4}$ mode gyrotron [39] as a function of beam current, beam voltage = 87 kV, gun anode voltage = 23 kV, magnetic field = 5.5 T.

The dashed lines correspond to numerical simulations with an average velocity ratio of 0.95 and 1.05.

With increasing operating frequency, power level and pulse duration a number of problems arise which necessitate significant changes in the gyrotron design approach. The main difficulties encountered in the realization of efficient megawatt CW mm-wave gyrotrons are connected with [4,46,49]:

- formation of an electron beam with sufficient orbital energy (velocity ratio $\alpha \geq 1.5$) and small velocity spread (electron gun design).
- propagation of the electron beam, spurious oscillations in the beam tunnel between the electron gun and the interaction cavity (see Fig. 1), voltage depression (dependent on R_e/R_0 , where R_e is the electron beam radius), space charge effects and beam instabilities.
- ohmic wall losses in the cavity (cavity heating).
- mode selectivity in a highly overmoded cavity, single mode operation, good mode separation of working mode from competing modes.
- unwanted mode conversion in the electrodynamic system of the tube.
- thermal loading of the electron beam collector.
- heating of the output window, selection of output mode.
- enhancement of efficiency up to 50-55 %.

Design trade-offs and operating limits will be necessary.

Electron Gun. The electron guns employed in gyrotrons provide a hollow beam of spiraling electrons which have a large fraction of their energy in velocity components transverse to the tube axis. Magnetron injection guns (MIGs) operating in a temperature limited mode have thus far been used most successfully. However, the experimental efficiency of present day gyrotrons (approx. 30 %) is mainly limited by velocity spread of the electron beam. The main factors producing the velocity spread are [12]: spread of the initial velocities, roughness of the emitting surface, azimuthally inhomogeneous emission, space charge effects within the beam, inhomogeneous fields on the cathode and nonadiabatic fields in the intermediate region (compression zone) between the cathode and the interaction cavity. Relatively high compression ratios of up to 30-40 are used [39]. Diode-type guns [12,39] as well as triode-type guns with a modulation anode [4,39], which give the option of powerless modulation of the electron beam and thus of the output power for heat pulse propagation experiments [38] are employed. The cathode size is limited to a technologically feasible diameter (≈ 100 mm) and the current density should be chosen not too high to assure a long cathode lifetime. The use of diode-type electron guns reduces the complexity of the required high voltage power supplies and automatically provides a desirable α, γ -beam evaluation during startup which permits one to obtain highly efficient single-mode operation [39].

Electron Beam Tunnel. The beam tunnel (compression region in which the wall and electron beam radii are reduced starting from the MIG and ending at the entrance of the interaction cavity) often has a sophisticated alternating metal - damping ceramics ring structure with specially shaped rings of lossy ceramics to suppress spurious oscillations and beam instabilities [4].

Interaction Cavity. The choice of the working mode of a high-power CW mm-wave gyrotron is based on an intricate set of design trade-offs. The first 140 GHz gyrotrons [e.g. 4,38] employed rotationally symmetric TE_{03} mode cavities. The TE_{0n} circular symmetric family of modes is part of a general class of modes called volume modes. Most of the stored energy in a volume mode resides in the central region of the cavity. As a result, for optimum coupling, the electron beam is placed on an inner maximum of the resonator electric field. Consequently the beam radius is relatively small compared with the size of the cavity.

For frequencies above 100 GHz and power levels approaching 1 MW, ohmic losses in the cavity walls necessitate the use of larger higher order mode cavities. If the electron beam remains located on one of the inner maxima, potential depression quickly limits the amount of beam current that may be passed through the resonator for a given beam voltage and pitch factor α . In addition, the problem concerning mode competition with the neighbouring TE_{2n} mode becomes more severe. With increasing n , frequency spacing between the TE_{0n} and TE_{2n} modes decreases. If the electron beam is placed on one of the outer maxima the cavity Q has to be increased to keep the efficiency high enough, thereby nullifying much of the ohmic loss reduction realized in using a higher order cavity.

The problems posed by the conflicting requirements on cavity wall losses, potential depression, mode competition and efficiency considerations are alleviated by using a different interaction approach. Only rotating asymmetric volume modes (AVM: TE_{mn} with $m \gg 1$ and $n > 2$, e.g. $TE_{22,6}$ at 140 GHz and $TE_{28,8}$ at 170 GHz) are now considered to have the potential to meet high power requirements (1 MW in CW operation) at frequencies between 140 and 170 GHz [32,34,36-50].

A general scaling law for the maximum power density P_{Ω} in the cavity walls is approximately given by [4,38]:

$$P_{\Omega} = K P_{\text{out}} Q f^{5/2} / (X_{\text{mn}}'^2 - m^2) \quad (7)$$

when P_{out} is the power output and K is a scaling constant which depends upon a number of factors including material selection, surface finish, manufacturing process, operating temperature and thermal cycling history of the cavity.

Typical limits for P_{Ω} given in the literature are about 3 kW/cm^2 (without extending to exotic cooling techniques) leading with $Q \cong 700\text{-}1000$ to working modes satisfying

$$\begin{aligned} X_{\text{mn}}'^2 - m^2 &\geq 500 \text{ for } P_{\text{out}} = 0.5 \text{ MW} \\ &1000 \text{ for } P_{\text{out}} = 1.0 \text{ MW} \end{aligned} \quad (8)$$

In an oversized electrodynamic system the mode spectrum is very dense; therefore the cyclotron resonance condition (see the dispersion diagram Fig. 3) can be fulfilled for the operating mode and several neighbouring modes simultaneously. Mode competition may result in unstable oscillations, efficiency reduction and complete quenching of the operating mode oscillations. Usually, to provide mode selection one tries to diminish the Q factors and the coupling impedances of the parasitic modes with the electron beam. The coupling of the desired working mode with beam electrons is strongest if the nominal beam radius in the resonator coincides with the inner electric field maximum (approx. caustic radius of the mode) as shown in Fig. 11 for the $\text{TE}_{10,4}$ mode of the FZK gyrotron [38]. In order to avoid problems with beam voltage depression and possible beam instabilities a ratio $R_e/R_0 \geq 0.45$ is required.

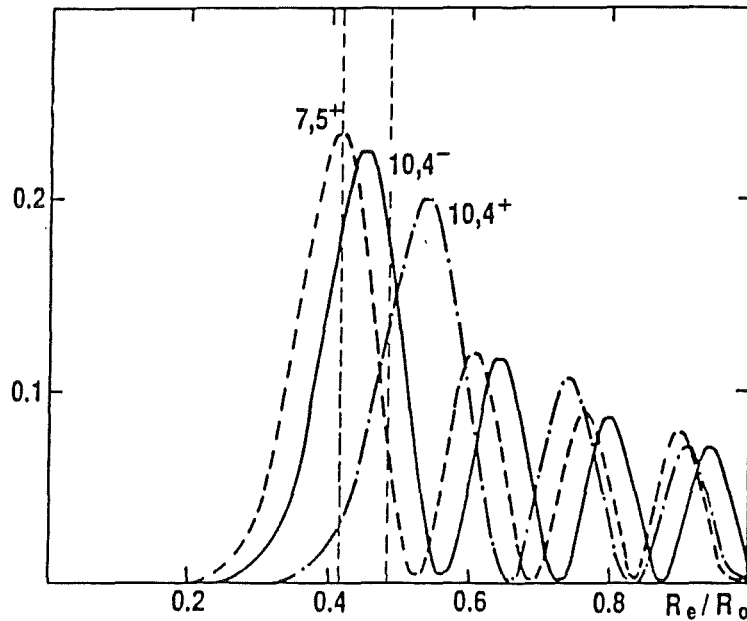


Fig. 11: Coupling coefficients vs normalized radius for the $\text{TE}_{10,4\pm}$ and $\text{TE}_{7,5+}$ modes. The vertical lines delineate the beam position (a beam of thickness $4r_L$ is assumed to be centered at $R_e = 3.65 \text{ mm}$ for $R_0 = 8.11 \text{ mm}$).

Up to now, stable single mode oscillations have been obtained for AVMs in simple cavities having a diameter of up to 23λ [50]. Higher efficiencies and more stable operation can be achieved if the working mode is chosen to be as isolated as possible from possible competing modes. Since there will be many modes close in frequency to the candidate mode, one searches for modes such that nearby possible competitors couple only weakly to the beam.

This requires also good beam quality and careful choice of beam radius. For a first overview the starting current relation for candidate (c) and parasitic (p) mode and the frequency separation can be considered. Good candidates satisfy the criterion that $I_p/I_c > R$ when $|\Delta f|/f = |1 - f_p/f_c| < \epsilon$ with R and ϵ as large as possible [38]. TE_{mn} modes with $m = 22$ and $n = 5$ or 6 are promising candidates for megawatt 140 GHz gyrotrons [32,39,40,45-49].

At the upper limit $D/\lambda \approx 20$ the experimental efficiency of approximately 25 % could be improved to 35 % by taking additional mode selection measures utilizing a coaxial cavity (see Fig. 12). Introduction of an inner rod conductor into the cylindrical resonator lowers the voltage depression (higher efficiency) and permits one to affect the Q factor of modes with high radial indices n whose fields are disturbed by this rod. If the inner conductor tapers to the output of the cavity, the rays forming the space extended mode fields are ejected from the cavity, i.e., the Q factors of these modes decrease. At the same time, the inner conductor weakly affects the Q factor and the effective field length of the working mode if its radius is smaller than the caustic radius [3,51]. Mode converting or impedance corrugations on the inner rod and mode converting, longitudinal slots on the outer cavity wall further improve mode selection [52]. High efficiency of electrodynamic mode selection in a coaxial cavity was experimentally proved [3,46,52,53]. Table VI summarizes the present performance parameters of short pulse (50 μ s) coaxial cavity gyromonotrons. The coaxial tubes employ a so called inverse MIG with an inner rod surrounded by the cathode emitter ring [52]. This construction allows fixing and cooling of the inner conductor since it is close to ground potential.

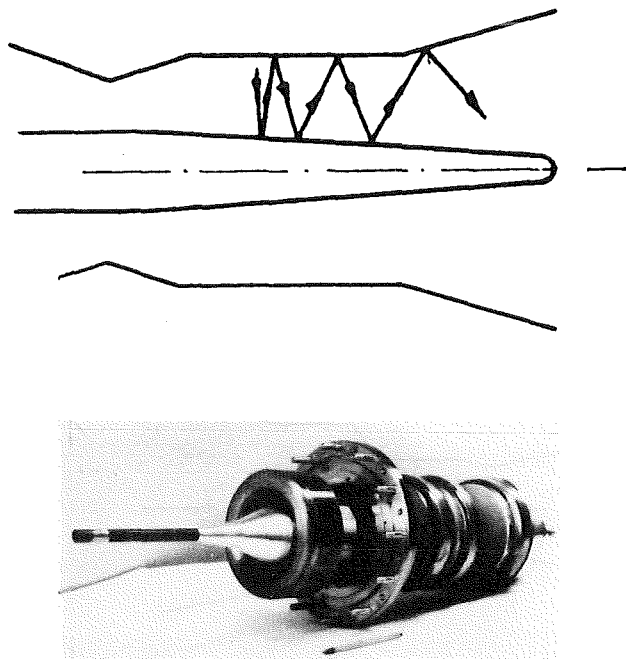


Fig. 12: Profile of a coaxial resonator with tapered inner rod and photograph of an inverse magnetron injection gun [52].

Institution	Frequency [GHz]	Mode		Power [MW]	Efficiency [%]	Corrug. Cavity	
		cavity	output			inner	outer
IAP, Nizhny Novgorod [3,53]	45	TE _{15,1}	TE _{15,1}	1.25	43	no	no
	100	TE _{20,13}	TE _{20,13}	2.1	30	no	no
	100	TE _{21,18}	TE _{21,18}	1.0	35	yes	no
				0.5	20	no	no
	110	TE _{17,7}	TE _{17,7}	0.7	25	no	no
	110	TE _{20,13}	TE _{20,13}	1.15	35	yes	no
	110	TE _{21,13}	TE _{21,13}	1.0	35	yes	no
	113	TE _{22,13}	TE _{22,13}	1.0	40	yes	yes
				0.7	30	yes	no
				0.3	14	no	no
0.1				11	yes	no	
224	TE _{33,8} (2Ω _c)	TE _{33,8}	0.1	11	yes	no	
IAP, FZK Karlsruhe [52]	133	TE _{27,15}	TE _{27,15}	1.3	29	no	no
	140	TE _{28,16}	TE _{28,16}	1.0	23	no	no

Table IV: Present experimental development status of short pulse (50 μs) coaxial cavity gyrotron oscillators.

Improved radial mode selection and higher efficiency may also be achieved using a two section cavity with a prebunching cutoff waveguide section [54] or using coupled (complex) cavities [53,55,56] (see Fig. 13), wherein a TE_{m,n} mode is excited in the narrow part at the same frequency as the mode with a larger radial index, TE_{m,n+p} but the same azimuthal index in the broad part of the resonator. Because of identical eigenfrequencies this pair of partial modes is coupled and forms a normal mode distributed throughout the resonator, while the other partial modes with different eigenfrequencies are localized in one of the two parts of the resonator and, correspondingly, have a much higher starting current.

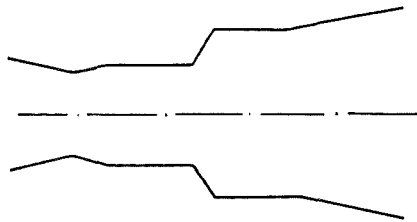


Fig. 13: Profile of a two section-coupled resonator.

Slow frequency step tuning by variation of the magnetic field and corresponding change of the operating mode (series of $TE_{m,n}$ modes with $n=\text{const}$) has been demonstrated experimentally [10,11,40] (see Fig. 14). Recent computational studies performed at FZK [57] show that fast frequency tunability may be feasible by simultaneously changing beam and modulation anode voltage.

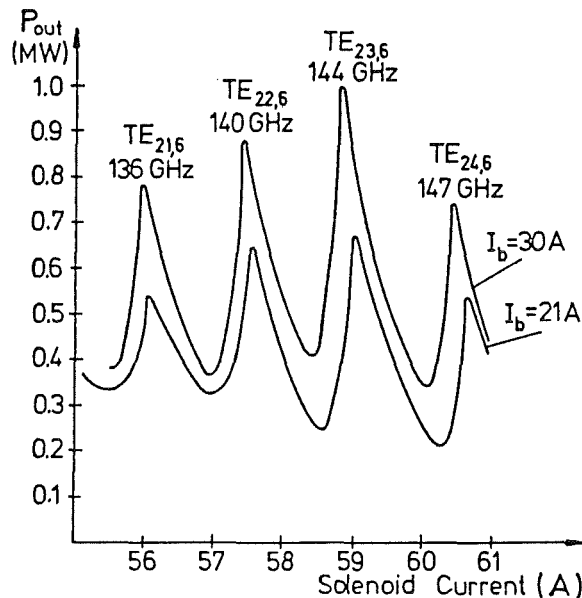


Fig. 14: Output power versus magnetic field of IAP-SALUT 140 GHz gyrotron [11,46].

The use of dispersion strengthened copper ($\text{Cu: Al}_2\text{O}_3$) as cavity material and advanced cooling techniques significantly improve the thermomechanical features of the cavity. Smooth transitions in the resonator-waveguide profile and a nonlinear contour of the uptaper guarantee a mode purity of almost 99 % [58]. High quality and long term stability of gyrotron and superconducting magnet alignment is required (< 0.1 mm) [47].

Electron Beam Collector. CW gyrotron oscillators having the classical cylindrical configuration employ standard output coupling where the electron beam collector also serves as the output waveguide. A nonlinear uptaper links the interaction cavity to the large diameter collector and in high-power long-pulse tubes, a nonlinear downtaper is sometimes incorporated between the collector and the output window waveguide. The entire uptaper/collector/downtaper combination is designed to preserve the purity of the mode generated in the cavity [4]. Usually a series of small magnet coils is employed along the length of the collector to aid in spreading the spent electron beam uniformly over a sufficiently large area to avoid heat load limits or RF breakdown in the collector. Mode purity requirements preclude the option of very large diameter collectors. For 1 MW, CW tubes the implementation of an output coupling approach that separates the spent electron beam from the outgoing RF power is required in order to increase the beam interception area. Such a configuration additionally allows the use of a depressed collector to improve the system efficiency by partially recovering the energy of the spent electron beam and leads to a reduction of the overall height of the tube. Fig. 15 shows the schematic layout of an AVM gyrotron with q.o. mode converter and Fig. 16 shows a photograph of the "Hercules" gyrotron (GYCOM/TORIY: 140 GHz, 0.55 MW, 3s). For beam sweeping a special collector coil is used which is fed with a sawtooth-shaped current generating an alternating magnetic field. Both the collector profile and distribution of the magnetic field in the collector are optimized to provide a temperature increase below an admissible one ($\leq 300^\circ$ C) and as homogeneous thermal load as possible [45-47].

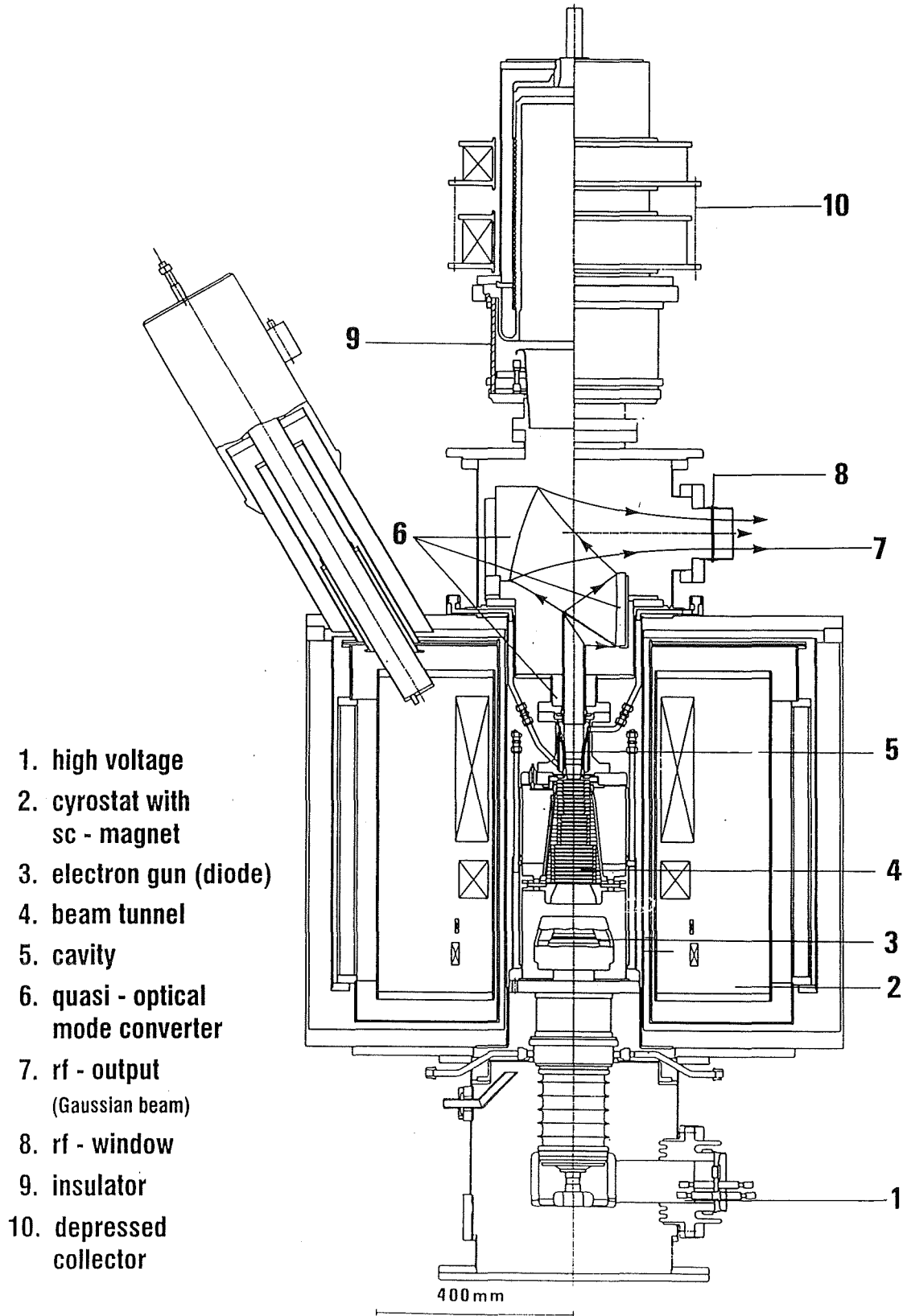


Fig. 15: Schematic layout of an advanced asymmetric volume mode (AVM) gyrotron with quasi-optical converter [40].

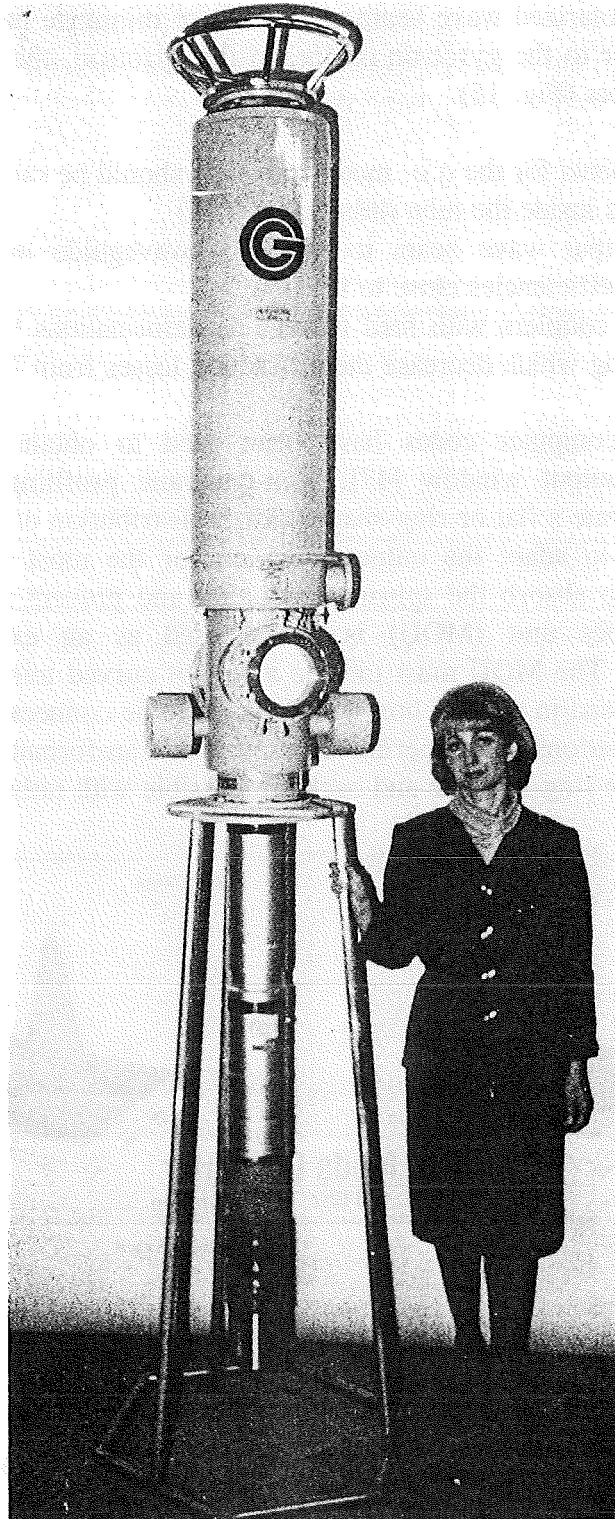


Fig. 16: Photograph of the Russian "Hercules" gyrotron (GYCOM/TORIY: 140 GHz, 0.55 MW, 3.0 s) [40].

Quasi-Optical Mode Converter. The q.o. mode converter is a part of the internal electrodynamic system of the tube as the cavity and the uptaper. The converter separates the RF radiation from the spent electron beam, transforms a complicated cavity mode to an easily transportable linearly polarized wave beam and allows to minimize harmful effects of possible reflections of RF power to the gyrotron cavity. In the gyrotron, the converter consists of an irradiator and 2-3 mirrors (Fig. 15).

The following requirements for the q.o. mode converter should be satisfied:

- low diffraction losses inside the tube (less than 5-7 %)
- matching of the output wave beam to the HE_{11} waveguide mode or the fundamental Gaussian beam with efficiencies close to 95 %.

Improved quasi-optical couplers with feed waveguide deformations [40,59] provide axial and azimuthal mode bunching which decrease the diffraction losses from 20 % to 5 % (Fig. 17).

In Russia, advanced computer codes have been used to obtain an optimal RF power distribution over the output window [47]. Non-quadratic profiling of the internal mirror surfaces allows to generate a flat or ring-shaped power distribution of the output wave beam at the window. In order to adapt the output radiation for the most effective excitation of a transmission line and to absorb the spurious radiation and prevent possible breakdowns, an external matching optics unit (MOU) is to be used as an extension of the internal electrodynamic system. The MOU must include a pair of curved mirrors and pipes absorbing spurious radiation enclosed in a metal box with a flange to be connected to a transmission line. Electrodynamical calculations and experiments show that transformation of the field structure from the Gaussian to the ring-like one and back are possible with rather low RF losses.

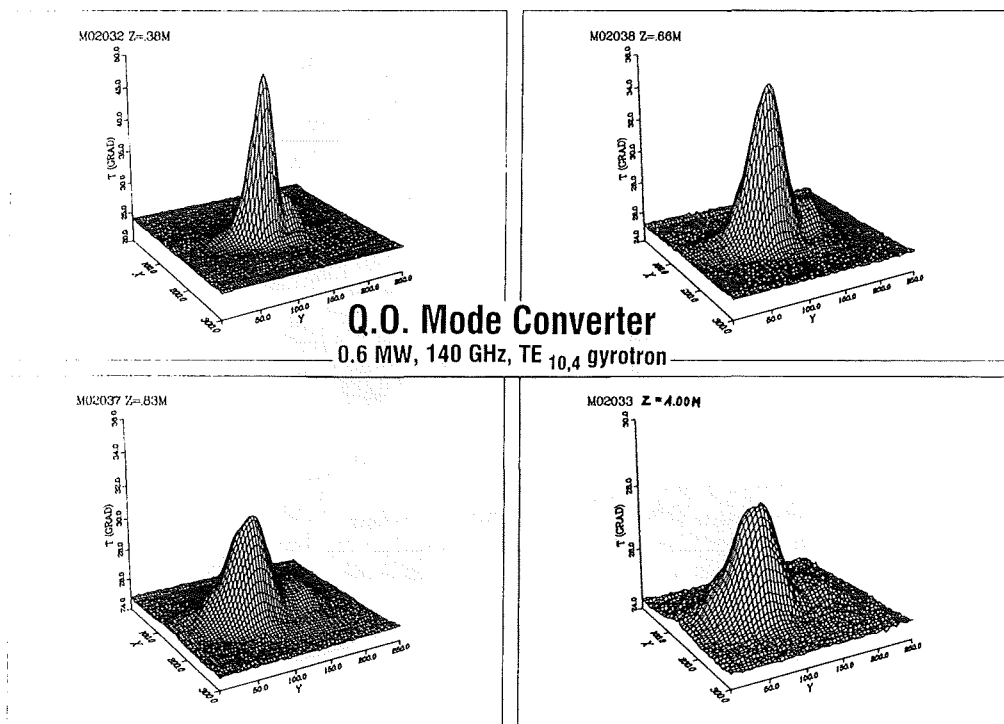


Fig. 17: Distribution of millimeter-wave-beam output power at different distances from the output window of the 140 GHz - 0.5 MW - $TE_{10,4}$ -mode FZK gyrotron with built-in high-efficiency mode converter. The measured mode purity is $94.5 \pm 1 \%$.

Energy Recovery Systems with Depressed Collector. The JAERI/TOSHIBA gyrotron development group and FZK Karlsruhe have recently tested gyrotrons with internal quasi-optical mode converter and single-stage depressed collector at 110 GHz and 140 GHz, respectively [40,44]. In Fig. 18 the configuration of the Japanese 110 GHz gyrotron and power supply system is illustrated. A relatively long insulator is installed between body and collector and the body section is also electrically insulated from the tube casing. The collector is grounded. These insulators make it possible to apply high voltages up to 50 kV to the body resulting in an electron retarding voltage at the gap between body and collector (single-stage depressed collector). The electron beam is accelerated and the beam characteristics are determined only by the beam acceleration power supply ($V_a = 80$ kV, $I_{\text{body}} \leq 0.3$ A) but the beam power is provided by the main power supply ($V_c = 50$ -80 kV, $I_{\text{beam}} = 30$ A). The beam deceleration voltage $V_r = V_a - V_c$ appears between body and collector. The collector permits the application of a retarding potential up to the minimum energy of the spent beam (≈ 30 kV). The system efficiency is enhanced by the factor V_a/V_c . Fig. 19 shows experimental results for the dependence of output power, output efficiency $P_{\text{out}}/(V_a I_{\text{beam}})$, total efficiency $P_{\text{out}}/(V_c I_{\text{beam}})$ and leakage current to the body section I_{body} on the electron retarding potential V_r . The pulse duration was approx. 50 ms. The results indicate that the output power (610 kW) is not affected by the applied voltage depression up to $V_r \approx 30$ kV. Above this retarding potential a body current I_{body} appears and the power starts to decrease. The output efficiency is 30 % and the total efficiency reached 50 %.

A single -stage depressed collector has been added to the FZK experiment (Fig. 15). The collector was depressed by inserting a variable high voltage resistance ($R_{\text{coll}} \leq 2.5$ k Ω) between the collector and ground, making the collector voltage dependent on the collector current. The measurements have been performed such that at a given set of gyrotron operating parameters (U_{cath} , I_{beam} , U_{mod} , $B_0(z)$) the following values have been measured : I_{coll} = current to collector, I_{body} = current to the grounded parts of the the tube ($I_{\text{beam}} = I_{\text{coll}} + I_{\text{body}}$), U_{coll} = collector voltage, and RF output power P_{out} . Proof of principle experiments yielded an increase of the output efficiency from 32 % to approximately 50 % ($U_{\text{coll}} = 31$ kV). Fig. 20 shows body current and output power versus the collector depression voltage U_{coll} for the parameter set $U_{\text{cath}} = 80$ kV, $I_{\text{beam}} = 25$ A, $U_{\text{mod}} = 23$ kV and $\tau = 0.5$ ms. The body leakage current in the FZK experiment is significantly higher than that measured in the JAERI/TOSHIBA tube since in this case the insulator is located much closer to the collector (compare Fig. 15 and Fig. 18). Owing to this location of the retarding potential at low magnetic field, the reflected electrons are trapped between the magnetic mirror at the cavity output and the retarding potential at the collector and thus fully contribute to the body current via radial diffusion. The FZK gyrotron with single-stage depressed collector was also operated at 155 GHz (TE_{12,4} cavity mode and Gaussian output). The efficiency of the TE_{12,4} mode is lower since the cavity is optimized for TE_{10,4} at 140 GHz. Additionally, it is not clear how well the improved TE_{10,4} q.o. mode converter operates at 155 GHz for the TE_{12,4} mode. Table V summarizes the present development status of high frequency gyrotron oscillators with depressed collector. The very first experiments on a gyrotron with single-stage depressed collector where conducted at NRL using a quasi-optical gyrotr [60].

The application of beam energy recovery by using a depressed collector has proven to be an effective method for efficiency enhancement of gyrotrons. This would give a strong impact on the design and costs of ECH/ECCD systems. As an example, we consider the effect for a 50 MW output plant (at the plasma torus) with 87 % trans power supply efficiency when the gyrotron efficiency is enhar

collector has proven to be an effective method for efficiency enhancement of gyrotrons. This would give a strong impact on the design and costs of ECH/ECCD systems. As an example, we consider the effect for a 50 MW output plant (at the plasma torus) with 87 % trans power supply efficiency when the gyrotron efficiency is enhar

**V_a : Voltage of Beam
Acceleration (~80 kV)**
**V_c : Voltage of Main Power
Supply (50~80 kV)**

$$\eta_{\text{Total}} = \eta_{\text{osc}} \times \frac{V_a}{V_c}$$

**By reducing V_c, Electron
deceleration voltage V_c - V_a
is applied between Collector
and Body**

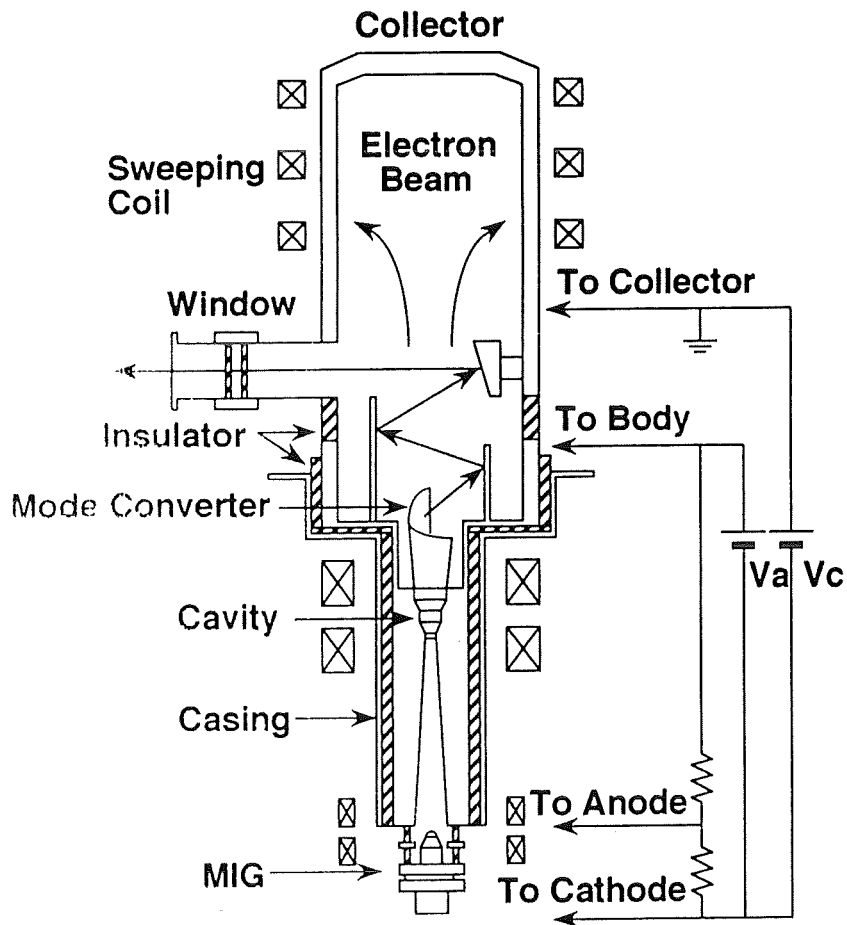


Fig. 18: Schematic layout of the JAERI/TOSHIBA 110 GHz-TE_{22,2}-mode gyrotron with q.o. mode converter and single-stage depressed collector together with the power supply system [44].

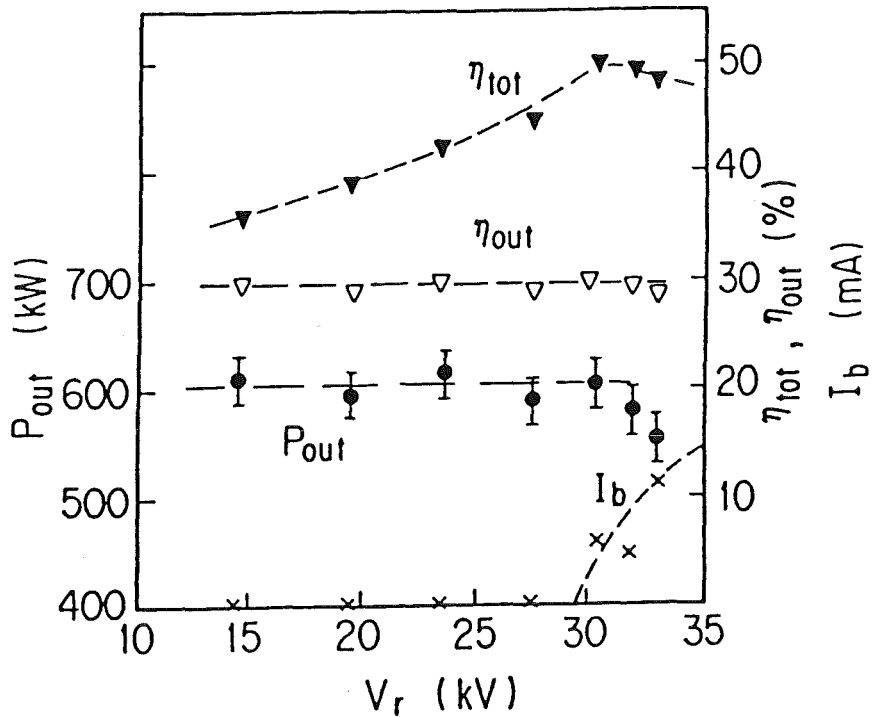


Fig. 19: Dependence of output power, body leakage current, output efficiency and total efficiency of the JAERI/TOSHIBA 110 GHz-TE_{22,2}-mode gyrotron with single-stage depressed collector on the retarding voltage V_r [44].

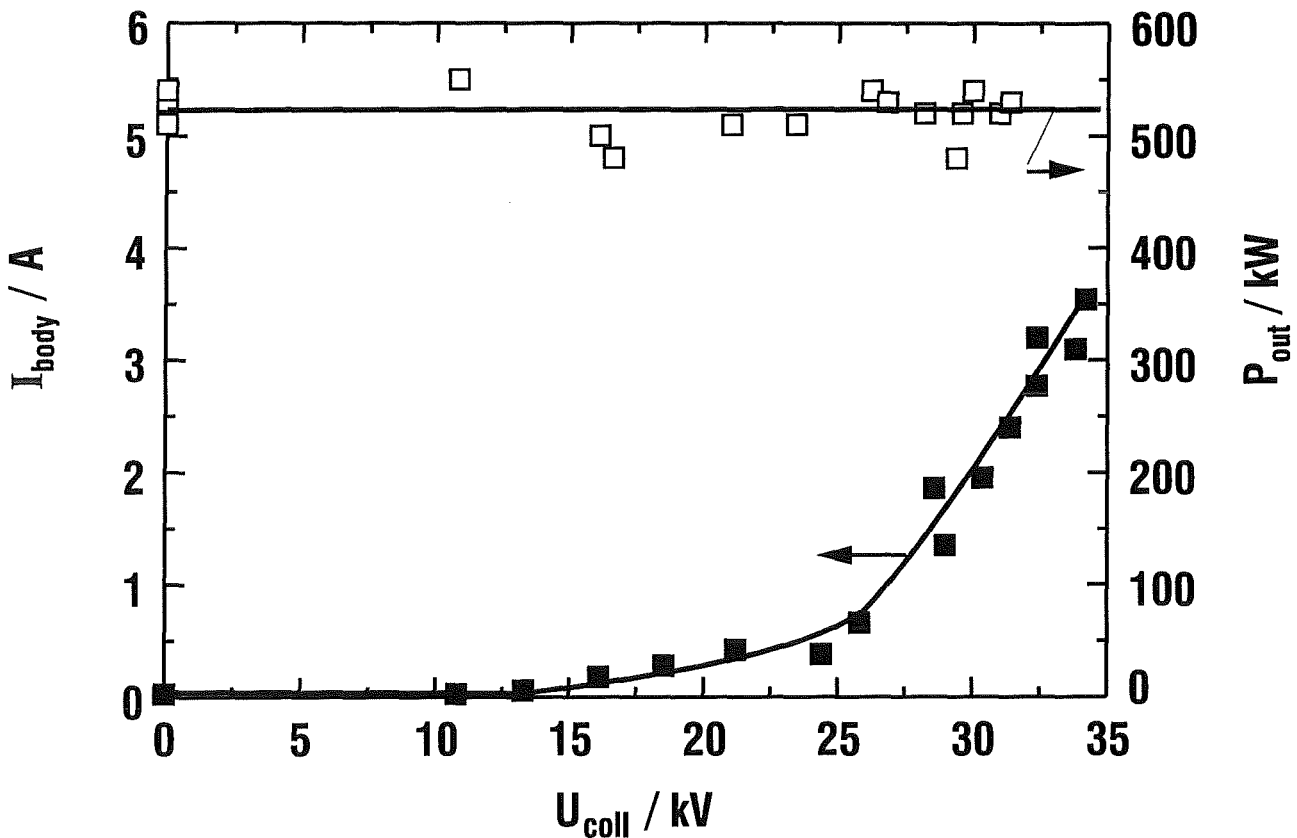


Fig. 20: Dependence of output power and body leakage current of the KfK-140 GHz-TE_{10,4}-mode gyrotron with single-stage depressed collector on the collector depression voltage U_{coll} [40].

Institution	Frequency [GHz]	Mode cavity output	Power [MW]	Efficiency [%]	Pulse length [s]
FZK, Karlsruhe [39,40]	140.2	TE _{10,4} TEM ₀₀	0.60	27	0.012
			0.50	32	0.03
			0.50	48(DEPCOL)	0.03
	140.5	TE _{10,4} TEM ₀₀	0.46	51(DEPCOL)	0.2
	154.8	TE _{12,4} TEM ₀₀	0.35	18	0.01
NRL, Washington D.C. [60]	115	QOG TEM ₀₀	0.35	27(DEPCOL)	0.005
			0.60	9	10 ⁻⁵
			0.43	12.7(DEPCOL)	10 ⁻⁵
TOSHIBA, JAERI Nasushiobara, Naka [43,44]	110	TE _{22,2} TEM ₀₀	0.20	16.1(DEPCOL)	10 ⁻⁵
			0.75	27.6	0.002
			0.61	30	0.05
			0.61	50(DEPCOL)	0.05
			0.42	48(DEPCOL)	2.6
			0.35	48(DEPCOL)	5.0

DEPCOL: Depressed Collector (single stage);

QOG: Quasi-Optical Gyrotron

Table V: Present development status of high frequency gyrotron oscillators with single-stage depressed collector (DEPCOL).

50 MW Output Plant	Power Supply Capacity	Cooling System Capacity	High-Power Fine Regulation
Ordinary Gyrotron ($\eta = 35\%$)	171 MW	121 MW	required
DEPCOL Gyrotron ($\eta = 50\%$)	109 MW	59 MW	not required
Gain Factor	1.57	2.05	

Table VI: Power supply and cooling system capacities required for a 50 MW output plant (at the plasma torus) with ordinary gyrotrons and gyrotrons with depressed collector.

Table VI summarizes the corresponding power supply and cooling system capacities required. The necessary power supply and cooling capacity is approximately 2/3 and 1/2 respectively, of that without energy recovery system. Only the low current accelerating power supply must have a high accuracy. Since the energy of the spent beam is substantially reduced ($U_{\text{coll}} = 30$ kV), the total amount of generated X-rays decreases significantly. It is obvious that all these favourable features bring a large cost reduction of ECW systems.

The advantages of a single stage collector are

- simple and efficient ($\eta_{\text{coll}} \approx 72\%$ for $\delta\beta_{\perp} = 0\%$)
- sweeping of the electron beam to lower the maximum power density on the collector as in an ordinary gyrotron
- less problems with backscattered electrons compared to a more complicated multi-stage depressed collector (e.g. $N_{\text{coll}} = 3$, $\eta_{\text{coll}} \approx 87\%$ for $\delta\beta_{\perp} = 0\%$)

Output window. From the viewpoint for the realization of 1 MW CW operation, essentially all components of present-day gyrotrons have been developed with the exception of the output window. At present, edge-cooled (water) single-disk windows as well as surface-cooled (FC-75) double disk sapphire windows are in use and cryogenically edge-cooled single disk sapphire windows and distributed windows are under test. The state-of-the-art is summarized in Table VII.

Material	Type	Power (kW)	Frequency (GHz)	Pulse Length (s)	Institution
alumina	single disk water edge cooled	200	60	0.1	VARIAN
water-free fused silica	single disk water edge cooled	200	60	5.0	UKAEA/Culham
boron nitride	single disk water edge cooled	600 550	140 140	2.0 3.0	SALUT TORIY
sapphire	single disk LN ₂ edge cooled	285* 500 370	140 140 140	3.0 0.5 1.3	IAP/INFK FZK/IAP/IPF/IPP FZK/IAP/IPF/IPP
sapphire	single disk with Cu anchor LHe edge cooled	410	110	1.0	JAERI/TOSHIBA
sapphire	double disk FC75 face cooled	500 350 200	110 110 140	2.5 5.0 CW	VARIAN JAERI/TOSHIBA VARIAN
sapphire	distributed water cooled	65**	110	0.3	GA/JAERI/ TOSHIBA

Power densities required for 1 MW-level (*) and 0.8 MW-level (**) gyrotrons (HE₁₁)

Tab. VII: Experimental parameters of high-power millimeter-wave vacuum windows.

As can be seen from Table VII, no windows for CW applications at the MW power level exist. To reach this goal, further developments of cryo-cooled sapphire windows are underway at several labs (CEA Cadarache, IAP Nizhny Novgorod, JAERI Naka, FZK Karlsruhe, TTE Thomson, Toshiba). In these designs, the extremely low absorption and the high thermal conductivity of pure sapphire in the temperature range between 20K and 77K will be utilized [61-67]. The theoretical power limits for CW transmission of a single disk, LN₂ edge-cooled sapphire window are given in Table VIII. It should be mentioned that in the case of gyrotron windows eventual "cryopumping" of a cryogenic window appears to be no problem.

	140 GHz	170 GHz	220 GHz
Gaussian Profile (G)	0.5 MW	0.4 MW	0.3 MW
Flattened Profile (F)	0.7 MW	0.6 MW	0.45 MW
Annular Profile (A)	1.0 MW	0.85 MW	0.65 MW

Table VIII: Maximum power transmittance of a single disk, LN₂ edge-cooled sapphire window with resonant thickness ($5\lambda/2$ at 140 GHz, $6\lambda/2$ at 170 GHz, $8\lambda/2$ at 220 GHz) for different power distributions.

A novel vacuum window has been developed at General Atomics which uses a planar slotted structure of alternating thin sapphire bars with micro-channel water-cooled niobium hexagonal tubes [68]. Analysis indicates that a window 100 mm x 100 mm in area can carry 1 MW in the HE₁₁ mode at 110 GHz and 1 MW with an appropriate HE₁₁/HE₁₂ mode mixture at 170 GHz.

As a potentially new material for noncryogenically cooled gyrotron windows, diamond is attractive due to its phenomenal tensile strength, modest dielectric constant, low loss and high thermal conductivity. Current chemical-vapor-deposition (CVD) capabilities have allowed for tests with samples of 2.5 cm diameter and $\lambda/2$ thickness at $f = 145$ GHz [69]. Another potential window material, an optimized silicon grade, is now also being investigated. For this material in the temperature range between 150 K and 200 K the loss tangent is a factor of 100 lower and the thermal conductivity is 3-4 times higher) than that of sapphire. Above 120 K the power carrying capability of a silicon window will exceed that of a comparable sapphire window. The temperature range around 180 K seems to be optimum for a silicon window.

If frequency tuning is needed, the window should be intrinsically broadband. A possible solution is an improved "moth-eye" configuration [70,71] with disks having grooves with optimized shape instead of pyramical corrugations. Multi-layer windows (variation of permittivity) or Brewster angle window are other possibilities.

In conclusion of this section on mm-wave vacuum windows Table IX summarizes possible options for 1 MW, CW, 170 GHz operation. Options ③ and ④ are also well suited for use as a torus window.

	Material	Type	RF-Profile	Cross-Section	Cooling
①	Sapphire	single disk	flattened Gaussian	rectangular (285 mm x 35 mm)	LN ₂ edge cooled (77 K) tan $\delta = 6.7 \cdot 10^{-6}$, k = 1000 W/mK
②	Sapphire	single disk	Gaussian	circular ($\varnothing = 100$ mm)	LNe or LHe edge cooled (27 K) tan $\delta = 1.9 \cdot 10^{-6}$, k = 2000 W/mK
③	Sapphire/Metal	distributed	flattened Gaussian	rectangular (100 mm x 100 mm)	Internally water cooled (300 K) tan $\delta = 2.5 \cdot 10^{-6}$, k = 40 W/mK
④	Diamond	single-disk	Gaussian	rectangular (200 mm x 50 mm)	water edge cooled (300 K) tan $\delta = 3.5 \cdot 10^{-6}$, k = 900 W/mK
			flattened Gaussian	circular ($\varnothing = 100$ mm)	
⑤	Silicon Au-doped	single-disk	flattened Gaussian	circular ($\varnothing = 100$ mm)	edge cooled (200 K), cryo-cooler (CHF ₃ , CF ₃ Cl) tan $\delta = 6.8 \cdot 10^{-6}$, k = 250 W/mK
			Gaussian	circular ($\varnothing = 100$ mm)	LN ₂ edge cooled (77 K) tan $\delta = 8 \cdot 10^{-6}$, k = 1500 W/mK

③ and ④ also torus windows

Table IX: Options for 1 MW, CW, 170 GHz gyrotron windows.

5 Very high frequency gyrotron oscillators

The development of high power gyrotrons for the short millimeter- and submillimeter-wave region is important for applications such as ECRH of high-field tokamak experiments with confining magnetic field $B_0 \geq 10\text{T}$ [50,72,73], for active plasma diagnostics such as mm-wave scattering to determine velocity distributions of ions and to study drift instabilities [12], and for radar and spectroscopy [24,25]. During the past several years excellent results have been obtained with pulsed and CW gyrotrons designed for operation at the second harmonic ($s=2$) of the electron cyclotron frequency employing superconducting [11,74-79] or Bitter magnets [80]. The most impressive recent results are given in Table X. The 3 dB frequency line width (FWHM) of gyrotron radiation was measured to be around ≤ 200 kHz [11, 80, 81]. A high spectral purity: ratio of noise power to total rf power $P_N/P_0 < 10^{-18}/\text{Hz}$, has been verified [35].

Fundamental cyclotron resonance interaction has been studied using a special pulsed high field solenoid for $B_0=14\text{-}27$ T [11] or a Bitter magnet rebuilt to operate at up to $B_0=14$ T [50,72,73]. Key issues to be addressed are: stability of electron beams with compression ratio ≥ 40 , mode competition in cavities with $D/\lambda \geq 20$ and improved cavity design, and step-tuning of frequency up to 327 GHz. Tables XI to XIII summarize the present capabilities and performance parameters of such gyrotrons. Operating at both fundamental and the 2nd harmonic of the electron cyclotron frequency enables the gyrotron to act as a medium power (several 100 W), step tunable, mm- and sub-mm wave source in the frequency range from 150 to 838 GHz [75-79].

Institution	Frequency [GHz]	Mode	Power [kW]	Efficiency [%]	Pulse length [ms]
IAP, N.Novgorod [12,74]	157	TE ₀₃	2.4	9.5	CW
	250	TE ₀₂	4.3	18	CW
	250	TE ₆₅	1	5	CW
	326	TE ₂₃	1.5	6.2	CW
MIT, Cambridge [73,80]	209	TE ₉₂	15	3.5	0.001
	241	TE _{11,2}	25	6.5	0.001
	302	TE ₃₄	4	1.5	0.0015
	339	TE _{10,2}	4	3	0.0015
	363	TE _{11,2}	7	2.5	0.0015
	417	TE _{10,3}	15	6	0.0015
	457	TE _{15,2}	7	2	0.0015
	467	TE _{12,3}	22	3.5	0.0015
	503	TE _{17,2}	10	5.5	0.0015
UNIVERSITY, Fukui [75-77]	383	TE ₂₆	3	3.7	1
	402	TE ₅₅	2	3	1
	576	TE ₂₆	1	2.5	0.5

Table X: Capabilities and performance parameters of mm- and submillimeter-wave gyrotrons operating at the second harmonic of the electron cyclotron frequency, with output power ≥ 1 kW.

Institution	Frequency [GHz]	Mode	Power [MW]	Efficiency [%]	Pulse length [μ s]
MIT, Cambridge [10,72,73]	140	TE _{15,2}	1.33	40	3
	148	TE _{16,2}	1.3	39	3
	188	TE _{18,3}	0.6		3
	225	TE _{23,3}	0.37		3
	231	TE _{38,5}	1.2	20	3
	236	TE _{21,4}	0.4		3
	287	TE _{28,4}	0.2		3
	280	TE _{25,13}	0.78	17	3
	267	TE _{22,5}	0.537	19	3
	320	TE _{29,5}	0.4	20	3
	327	TE _{27,6}	0.375	13	3
	IAP, Nizhny Novgorod [12]	250	TE _{20,2}	0.3	31
350			0.13	17	30 - 80
375			0.12	15	30 - 80
430			0.12	9.3	30 - 80
500		TE _{28,3}	0.1	8.2	30 - 80
555			0.063	6	30 - 80
600		TE _{38,2}	0.05	5	30 - 80
650			0.04	4	40

Table XI: Capabilities and performance parameters of pulsed millimeter- and submillimeter-wave gyrotron oscillators operating at the fundamental electron cyclotron resonance.

Institution	Frequency [GHz]	Mode	Voltage [kV]	Current [A]	Power [MW]	Efficiency [%]	
MIT, Cambridge [50]	187.7	TE _{32,4}	94	57	0.65	12	
	201.6	TE _{35,4}	97	54	0.92	18	
	209.5	TE _{33,5}	98	37	0.54	15	
	213.9	TE _{34,5}	95	51	0.89	18	
	218.4	TE _{35,5}	90	44	0.56	14	
	224.3	TE _{33,6}	91	60	0.90	17	
	228.8	TE _{34,6}	92	59	0.97	18	
				100	59	1.2	20
	265.7	TE _{39,7}	90	57	0.64	12	
	283.7	TE _{43,7}	92	35	0.33	10	
	291.6	TE _{41,8}	93	54	0.887	18	

Table XII: Step tuning of MIT gyrotron oscillator (with large MIG [50]) operating at the fundamental electron cyclotron resonance (pulse length 1.5 μ s).

Institution	Frequency [GHz]	Mode	Voltage [kV]	Current [A]	Power [MW]	Efficiency [%]
MIT, Cambridge [50]	249.6	TE _{24,11}	71	41	0.39	14
	257.5	TE _{23,12}	87	41	0.33	9
	267.5	TE _{25,12}	85	33	0.35	12
	277.2	TE _{27,12}	78	42	0.45	14
	280.1	TE _{25,13}	92	51	0.78	17
	285.2	TE _{26,13}	93	41	0.42	11
	282.8	TE _{23,14}	94	39	0.54	15
	287.9	TE _{24,14}	94	51	0.66	14
	292.9	TE _{25,14}	95	41	0.72	18
	302.7	TE _{27,14}	96	43	0.27	7

Table XIII: Step tuning of MIT gyrotron oscillator (with small MIG [50]) operating at the fundamental electron cyclotron resonance (pulse length 1.5 μ s).

6 Gyrotrons for technological applications

The use of gyrotron oscillators for technological applications as material processing and plasma chemistry [13] appears to be of great interest if relatively simple, low cost devices are realized which are easy in service such as magnetrons. In CW gyrotrons with medium output power from 10 to 30 kW relatively low operating modes can be used even in the mm-wave range. Reliability, efficiency, feasibility and simplicity are the main problems instead of the thermal load and mode selectivity problems of ECRH gyrotrons. Devices with low magnetic field (normal conducting magnet, permanent magnet or cryocooler cooled superconducting magnet), low anode voltage, high efficiency and simple output coupling are under development. The state of the art in this area is summarized in Table XIV. Fig. 21 shows the photograph of a gyrotron oscillator technological system (GOTS) for high-temperature processing of materials at $P \leq 10$ kW, $f = 30$ GHz, CW which was developed and manufactured at the IAP Nizhny Novgorod and is now installed at the FZK Karlsruhe.

Institution	Frequency [GHz]	Mode		Power [kW]	Efficiency [%]	Voltage [kV]
		cavity	output			
IAP, SALUT, Nizhny Novgorod, TORIY, Moscow [11,13,45,46]	15	TE ₀₁	TE ₀₁	4	50	15
	30 (2 Ω_c)	TE ₀₂	TE ₀₂	20	25-40	20
	37.5		TEM ₀₀	15	30	15
	78	TE ₃₂	TE ₁₁	10	30	30
	83	TE _{11,3}	TEM ₀₀	20	30	20
	150	TE ₀₃	TE ₀₃	22	30	40
VARIAN, Palo Alto [4]	160 (2 Ω_c)	TE ₀₃	TE ₀₃	2.4	9.5	18
	28	TE ₀₂	TE ₀₂	15	40	40

Table XIV: Performance parameters of present CW gyrotron oscillators for technological applications.

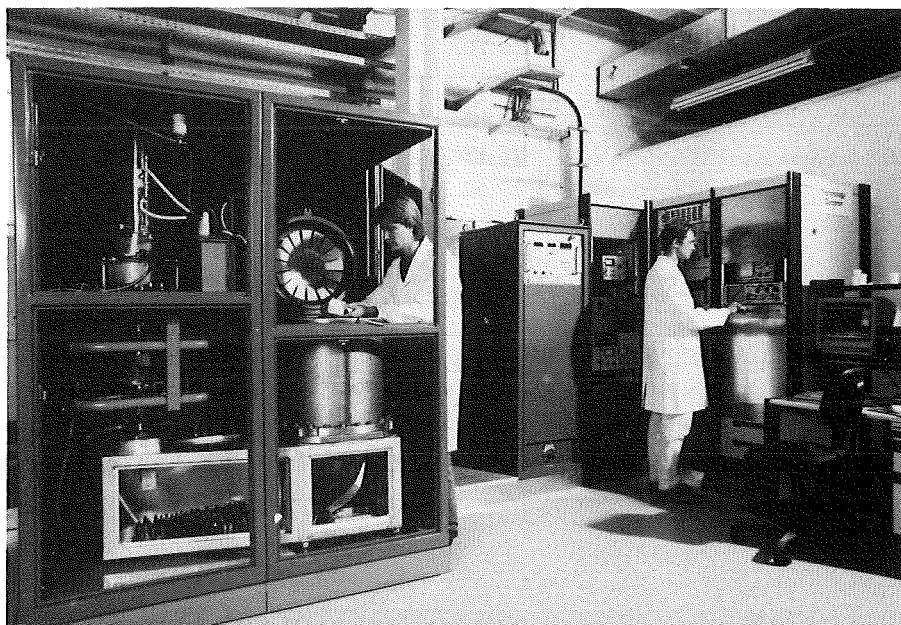


Fig. 21: Photograph of the IAP/FZK Gyrotron Oscillator Technological System (GOTS) for high-temperature processing of materials at $P \leq 10$ kW, $f = 30$ GHz, CW.

7 Relativistic gyrotrons

Some future applications of mm-wave radiation, such as deep-space radars and high-energy linear electron (and positron) accelerators may require substantially higher peak power levels than have been produced using conventional thermionic microwave technologies. The development of very high-peak-power gyrotron oscillators has profited from advances in intense relativistic electron beam technology using explosive emission cold cathodes with microwave pulse duration varying from 20 to 50 ns. Relativistic gyrotrons have two distinctive features compared to weakly relativistic gyrotrons [82]. First, increasing the beam energy reduces the microwave generation efficiency and second, since the coupling of the electron beam to TM modes is proportional to an additional factor of v_z^2 not found in the parameter describing the coupling to TE modes, in relativistic gyrotrons also TM-cavity operation can be achieved. The record for power in a relativistic gyrotron was achieved in the mid-1970s at the NRL in collaboration with scientists from Cornell University [83]. A total peak power of approximately 1 GW was generated which was spread over several interacting modes: 300 MW at 8.35 GHz, 600 MW at 8.5 GHz and 9 MW at both 11 and 13 GHz. The efficiency of microwave generation was very low (0.4 %). Single mode relativistic gyrotrons have been investigated primarily at the Institute of Applied Physics in Nizhny Novgorod (IAP) and the Lebedev/General Physics Institute in Moscow [84-88], and at the NRL in Washington D.C. [89,90]. In recent years, research has concentrated at NRL where step-tunable (28 to 49 GHz) $TE_{m,2}$ -mode gyrotrons ($m=4$ to 10) have produced hundreds of megawatts of output power. Step-tuning of relativistic short-pulse gyrotrons in the Ka band (26.5 to 40 GHz) and W band (75-110 GHz) at lower power levels in the several hundred kilowatt range has been investigated at the University of Strathclyde in Scotland [91]. The present status of relativistic multimegawatt gyrotron oscillators is summarized in Table XV. The Russian TM-mode gyrotron employed a slotted echelette grating cavity together with a central rod with slightly elliptical cross-section for radial and azimuthal mode selection in very high beam current operation [88]. Another approach to effectively employing high beam currents was the utilization of plasma-filled resonators for compensation of the static beam space charge. The output power of these experiments reached 60 MW at 10 GHz with an efficiency of 15 % [85].

Institution	Frequency [GHz]	Mode	Voltage [MV]	Current [kA]	Power [MW]	Efficiency [%]	
IAP, Nizhny Novgorod [88]	20	TM_{01}	0.5	0.7	40	11.4	
	79-107	TM_{1n}	0.5	2-6.5	30	3-1	slotted echelette cavity, $n = 3-10$
IAP, Nizhny Novgorod	10	TE_{13}	0.3	0.4	25	20	slotted cavity
Lebedev/General Phys. Inst. Moscow [85-88]	10	TE_{13}	0.3	1.0	60	15	slotted cavity with plasma
	40	TE_{13}	0.4	1.3	25	5	slotted cavity
UNIV. Michigan [92]	10	TE_{11}	0.4	0.025	0.6	6	
NRL, Washington D.C. [83,89,90]	8.35-13		3.3	80	1000	0.4	4-5 modes
		TE_{62}	0.6	2.0	100	8	
	35		1.15	2.5	275	10	
Tomsk Polytech. Inst. [84]	35	TE_{13}	0.9	0.65	35	6	slotted cavity
	3.1		0.75	8.0(30)	1800	8	also viractor interaction

Table XV: Present development status of relativistic gyrotron oscillators.

8 Quasi-optical gyrotrons

Although most gyrotron research has been based on the cylindrical waveguide cavity, results have also been obtained with a quasi-optical cavity [9,60,93]. The quasi-optical gyrotron is a gyro-device in which the interaction between the electromagnetic wave and the electron beam occurs in a Fabry-Perot type resonator placed transverse to the static magnetic field (Fig. 2). Operation in the mm-wave range of frequency and at megawatt power levels is possible since the ohmic heat load on the mirror surfaces can be kept within the usual limits of 1-3 kW/cm² by adjusting the resonator parameters. The operating mode is a high order Gaussian TEM_{00q} (with longitudinal mode index $q > 200$) so that the frequency can be tuned over a wide range by variation of the mirror distance (change of q). The separation between the spent electron beam and the microwaves allows easy implementation of a depressed collector in order to increase the overall system efficiency.

The-state-of-the art of quasi-optical gyrotrons is summarized in Table XVI. The two key issues of current research are the output coupling scheme and efficiency enhancement. Concerning the issue of a Gaussian output coupling scheme, the use of a grating mirror appears to be the best approach, as confirmed by hot test experiments where up to 99 % of the power was coupled into an HE₁₁ waveguide [94]. Three methods are being considered for efficiency enhancement [9,60,93]:

- the use of a sheet electron beam instead of the hollow MIG beam of conventional gyrotrons. Issues of sheet beam stability must still be investigated.
- the use of a depressed collector.
- the quasi-optical gyroklystron configuration. In this case the main difficulties lie in the necessity of amplitude and phase control by a feedback loop between the energy extracting resonator and the prebuncher. Mode priming and α -priming are being studied.

Institution	Frequency [GHz]	Mode resonator	Power [kW]	Efficiency [%]	Pulse length [ms]
ABB, Baden	[29] 92	TEM _{00q}	90	10	10
CRPP, Lausanne	[9] 90.8	TEM _{00q}	150	14	5
	100	TEM _{00q}	90	12	15
NRL, Washington D.C. [60,93]	110	TEM _{00q}	80	8	0.013
	115	TEM _{00q}	431	12.7(DEPCOL)	0.013
			197	16.1(DEPCOL)	0.013
	120	TEM _{00q}	600	9	0.013
TOSHIBA, Nasushiobara	[34] 112	TEM _{00q}	200	12	0.013
			100	12	5
	120	TEM _{00q}	26	10(DEB)	3

DEPCOL: Depressed Collector (single stage)

DEB: Dual Electron Beam (1 annular beam, 1 pencil beam)

Table XVI: Present development status of quasi-optical gyrotron oscillators.

9 Cyclotron autoresonance masers (CARMs)

CARM oscillators and amplifiers are presently only at the stage of proof of principle experiments but recent experimental successes show their intrinsic possibilities. The status of CARM performance parameters is summarized in Table XVII. The key issues for the future development of such devices are:

- Very high electron beam quality is required to obtain a high efficiency. The efficiency drops from 40% to 20% for $\Delta v_z/v_z \geq 2\%$. Recently, an efficiency of 10% has been achieved in 36 and 50 GHz, TE_{11} CARM oscillators employing an improved Bragg resonator [95-97]. By keeping the interaction region short (less than 10 cyclotron orbits), the effect of velocity spread is reduced. The interaction efficiency is found to be substantially increased when the axial magnetic field is tapered.
- High energy electron beam transport with low interception in the body.
- Competition between other interaction processes such as the gyrotron or the backward wave instabilities. These unwanted oscillations can be suppressed by choosing an optimum bunching parameter and a specific frequency dependence of the interaction circuit reflectivities [95-97].

Institution	Frequency [GHz]	Mode	Power [MW]	Efficiency [%]	Gain [dB]	B-Field [T]	Voltage [MV]	Current [kA]	Type
IAP	35.7	TE_{51}	25	10	-	1.12	0.4	0.6	oscil.
IAP, IHCE	37.5	TE_{11}	10	4	30	0.5	0.5	0.5	ampl.
IAP, IHCE, JINR	50	TE_{11}	30	10	-	0.7	1.0	0.3	oscil.
IAP	66.7	TE_{21}	15	3	-	0.6	0.5	1.0	oscil.
IAP, IHCE, JINR	68	TE_{11}	50	8	-	1.0	1.2	0.5	oscil.
IAP	69.8	TE_{11}	6	4	-	0.6	0.35	0.4	oscil.
IAP [95-97]	125	TE_{41}	10	2	-	0.9	0.5	1.0	oscil.
LLNL Livermore [98]	220	TE_{11}	50	2.5	-	3.0	2.0	1.0	oscil.
MIT Cambridge [99]	27.8	TE_{11}	1.9	5.3	-	0.6	0.45	0.080	oscil.
	30	TE_{11}	0.1	3	-	0.64	0.3	0.012	oscil.
	32	TE_{11}	0.11	2.3	-	0.63	0.32	0.015	oscil.
	35	TE_{11}	10	3	45	0.7	1.5	0.25	ampl.
UNIV. Michigan [100]	15	TE_{11}	7	1.5	-	0.45	0.4	1.2	oscil.

IAP Nizhny Novgorod, IHCE Tomsk, JINR Dubna

Table XVII: State-of-the-art of CARM experiments (short pulse).

10 Gyroklystrons, gyro-TWTs, gyrotwistrons, gyro-BWOs and other gyro-devices

As in the cases of gyromonotron and CARM, the efficiencies of gyroklystrons [101-109], gyro-TWTs [110-112], gyrotwistrons [104] and gyro-BWOs [113-115] strongly depend on beam quality. The longer interaction time in amplifiers allows the phase bunching of the electrons to be more degraded by velocity spread. Efficiency may be improved by keeping the gain per unit length high, and thus for a given overall gain, making the interaction region as short as possible. Improved electron guns (e.g. Pierce guns with kickers) are under development [95-97,115]. Electron beams with relatively low α ($\alpha = 0.8$) have resulted in stable saturated gyro-TWT operation at broad bandwidth at the expense of lower efficiency [111]. Dramatic improvement in performance appears to be achievable by tapering both the magnetic field (ramped field) and the wall radius along the axis of the interaction region to maintain the resonance condition over a wide frequency range [111,112]. The precise axial contouring is a topic of intensive current study. The gyro-TWT is potentially capable of much larger bandwidth than the gyroklystron. Key issues for gyroklystrons are stray oscillations in the drift regions between the different cavities, magnetic field profiling and penultimate tuning. Tables XVIII to XXI summarize the actual experimental parameters of gyroklystrons, gyro-TWTs, gyrotwistrons and gyro-BWOs, respectively. The duty factors of the gyroklystrons developed by VARIAN (Palo Alto), TORIY (Moscow) and IAP (Nizhny Novgorod) are 5 % (with 0.2 % bandwidth), 1 % (with 1.5 % bandwidth) and 0.05 % (with 0.5 % bandwidth), respectively. In the CW regime a peak output power of 2.5 kW at an efficiency of 25 % (beam voltage 22 kV, beam current 0.46 A) has been achieved in Russia [109]. The measured large-signal gain of this TE_{01} gyroklystron with 4 cavities is 30 dB and the experimental half-power bandwidth is 0.35 %. In general, the gyrotwistron tubes are more sensitive to instabilities and output loading than their gyroklystron relatives but they have a wider bandwidth [104]. The fundamental tubes have a wider bandwidth than their gyroklystron counterparts and the output power is in reasonable agreement with theory. The second-harmonic tubes experience more mode competition and cannot operate at the theoretical optimal point.

A relativistic gyro-TWT amplifier experiment operating in the TE_{11} mode at 35 GHz with a 0.9 MV, 200 A electron beam has demonstrated a linear growth rate of 2 dB/cm, total gain exceeding 30 dB, and an output power of 20 MW (11 % efficiency) [116]. Experiments on tapered-tube versus uniform-tube gyro-BWOs (4.4 -6 GHz) driven by an intensive electron beam with parameters: 0.8 MV, 1-4 kA, show higher microwave peak-power (few 10 MW) and more-reproducible long-pulse emission (400-500 ns) for the case of the tapered interaction circuit [117].

Rapid improvement in performance of gyro-amplifiers is expected in the near future since the development of those devices is in a considerably more preliminary state than the development of gyromonotrons.

Institution	Frequency [GHz]	Mode	No. of cavities	Power [MW]	Efficiency [%]	Gain [dB]	
NRL, Washington D.C. [24,60,101,102]	4.5	TE ₁₀	3	0.07	40	36	
	85	TE ₁₃	2	0.05		20	
	85.5	TEM ₀₀	2	0.082	19	18	QOGK
				0.082	30 (DEPCOL)	18	QOGK
IAP Nizhny Novgorod [106-108]	15.2	TE ₀₁	3	0.05	50	30	
	15.8	TE ₀₂	3	0.16	40	30	max. efficiency
	35	TE ₀₂ (2Ω _c)	2	0.2	18	15	tapered B-field
TORIY, Moscow [106-108]	35	TE ₀₂	2	0.75	24	20	max. power
			2	0.35	32	19	max. efficiency
	35	TE ₀₁	4	0.16	48	42	
			3	0.25	35	40	
IAP Nizhny Novgorod [109]	93.2	TE ₀₁	4	0.065	26	35	max. power
			4	0.057	34	40	max. efficiency
VARIAN, Palo Alto [24]	10	TE ₀₁	3	0.02	8.2	10	
	28	TE _{01/02}	2	0.076	9	41	

QOGK: Quasi-Optical Gyroklystron;

DEPCOL: Depressed Collector (single stage)

Institution	Frequency [GHz]	Mode	No. of cavities	Power [MW]	Efficiency [%]	Gain [dB]	
UNIV. MARYLAND [103-105]	9.87	TE ₀₁	2	24	32	34	
	9.87	TE ₀₁	3	27	32	37	max. power
			3	16	37	33	max. efficiency
			3	20	28	50	max. gain
	19.75	TE ₀₂ (2Ω _c)	2	32	28	27	
	29.63	TE ₀₃ (3Ω _c)	2	1	1.2	18	

Table XVIII: Gyroklystron experimental results (short pulse, bandwidth ≤ 2 %).

Upper part: weakly relativistic gyroklystrons,

lower part: relativistic gyroklystrons.

Institution	Frequency [GHz]	Mode	Power [kW]	Efficiency [%]	Gain [dB]	Bandwidth [%]	
UC LOS ANGELES [110]	10	TE ₁₀	55	11	27	11	diel.coat.w.g.
	15.7	TE ₂₁ (2Ω _c)	202	13	16	2	slotted w.g.
UNIV. HSINCHU [111]	35.8	TE ₁₁	18.4	18.6	18	10	
	35.8	TE ₁₁	28.8	16	35	8	2-stage
NRL, Washington D.C. [24,112]	32.5	TE ₁₀	6.3	10	16.7	33	
	32.5	TE ₁₀	8	16	25	20	2-stage
	34.3	TE ₀₁	16.6	7.8	20	1.4	
VARIAN, Palo Alto [24]	5.18	TE ₁₁	120	26	20	7.3	
	95	TE ₁₁	15	6.3	30	1.6	

Table XIX: Present development status of gyro-TWTs (short pulse).

Institution	Frequency [GHz]	Mode	No. of cavities	Power [MW]	Efficiency [%]	Gain [dB]
UNIV. MARYLAND [104]	8.57	TE ₀₁	2	21.6	22	24
	17.14	TE ₀₂ (2Ω _c)	2	12	12	22

Table XX: State-of-the-art of gyrotwistron experiments (short pulse).

Institution	Frequency [GHz]	Mode	Power [kW]	Efficiency [%]	Bandwidth [%]	
NRL, Washington D.C.	[113]	29.2	TE ₁₀	6	15	3 electr. tuning
						13 magn. tuning
UNIV. HSINCHU	[114]	34	TE ₁₁	20-67	6.5-21.7	5
				113	19	1
MIT, Cambr., LLNL, Liverm.	[115]	138	TE ₁₂	1	0.5	6.5

Table XXI: First experimental results on gyro-BWOs (short pulse).

So far, we have considered gyro-devices driven by the kinetic energy stored in the small-orbit Larmor gyration of electrons in a magnetic field. By contrast, in the large-orbit gyrotron (also known as a gyromagnetron or cusptron [24,25]), a beam of electrons is passed through a magnetic cusp so that the beam goes into a fast rotational mode in which all of the electrons have axis-encircling orbits. This large-orbit beam then interacts downstream in a cavity with a magnetic field to produce microwaves. Although not as efficient as conventional gyrotrons operating at the fundamental, large-orbit gyrotrons have demonstrated an ability to run at very high multiples (e.g., 10 to 20) of the cyclotron frequency. The magnicon, an enhancement of the original gyrocon [24] and finally the peniotron are other large-orbit devices.

The peniotron is based on an interaction first described by Ono and his coworkers in 1962 [118], shortly after the discovery of the ECM. The peniotron mechanism, however, is very different from the ECM interaction in two respects. First, it operates in a mode with azimuthal index m , which must be related to the cyclotron harmonic index s by

$$m = s + 1 \quad ; \quad \text{i.e.} \quad \omega = (m - 1) \Omega + k_z v_z \quad (9)$$

such that each electron "sees" one complete cycle of the rf electric field during each orbit. Second, the gain mechanism underlying the peniotron interaction occurs due to the coherent drift of the guiding centers of the electron orbits into regions of strong decelerating rf electric field. As a result, all electrons, regardless of their initial phases relative to the wave, convert roughly the same amount of their kinetic energy into wave energy. There are no bad phase electrons and there is no bunching [119]. As a consequence, the efficiencies predicted by ideal theories are quite high, higher than in ECMs, where bunching occurs and a minority of the electrons actually draw energy from the fields. High efficiencies at cyclotron harmonics are also possible. Selection of modes with large azimuthal wavenumbers at high cyclotron harmonics is accomplished with a magnetron-like structure in the cavity, as in a large-orbit gyrotron. Effective coupling of the beam and fields is effected by using beams placed close to

the wall with axis-encircling orbits. Computer simulations indicate that the efficiency is rather insensitive to spreads in the guiding center locations for the beam electrons, but that beam loss to the nearby wall is a limiting factor [119].

In the gyropeniotron, the electrons entering the cavity are moving in smaller, off-axis orbits as in a gyrotron [120]. The electron beam radius is placed on the circle at which the rf electric field is zero, so that there is no gyrotron interaction.

Tables XXII and XXIII summarize the experimental results of peniotrons and gyropeniotrons achieved by the TOHOKU University Group at Sendai, Japan. Up to now, there is still no convincing evidence to assure that high efficiency interaction has been achieved in any of the experiments.

Institution	Frequency [GHz]	Mode	Power [kW]	Efficiency [%]	Pulse Length [ms]
UNIV. TOHOKU, Sendai [121-123]	10.0	TE_{11}^r	10	36	0.02
	10.5	$TE_{31}^c(2\Omega_c)$	0.7	10	magnetron- type cavity auto-res.
			1.3	7	
10	TE_{21}^c	1.5	25		

Table XXII: Experimental results of peniotrons.

Institution	Frequency [GHz]	Mode	Power [kW]	Efficiency [%]	Pulse Length [ms]
UNIV. TOHOKU, Sendai					
TOSHIBA, Nasushiobara	69.85	$TE_{02}(3\Omega_c)$	8	6.75	0.2
UNIV. FUKUI [124]	140	$TE_{03}(3\Omega_c)$	8	1	1

Table XXIII: Experimental results of gyropeniotrons.

11 Free electron masers (FEMs)

Free electron masers (FEMs) differ from the other high-power microwave sources considered in this report in that they have demonstrated output over a range of frequencies extending far beyond the microwave spectrum, well into the visible and ultraviolet range (free electron lasers) [24,25,125-127]. To achieve this spectral versatility, FEMs exploit relativistic beam technology to upshift the electron "wobble" frequency by an amount roughly proportional to γ^2 (see Fig. 22 and Section 2). In this respect, perhaps a more descriptive name is that coined by R.M. Phillips [128]: UBITRON, for an "undulated beam interaction electron" tube. The magnetostatic wiggler is the most common, but not the sole means, for providing electron undulation. An electrostatic wiggler or the oscillatory field of a strong electromagnetic wave can also play this role. Devices with such electromagnetic wigglers are sometimes called scattrons [1,16].

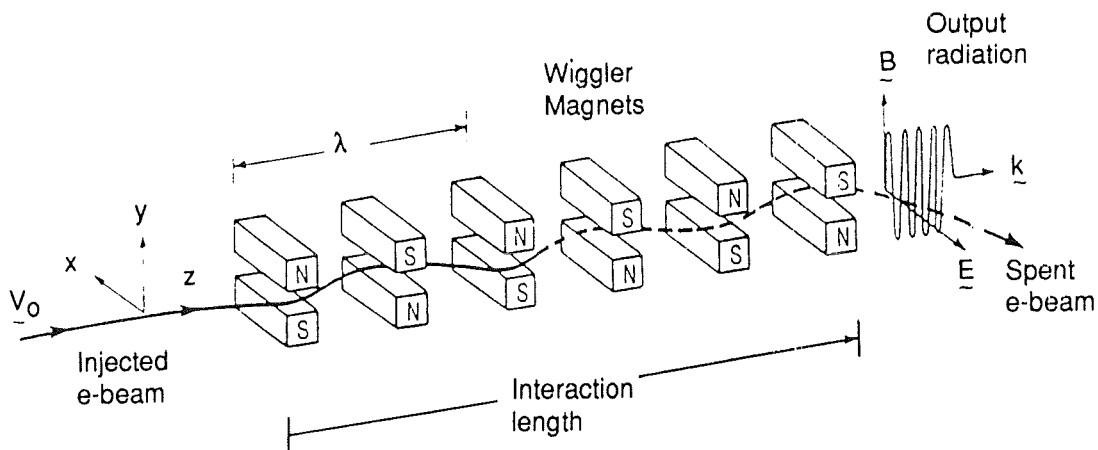


Fig. 22: The basis FEM configuration. Electrons in a injected electron beam undulate in the periodic magnetic field of the wiggler.

11.1 Possibilities

The FEM appears to be potentially capable of fulfilling all the requirements for a frequency tunable high power mm-wave source. Coverage of the entire frequency range of 130-260 GHz presents no severe problems, and even higher frequencies are quite feasible. Rapid tunability over more than $\pm 5\%$ could be obtained by variation of the beam energy. The interaction occurs in a cavity operating in low-order modes, which have very good coupling to a Gaussian beam output. The relatively low RF wall loading and the use of high electron beam energy (>0.5 MeV) are compatible with a high unit power if the electron beam interception could be maintained at an acceptable level. A survey of FEM development status (experiments) is presented in Table XXIV.

Institution	Frequency [GHz]	B_w [T]	λ_w [mm]	Mode	Power [MW]	Efficiency [%]	Gain [dB]	Voltage [MV]	Current [kA]	Accelerator	Pulse-Length [μ s]	Type
CESTA, Le Barp [130]	33-36	0.2	120	TE ₁₁ ^c	0.22	0.3		2.4	0.3(5)	Pulse Line	0.003	superrad.
COLUMBIA U. NY [131,132]	24	0.05	34	TE ₁₁ ^c /TM ₁₁ ^c	2	3.3	20	0.6	0.1	Pulse Line	0.15	amplifier
ENEA Frascati [133]	110-140	0.61	25	TE ₀₁ ^r	0.001	1.1·10 ⁻⁴		2.3	0.004	Microtron	4	oscillator
EP Palaiseau [134]	120	0.03	20	TE ₁₁ ^c	11.5	6.4		0.6	0.3	Electrostatic	0.02	superrad.
General Electric	2.6	0.04		TE ₀₁ ^r	1.2	10		0.17	0.07	Electrostatic		oscillator
Microwave Lab, Palo Alto [128]	2.8	0.04		TE ₀₁ ^r	0.9	9.2	6	0.14	0.07	Electrostatic		amplifier
	15.7			TE ₀₁ ^r	1.65	6		0.23	0.125	Electrostatic		oscillator
	54			TE ₀₁ ^r	0.15	6	30	0.07	0.04	Electrostatic		amplifier
IAP, Nizhny Novgorod [135]	16.7	0.02		TE ₀₁ ^c	300	11		0.6	4.5	Electrostatic	0.03	oscillator
ILE Osaka [136]	250	0.05	30	TE ₁₁ ^c	0.6	0.5	110	0.6	0.2	Ind. LINAC	0.04	amplifier
JAERI, Ibaraki [137]	45	0.18	45	TE ₁₁ ^c	6	2.9	52	0.82	0.25(2.0)	Ind. LINAC	0.03	amplifier
KEK, Tsukuba [138]	9.4	0.12	160	TE ₀₁ ^r	100	4.5	33	1.5	0.65(1.5)	RF LINAC	0.015	amplifier
LLNL, Livermore [17,139]	34.6	0.37	98	TE ₀₁ ^r	1000	34	52	3.5	0.85(4.0)	Ind. LINAC	0.02	amplifier
[140]	140	0.17	98	TE ₁₁ ^c	2000	13.3	58	6.0	2.5 (3.0)	Ind. LINAC	0.02	amplifier
MIT, Cambridge [99,141]	9.3	0.02	33	TE ₁₁ ^c	0.1	10	6	0.18	0.0055	Electrostatic	0.02	amplifier
	27.5	0.05	30	TE ₁₁ ^c	1	10.3	-	0.32	0.03(0.05)	Electrostatic	1	oscillator
	33.4	0.15	32	TE ₁₁ ^c	61	27	50	0.75	0.3	Electrostatic	0.03	amplifier
	35.2	0.05	30	TE ₁₁ ^c	0.8	8.6	26	0.31	0.03(0.05)	Electrostatic	1	amplifier
NRL, Washington D.C. [142]	12.5-16.5	0.1	30	TE ₀₁ ^r	0.7	3		0.25	0.1			amplifier
	23-31	0.06	40	TE ₀₁ ^c	4	3		0.7	0.2	Ind. LINAC	0.035	amplifier
	35	0.14	30	TE ₁₁ ^c	17	3.2	50	0.9	0.6	Pulse Line	0.02	amplifier
	75	0.08	30	TE ₁₁ ^c	75	6	50	1.25	1.0	Pulse Line	0.02	superrad.
RI, Moscow [143]	6-25	0.03	48	TE ₁₁ ^c /TM ₀₁ ^c	10	1.7		0.6	1	Pulse Line	2	superrad.
SIAE, Chengdu [144]	37	0.125	34.5	TE ₁₁ ^c	7.6	5.4		0.5	0.28	Electrostatic	0.015	oscillator
SIOFM, Shanghai [145,146]	37.5	0.12	21	TE ₁₁ ^c	12	3.7	50	0.4	0.8	Pulse Line	0.02	amplifier
	39	0.126	22	TM ₀₁ ^c	14	4.4		0.4	0.8	Pulse Line	0.02	oscillator
	85.4	0.1	10	TE ₁₁ ^c /TM ₀₁ ^c	0.6	0.5		0.3	0.4	Pulse Line	0.02	superrad.
TRW, Redondo Beach [147]	35	0.16	20	TE ₀₁ ^r	0.1	9.2		0.3	0.004	Electrostatic	10	oscillator
	35	0.16	20	TE ₀₁ ^r	0.1	9.2	2	0.29	0.0001	Electrostatic	10	amplifier
UCSB Santa Barbara [148]	120-880	0.15	71.4		0.027	0.5		2-6	0.002	Electrostatic	1-20	oscillator

r: rectangular waveguide; c: circular waveguide

Table XXIV: State-of-the-art of millimeter- and submillimeter wave FEMs.

11.2 Accelerator options and key issues

In principle, for the mm-wave range, the FEM could be powered by either an induction LINAC, and RF LINAC with beam energy at 3 - 10 MeV, or an electrostatic accelerator at 0.5-3 MeV. One of the problems of the induction LINAC is the large size and complexity of the device. Another difficulty is the very high peak power at low repetition rate and, therefore, the possible impact of nonlinear effects associated with pulsed output at GW peak power. The RF-LINAC is also a pulsed device with a peak power up to 50 MW; this is deemed to be acceptable for ECW interaction in the linear regime. Development of a source having an average output of 1 MW should be possible using proven technology. An oscillator with a high system efficiency requires a sophisticated recirculation and recovery scheme. A FEM amplifier with a tapered undulator has already achieved a high extraction efficiency per pass (40 %) without energy recovery. The electrostatic accelerator allows true CW operation and has the potential of achieving efficiencies in the 50 % range through energy recovery (but very good beam quality is required).

Key issues common for both accelerator options are:

- the design of the output coupling scheme,
 - the implementation of techniques to suppress the side-band instability.
- Both problems may be solved using a special interaction circuit employing a stepped rectangular HE_{11} waveguide together with phased plane 100 % reflectors [129].

The electrostatic accelerator would also require:

- development for the transport of a multiampere beam at energies around or larger than 1 MeV at extremely low (<0.5 %) body current on the undulator channel.
- development of a short-period undulator (period below 2 cm) at frequencies larger than 260 GHz.

The specific important issue for RF LINAC is:

- an efficient energy recovery system (the system efficiency is a sensitive function of the "recovery" efficiency: 96 % (resp. 89 %) is necessary to obtain 20 % (resp. 10 %) system efficiency).

11.3 The FOM-Fusion FEM

A free electron maser is being designed at the FOM Institute "Rijnhuizen" for ECRH applications on future fusion devices [126]. The FEM will have an output power of 1 MW, a central frequency of 200 GHz and will be adjustable over the complete frequency range of 130 GHz to 260 GHz. The FEM is driven by a thermionic electron gun. Fast tunability is achieved by variation of the terminal voltage of the 2 MeV electrostatic accelerator. The undulator and mmw system are located in a terminal at a voltage of 2 MV, inside a vessel at 7 bar (see Fig. 23). After interaction with the mm waves in the undulator, the energy of the electron beam will be recovered by means of a decelerator and a multi-stage depressed collector. The low emittance electron beam will be completely straight to minimize current losses to less than 20 mA. This current is to be delivered by the 2 MV dc accelerating voltage power supply. Simulations indicate that the overall efficiency should be over 50 %.

The FOM-FEM will be an oscillator, consisting of a waveguide amplifier section and a feedback system (see Fig. 23). For the oversized waveguide inside the undulator a rectangular corrugated HE_{11} waveguide is chosen with a cross section of 15 x 20 mm². Directly behind the undulator the mm waves will be separated from the electron beam by means of a stepped waveguide. Here the width of the waveguide changes step-wise. Because of this step, the initial HE_{11} beam is split into two identical HE_{11} beams at about 1.5 m from the step. At this position two mirrors can be located with a hole in between, large enough to let the electron beam pass without disturbing the mmw beams (see Fig. 24). The two mmw beams at the location of the mirror are reflected with adjustable phases by changing the position of the mirrors. This enables a 0-100 % variation of the reflection coefficient (the fraction of the power that goes back through the interaction waveguide to the input side of the undulator, where a similar 100 % reflector is located, Fig. 25 and 26). The remaining power is evenly divided into two output beams; these can be recombined to make the 1 MW output. Low-power measurements on a prototype separation system are very encouraging. The width of the waveguide a (after the step) is given by $a = \sqrt{2\lambda L}$, where L is the length of the electron-beam/mmw splitter: 1.5 m. At present a system is being designed to move the sidewalls of the splitter in order to optimize the dimension a for all frequencies from $a = 60$ mm for 260 GHz to $a = 85$ mm for 130 GHz. This system enables to vary the frequency over the complete range of 130 to 260 GHz by just changing the accelerator voltage, the splitter width and the reflection coefficient. All this can be controlled remotely. Table XXV summarizes the design parameters of the planned FOM-FEM experiment.

Detailed simulations which take into account the propagation of the millimeter wave beam in the cavity and the interaction with the electron beam show that 99.8 % of the rf power is in the HE_{11} mode.

Transport of the mm waves to earth potential is done quasi-optically through a tube similar to the acceleration tube. By this method of transport a vacuum window at a pressure of 7 bar can be avoided.

Since frequency tuning is an important feature of the FEM, the output window has to be broadband. Some promising solutions are discussed in [71].

1 MW, 130-250 GHz FOM-Fusion-FEM

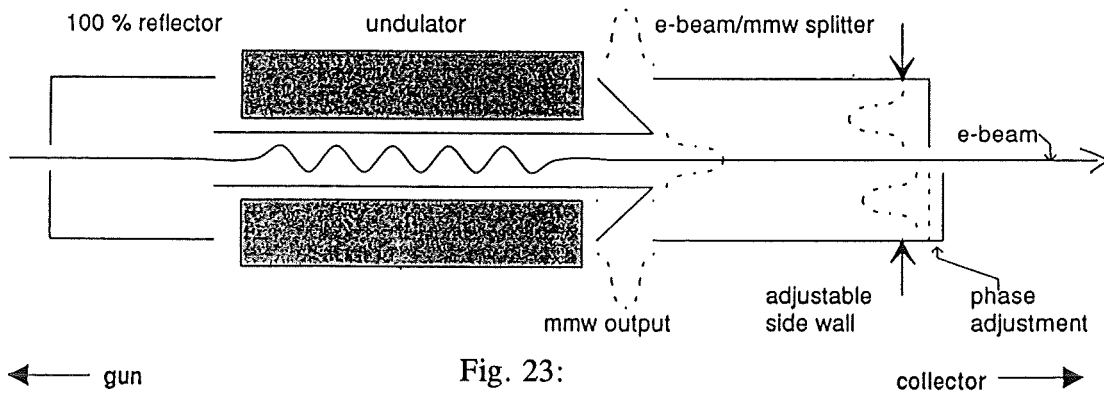
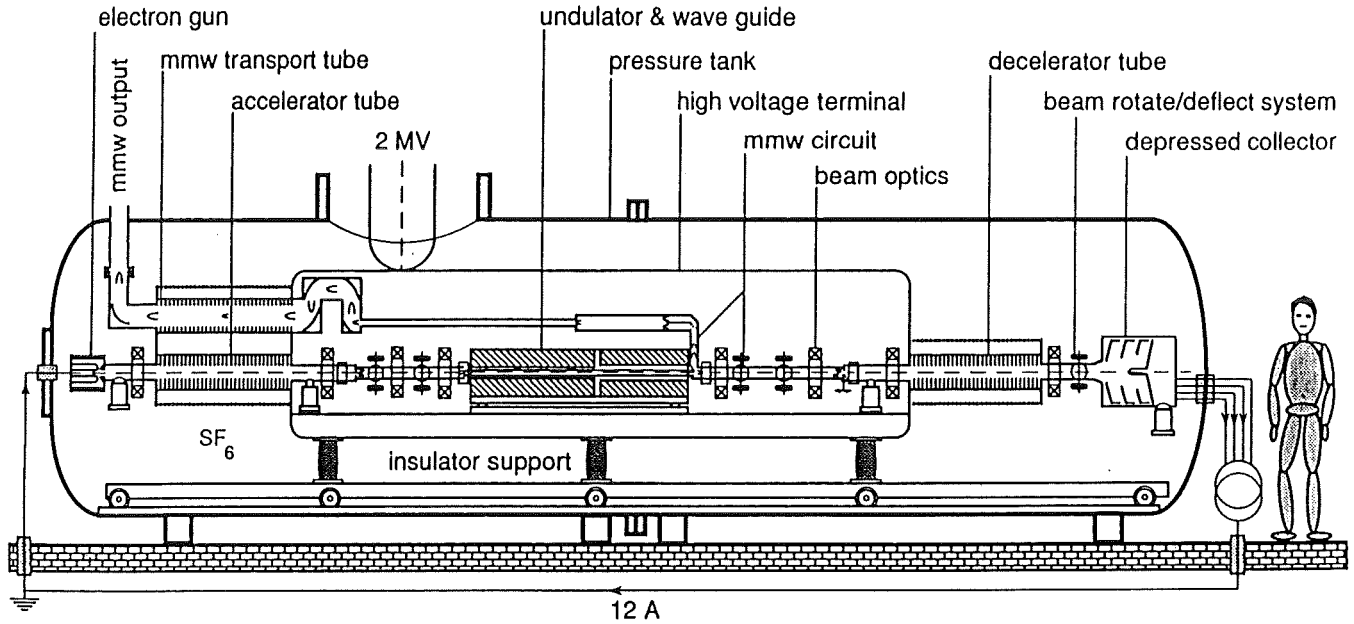


Fig. 23:
The mmw system

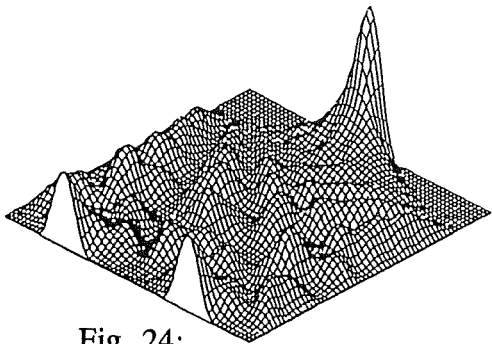


Fig. 24:
Splitting of one HE_{11}
beam into 2 beams

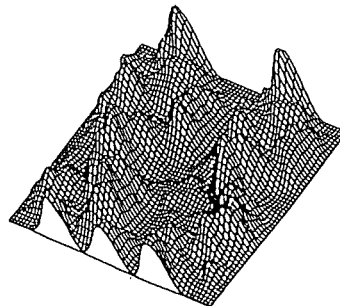


Fig. 25:
Two beams are transformed into
3 beams at a phase shift of 0.63π

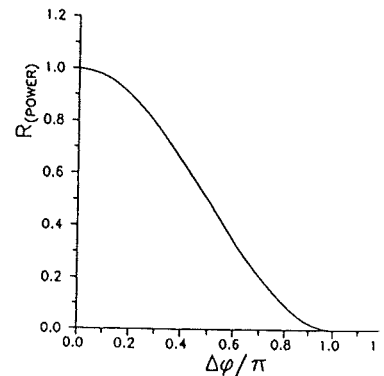


Fig. 26:
Reflection coefficient
vs phase shift

- power 1 MW
 - sufficient for FEM demonstration
 - comparable to largest gyrotrons

- center frequency 130 GHz, 200 GHz, 250 GHz
 - future use on fusion devices
 - higher than gyrotron frequencies

- frequency tunability in ms time scale 10 % via e-beam energy (high-voltage)
 - to demonstrate advantage of FEM
 - for tracking of plasma disruptions

- gain 3 (saturation)
 - to limit intra-cavity power
 - ≈ 7 (small signal gain)
 - fast start-up ($\approx 1 \mu\text{s}$)

- extraction eff., η 5 %

- pulse duration 100 ms
 - eventually CW but at first 100 ms to avoid severe cooling problems

- power efficiency $\approx 60 \%$ (grid \rightarrow millimeter wave power)

- electron beam

12A, @	V =	2.0,	1.75,	1.35 MeV
for	f =	250,	200,	130 GHz

- undulator
 - period = 40 mm, 2 sections
 - section 1: 20 cells, B = 0.20 T
 - gap: 25 mm
 - section 2: 14 cells, B = 0.16 T

Table XXV: Design parameters of the planned FOM-FEM [126]

12 Comparison of gyrotron and FEM for nuclear fusion

Table XXVI lists a comparison of the main performance parameters and features of gyrotron oscillators and FEMs for ECRH of plasmas in nuclear fusion research. The important advantage of the FEM is its a and continuous frequency tunability and the possibility of high unit power but the gyromonotron is a much simpler device. Up to now, the cylindrical cavity gyrotron is the only millimeter wave source which has had an extensive on-the-field experience during ECRH experiments over a wide range of frequencies and power levels (28-140 GHz, 0.1-0.5 MW).

	Gyrotron Oscillator (cyclotron resonance maser axial magnetic field)	Free Electron Maser Oscillator (periodic transverse magnetic field)
1. Beam voltage	low (70 - 90kV)	high (0.2 - 2 MV)
2. Magnetic field (140 GHz)	high (5.5 T, 1st harmonic)	low (0.2 T, wiggler)
3. Frequencies	8 - 250 GHz	9 - 250 GHz
4. Frequency tunability	ΔB : slow step tuning $\Delta U_{\text{beam}} + \Delta U_{\text{mode}}$: fast step tuning (few steps)	ΔU_{beam} : fast continuous tuning (10%)
5. Electron beam	magnetron injection gun	Pierce electron gun, acceleration and deceleration tubes, beam optics
6. Ohmic losses in cavity	cutoff cavity 2 kW/cm ²	oversized circuit far away from cutoff
7. Power density in cavity	high	low
8. Longitudinal mode competition in cavity	single mode operation	nonlinear temporal dynamics can bring broad frequency spectrum (noise source?)
9. Linearly polarized output mode	generated by internal quasi-optical converter	linearly polarized, low-order resonator mode
10. Power density on first mirror (1 MW, 140 GHz)	1 kW/cm ²	2kW/cm ²
11. Number of internal quasi-optical mirrors	2-3	4-14 phase coherence required
12. Internal microwave diagnostics	not required	required
13. Output power present status (140 GHz)	high average power 0.6 MW/2s	2GW/20ns but very low duty cycle (LLNL amplifier)
14. Exp. system efficiency without energy recovery	high 30-40 %	low 5-10 %
15. Collector loading	relatively low	high
16. Theor. system efficiency with depressed collector	55 %	55 % (but halo current ?)
17. Physical size	relatively small	large
18. Power per unit (140 GHz)	1-2 MW	1-5 MW

Table XXVI: Comparison of parameters and features of gyrotron oscillators and FEMs for ECRH.

Acknowledgments

The author would like to thank M. Pain (CEA, Cadarache), M.Q. Tran and D. Whaley (CRPP, Lausanne), R. Heidinger, C. Iatrou, H.-U. Nickel, B. Piosczyk and P. Norajitra (Forschungszentrum Karlsruhe), A.G.A. Verhoeven (FOM Institute "Rijnhuizen"), T. Idehara (Fukui University), J.L. Doane, R. Freeman and C.P. Moeller (General Atomics, San Diego), A. Litvak (GYCOM), V.L. Bratman, G.G. Denisov, V.A. Flyagin, V.A. Goldenberg, A.N. Kuftin, M.I. Petelin, A.B. Pavelyev, Sh.E. Tsimring and V.E. Zapevalov (IAP, Nizhny Novgorod), M. Makowski, T. Nagashima and D. Remsen (ITER, Worksite Garching), T. Imai and K. Sakamoto (JAERI, Naka), R.J. Temkin (MIT, Cambridge), T. Kikunaga (MITSUBISHI, Amagasaki), Y. Tsunawaki (Osaka Sangyo University), H.-G. Mathews, G. Mourier and P. Garin (THOMSON, Velizy), S. Ono and K. Yokoo (Tohoku University Sendai), Y. Okazaki (TOSHIBA, Ohtawara), D.B. McDermott (UCLA), V.L. Granatstein and W. Lawson (University of Maryland) and T.S. Chu, K. Felch and H. Jory (VARIAN, Palo Alto). This work could not have been done without their help, stimulating suggestions and useful discussions. The author also wish to express his deep gratitude to Mrs. Mosbacher for her thorough typing, as well as E. Borie and B. Piosczyk for critical reading of this manuscript.

This work was supported by the European Community as part of the European Fusion Technology Program under the auspices of the Project Nuclear Fusion (Projekt Kernfusion) at the Forschungszentrum Karlsruhe.

References

- [1] Flyagin, V.A., Gaponov, A.V., Petelin, M.I., Yulpatov, V.K., 1977, The gyrotron. *IEEE Trans. Microwave Theory and Techniques*, **MTT-25**, 514-521.
Andronov, A.A., Flyagin, V.A., Gaponov, A.V., Goldenberg, A.L., Petelin, M.I., Usov, V.G., Yulpatov, V.K., 1978, The gyrotron: high power sources of millimetre and submillimetre waves. *Infrared Physics*, **18**, 385-393.
Petelin, M.I., *Physics of advanced gyrotrons. Plasma Phys. and Contr. Nucl. Fusion*, **35**, Supplement B, 343-341.
- [2] Flyagin, V.A., Goldenberg, A.L., Nusinovich, G.S., 1984, Powerful gyrotrons, in *Infrared and Millimeter Waves*, **Vol. 11**, ed. K.J. Button, Academic Press, New York, 179-226.
- [3] Flyagin, V.A., Nusinovich, G.S., 1988, Gyrotron oscillators. *Proceedings of the Institute of Electrical and Electronics Engineers*, **76**, 644-656 and, 1985, Powerful gyrotrons for thermonuclear research, in *Infrared and Millimeter Waves*, **Vol.13**, ed. K.J. Button, Academic Press, New York, 1-17.
- [4] Felch, K., Huey, H., Jory, H., 1990, Gyrotrons for ECH application. *J. Fusion Energy*, **9**, 59-75.
- [5] Prater, R., 1990, Recent results on the application of electron cyclotron heating in tokamaks. *J. Fusion Energy*, **9**, 19-30.
- [6] Erckmann, V., WVII-AS Team, Kasperek, W., Müller, G.A., Schüller, P.G., and Thumm, M., 1990, Electron cyclotron resonance heating transmission line and launching system for the Wendelstein VII-AS stellarator. *Fusion Technology*, **17**, 76-85.
- [7] Thumm, M., 1995, Advanced electron cyclotron heating systems for next step fusion experiments. *Fusion Engineering and Design*, accepted for publication.
- [8] Henle, W., Jacobs, A., Kasperek, W., Kumric, H., Müller, G.A., Schüller, P.G., Thumm, M., Engelmann, F., Rebuffi, L., 1991, Conceptual study of multi-megawatt millimeter wave transmission and antenna systems for electron cyclotron wave applications in NET/ITER. *Fusion Technology* **1990**, eds. B.E. Keen, M. Huguet, R. Hemsworth. Elsevier Science Publishers B.V., 238-242.
- [9] Alberti, S., Tran, M.Q., Hogge, J.P., Tran, T.M., Bondeson, A., Muggli, P., Perrenoud, A., Jödicke, B., Mathews, H.G., 1990, Experimental measurements on a 100 GHz frequency tunable quasi-optical gyrotron. *Phys. Fluids*, **B2**, 1654-1661.
- [10] Kreischer, K.E. Temkin, R.J., 1987, Single-mode operation of a high-power, step-tunable gyrotron. *Phys. Rev. Lett.*, **59**, 547-550.
- [11] Kurbatov, V.I., Malygin, S.A., Vasilyev, E.G., 1990, Commercial gyrotrons for thermonuclear investigations. *Proc. Int. Workshop on Strong Microwaves in Plasmas*, Suzdal, Inst. of Applied Physics, Nizhny Novgorod, 1991, 765-772.
Bogdanov, S.D., Kurbatov, V.I., Malygin, S.A., Orlov, V.B., Tai, E.M., 1993, Industrial gyrotrons development in Salut. *Proc. 2nd Int. Workshop on Strong Microwaves in Plasmas*, Moscow - Nizhny Novgorod - Moscow, ed. A.G. Litvak, Inst. of Applied Physics, Nizhny Novgorod, 1994, **Vol. 2**, 830-835.
- [12] Flyagin, V.A., Kuftin, A.N., Luchinin, A.G., Nusinovich, G.S., Pankratova, T.B., Zapevalov, V.E., 1989, Gyrotrons for electron cyclotron heating and active plasma diagnostics. *Proc. Joint IAEA Techn. Committee Meeting on ECE and ECRH (EC-7 Joint Workshop)*, Hefei, P.R. China, 355-372.
Flyagin, V.A., Luchinin, A.G., Nusinovich, G.S., 1983, Submillimeter-wave gyrotrons: theory and experiment. *Int. J. Infrared and Millimeter Waves*, **4**, 629-637.

- [13] Bykov, Y., Goldenberg, A.F.L., Flyagin, V.A., 1991, The possibilities of material processing by intense millimeter-wave radiation. *Mat. Res. Soc. Symp. Proc.*, **169**, 41-42.
- Sklyarevich, V., Detkov, A., Shevelev, M., Decker, R., 1992, Interaction between gyrotron radiation and powder materials, *Mat. Res. Soc. Symp. Proc.*, **269**, 163-169.
- [14] Granatstein, V.L., Lawson, W., Latham, P.E., 1988, Feasibility of 30 GHz gyrokystron amplifiers for driving linear supercolliders. *Conf. Digest, 13th Int. Conf. on Infrared and Millimeter Waves, Honolulu, Hawaii, Proc.*, SPIE **1039**, 230-231.
- Granatstein, V.L., Nusinovich, G.S., 1993, On the optimal choice of microwave systems for driving TeV linear colliders. *Proc. 2nd Int. Workshop on Strong Microwaves in Plasmas, Moscow - Nizhny Novgorod - Moscow*, ed. A.G. Litvak, Inst. of Applied Physics, Nizhny Novgorod, 1994, **Vol. 2**, 575-586.
- [15] Manheimer, W.M., Mesyats, G.A., Petelin, M.I., 1993, Super-high-power microwave radars, *Proc. 2nd Int. Workshop on Strong Microwaves in Plasmas, Moscow - Nizhny Novgorod - Moscow*, ed. A.G. Litvak, Inst. of Applied Physics, Nizhny Novgorod, 1994, **Vol. 2**, 632-641.
- Manheimer, W.M., 1992, On the possibility of high power gyrotrons for super range resolution radar and atmospheric sensing. *Int. J. Electronics*, **72**, 1165-1189.
- [16] Bratman, V.L., Denisov, G.G., Ginzburg, N.S., and Petelin, M.I., 1983, FEL's with Bragg reflection resonators. Cyclotron autoresonance masers versus ubitrons. *I.E.E.E. Journal Quantum Electronics*, **QE-19**, 282-296.
- [17] Stone, R.R., Jong, R.A., Orzechowski, T.J., Scharlemann, E.T., Throop, A.L., Kulke, B., Thomassen, K.I., Stallard, B.W., 1990, An FEL-based microwave system for fusion. *J. Fusion Energy*, **9**, 77-101.
- [18] Hirshfield, J.L., Granatstein, V.L., 1977, Electron cyclotron maser - an historical survey. *IEEE Trans. Microwave Theory Tech.*, **MTT-25**, 522-527.
- [19] Twiss, R.Q., 1958, Radiation transfer and the possibility of negative absorption in radio astronomy. *Aust. J. Phys.*, **11**, 564-579; Twiss, R.Q., Roberts, J.A., 1958, Electromagnetic radiation from electrons rotating in an ionized medium under the action of a uniform magnetic field. *Aust. J. Phys.*, **11**, 424.
- [20] Schneider, J., Stimulated emission of radiation by relativistic electrons in a magnetic field. 1959, *Phys. Rev. Lett.*, **2**, 504-505.
- [21] Gaponov, A.V., Addendum, 1959, *Izv. VUZ Radiofiz.*, **2**, 837, an addendum to Gaponov, A.V., 1959, Interaction between electron fluxes and electromagnetic waves and waveguides. *Izv. VUZ Radiofiz.*, **2**, 450-462.
- [22] Hirshfield, J.L., Wachtel, J.M., 1964, Electron cyclotron maser. *Phys. Rev. Lett.*, **12**, 533-536.
- [23] Gaponov, A.V., Petelin, M.I. and Yulpatov, V.K., 1967, The induced radiation of excited classical oscillators and its use in high frequency electronics. *Izv. VUZ Radiofiz.* **10**, 1414 (*Radiophys. Quantum Electr.*, **10**, 794-813).
- [24] Granatstein, V.L., Alexeff, I., eds., 1987, *High-power microwave sources*. Artech House, Boston, London.
- Gaponov-Grekhov, A.V., Granatstein, V.L., 1994, *Application of high-power microwaves*. Artech House, Boston, London.
- [25] Benford, J. Swegle, J., 1992, *High-power microwave sources*. Artech House, Boston, London.
- [26] Edgcombe, C.J., ed., 1993, *Gyrotron oscillators-their principles and practice*. Taylor & Francis, London.
- [27] Pendergast, K.D., Danly, B.G., Menninger, W.L., Temkin, R.J., 1992, A long-pulse CARM oscillator experiment. *Int. J. Electronics*, **72**, 983-1004.

- [28] Granatstein, V.L., Read, M.E., Barnett, L.R., 1982, Measured performance of gyrotron oscillators and amplifiers, in *Infrared and Millimeter Waves*, Vol. 5, ed. K.J. Button, Academic Press, New York, 267-304.
- [29] Mathews, H.-G., Tran, M.Q., 1991, private communication, ABB, Baden, Switzerland.
- [30] Chen, Z.-G., 1992, private communication, Institute of Electronics, Academia Sinica (IEAS), Beijing, P.R. China and Guo, H., Wu, D.S., Liu, G., Miao, Y.H., Qian, S.Z., Qin, W.Z., 1990, Special complex open-cavity and low-magnetic field high power gyrotron. *IEEE Trans. on Plasma Science*, **18**, 326-333.
- [31] Behm, K, Jensen, E., 1986, 70 GHz gyrotron development at Valvo. *Conf. Digest 11th Int. Conf. on Infrared and Millimeter Waves*, Pisa, 218-220.
- [32] Bogdanov, S.D., Gyrotron Team, Solujanava, E.A. 1994, Industrial gyrotrons from GYCOM. *Conf. Digest 19th Int. Conf. on Infrared and Millimeter Waves*, Sendai, JSAP Catalog No.: AP 941228, 351-352.
- [33] Mourier, G., 1990, Current gyrotron development at Thomson Tubes Electroniques. *Proc. Int. Workshop on Strong Microwaves in Plasmas*, Suzdal, Inst. of Applied Physics, Nizhny Novgorod, 1991, 751-764 and, 1993, private communication.
- [34] Nagashima, T., Sakamoto, K., Maebara, S., Tsuneoka, M., Okazaki, Y., Hayashi, K., Miyake, S., Kariya, T., Mitsunaka, Y., Itoh, Y., Sugawara, T., Okamoto, T., 1990, Test results of 0.5 MW gyrotron at 120 GHz and 1.5 MW at 2 GHz Klystron for fusion application. *Proc. Int. Workshop on Strong Microwaves in Plasmas*, Suzdal, Inst. of Applied Physics, Nizhny Novgorod, 1991, 739-750 and, Okazaki, Y., 1994, private communication, Toshiba, Nasushiobara, Japan.
- [35] Felch, K., Chu, T.S., Feinstein, J., Huey, H., Jory, H., Nielson, J., Schumacher, R., 1992, Long-pulse operation of a gyrotron with beam/rf separation. *Conf. Digest 17th Int. Conf. on Infrared and Millimeter Waves*, Pasadena, Proc., SPIE **1929**, 184-195.
Lawrence Ives, R., Jory, H., Neilson, J., Chodorow, M., Feinstein, J., LaRue, A.D., Zitelli, L., Martorana, R., 1993, Development and test of a 500 kW, 8-GHz gyrotron. *IEEE Trans. on Electron Devices*, **40**, 1316-1321.
- [36] Shimozuma, T., Sato, M., Takita, Y., Kubo, S., Idei, H., Ohkubo, K., Kuroda, T. Tubokawa, Y., Huey, H., Jory, H., 1994, Development of a high power 84 GHz gyrotron. *Conf. Digest 19th Int. Conf. on Infrared and Millimeter Waves*, Sendai, JSAP Catalog No.: AP 941228, 65-66.
- [37] Thumm, M., 1986, High power mode conversion for linearly polarized HE_{11} hybrid mode output. *Int. J. Electronics*, **61**, 1135-1153.
- [38] Piosczyk, B., Kuntze, M., Borie, E., Dammertz, G., Dumbrajs, O., Gantenbein, G., Möbius, A., Nickel H.-U., Thumm, M., 1992, Development of high power 140 GHz gyrotrons at KfK for applications in fusion. *Fusion Technology* **1992**, eds. C. Ferro, M. Gasparotto, H. Knoepfel. Elsevier Science Publishers B.V., 1993, 618-622.
- [39] Borie, E., Dammertz, G., Gantenbein, G., Kuntze, M., Möbius, A., Nickel, H.-U., Piosczyk, B., Thumm, M., 1993, 0.5 MW/140 GHz $TE_{10,4}$ Gyrotron with built-in highly efficient quasioptical converter. *Conf. Digest 18th Int. Conf. on Infrared and Millimeter Waves*, Colchester (Essex, UK), Proc., SPIE **2104**, 519-520.
Thumm, M., Borie, E., Dammertz, G., Kuntze, M., Möbius, A., Nickel, H.-U., Piosczyk, B., Wien, A., 1993. Development of high-power 140 GHz gyrotrons for fusion plasma applications. *Proc. 2nd Int. Workshop on Strong Microwaves in Plasma*, Moscow - Nizhny Novgorod -Moscow, Inst. of Applied Physics, Nizhny Novgorod, 1994, Vol. 2, 670-689.
Gantenbein, G., Borie, E., Dammertz, G., Kuntze, M., Nickel, H.-U., Piosczyk, B., Thumm, M., 1994, Experimental results and numerical simulations of a high power 140 GHz gyrotron. *IEEE Trans. Plasma Science*, **22**, 861-870.

- [40] Thumm, M., Borie, E., Dammertz, G., Höchtl, O., Kuntze, M., Möbius, A., Nickel, H.-U., Piosczyk, B., Semmler, C., Wien, A., 1994, Development of advanced high-power 140 GHz gyrotrons at KfK. Conf. Digest 19th Int. Conf. on Infrared and Millimeter Waves, Sendai, JSAP Catalog No.: AP 941228, 57-58.
- [41] Shimozuma, T., Kikunaga, T., Asano, H., Yasojima, Y., Miyamoto, K., Tsukamoto, T., 1993, A 120 GHz high-power whispering-gallery mode gyrotron. *Int. J. Electronics*, **74**, 137-151.
- [42] Asano, H., Kikunaga, T., Shimozuma, T., Yasojima, Y., Tsukamoto, T., 1994, Experimental results of a 1 Megawatt gyrotron. Conf. Digest 19th Int. Conf. Of Infrared and Millimeter Waves, Sendai, JSAP Catalog No.: AP 941228, 59-60.
- [43] Sakamoto, K., Tsuneoka, M., Maebava, S., Kasugai, A., Fujita, H., Kikuchi, M., Yamamoto, T., Nagashima, T., Kariya, T., Okazaki, Y., Shirai, N., Okamoto, T., Hayashi, K., Mitsunaka, Y., Hirata, Y., 1992, Development of a high power gyrotron for ECH of tokamak plasma. Conf. Digest 17th Int. Conf. on Infrared and Millimeter Waves, Pasadena, SPIE **1929**, 188-189.
- Sakamoto, K., Tsuneoka, M., Kasugai, A., Maebara, S., Nagashima, T., Imai, T., Kariya, T., Okazaki, Y., Shirai, N., Okamoto, T., Hayashi, K., Mitsunaka, Y., Hirata, Y., 1993, Development of a high power gyrotron for fusion application in JAERI. Proc. 2nd Int. Workshop on Strong Microwaves in Plasmas, Moscow - Nizhny Novgorod - Moscow, ed. A.G. Litvak, Inst. of Applied Physics, Nizhny Novgorod, 1994, Vol. 2, 601-615.
- [44] Sakamoto, K., Tsuneoka, M., Kasugai, A., Takahashi, K., Maebara, S., Imai, T., Kariya, T., Okazaki, Y., Hayashi, K., Mitsunaka, Y., Hirata, Y., 1994, Development of 110 GHz CPD gyrotron. Conf. Digest 19th Int. Conf. on Infrared and Millimeter Waves, Sendai, JSAP Catalog No.: AP 941228, 63-64.
- [45] Myasnikov, V.E., Cayer, A.P., Bogdanov, S.D., Kurbatov, V.I., 1991, Soviet industrial gyrotrons. Conf. Digest 16th Int. Conf. on Infrared and Millimeter Waves, Lausanne, SPIE **1576**, 127-128.
- [46] Flyagin, V.A., Goldenberg, A.L., Zapevalov, V.E., 1993, State of the art of gyrotron investigation in Russia. Conf. Digest 18th Int. Conf. on Infrared and Millimeter Waves, Colchester (Essex, UK), Proc., SPIE **2104**, 581-584.
- Denisov, G.G., Flyagin, V.A., Goldenberg, A.L., Khizhnyak, V.I., Kuftin, A.N., Malygin, V.I., Pavelyev, A.B., Pulin, A.V., Zapevalov, V.E., 1991, Investigation of gyrotrons in IAP. Conf. Digest 16th Int. Conf. on Infrared and Millimeter Waves, Lausanne, SPIE **1576**, 632-635.
- [47] Agapova, M.V., Axenova, L.A., Alikae, V.V., Cayer, A.P., Denisov, G.G., Flyagin, V.A., Fix, A.Sh., Iljin, V.I., Ilyin, V.N., Khmara, V.A., Kostyna, A.N., Kuftin, A.N., Mjasnikov, V.E., Popov, L.G., Zapevalov, V.E., 1994, Long-pulsed 140 GHz/0.5 MW gyrotron: problems and results. Conf. Digest 19th Int. Conf. on Infrared and Millimeter Waves, Sendai, JSAP Catalog No.: AP 941228, 79-80.
- [48] Felch, K., Chu, T.S., DeHope, W., Huey, H., Jory, H., Nielson, J., Schumacher, R., 1994, Recent test results on a high-power gyrotron with an internal, quasi-optical converter. Conf. Digest 19th Int. Conf. on Infrared and Millimeter Waves, Sendai, JSAP Catalog No.: AP 941228, 333-334.
- [49] Gantenbein, G., Borie, E., Möbius, A., Piosczyk, B., Thumm, M., 1991, Design of a high-power 140 GHz gyrotron oscillator operating in an asymmetric volume mode at KfK. Conf. Digest 16th Int. Conf. on Infrared and Millimeter Waves, Lausanne, Proc., SPIE **1576**, 264-265.
- [50] Grimm, T.L., Kreischer, K.E., Guss, W.C., Temkin, R.J., 1992, Experimental study of a megawatt 200-300 GHz gyrotron oscillator. *Fusion Technology*, **21**, 1648-1657 and, 1993, *Phys. Fluids*, **B5**, 4135-4143.

- [51] Vlasov, S.N., Zagryadskaya, L.I., Orlova, I.M., 1976, Open coaxial resonators for gyrotrons. *Radio Eng. Electron. Phys.*, **21**, 96-102.
- [52] Flyagin, V.A., Khishnyak, V.I., Manuilov, V.N., Pavelyev, A.B., Pavelyev, V.G., Piosczyk, B., Dammertz, G., Höchtl, O., Iatrou, C., Kern, S., Nickel, H.-U., Thumm, M., Wien, A., Dumbrajs, O., 1994, Development of a 1.5 MW coaxial gyrotron at 140 GHz. *Conf. Digest 19th Int. Conf. on Infrared and Millimeter Waves, Sendai, JSAP Catalog No.: AP 941228*, 75-76.
- [53] Gaponov, A.V., Flyagin, V.A., Goldenberg, A.L., Nusinovich, G.S., Tsimring, Sh.E., Usov, V.G., Vlasov, S.N., 1981, Powerful millimeter-wave gyrotrons. *Int. J. Electronics*, **51**, 277-302.
- [54] Xu, K.Y., Kreisler, K.E., Guss, W.C., Grimm, T.L., Temkin, R.J., 1990, Efficient operation of a megawatt gyrotron. *Conf. Digest 15th Int. Conf. on Infrared and Millimeter Waves, Orlando, Proc., SPIE 1514*, 324-326.
- [55] Carmel, Y., Chu, K.R., Dialetis, D., Fliflet, A., Read, M.E., Kim, K.J., Arfin, B., Granatstein, V.L., 1982, Mode competition, suppression, and efficiency enhancement in overmoded gyrotron oscillators. *Int. J. on Infrared and Millimeter Waves*, **3**, 645-665.
- [56] Zapevalov, V.E., Malygin, S.A., Pavelyev, V.G., Tsimring, Sh.E., 1984, Coupled resonator gyrotrons with mode conversion. *Radiophys. Quantum Electron.*, **27**, 846-852.
- [57] Dumbrajs, O., Nusinovich, G.S., 1992, Theory of a frequency-step-tunable gyrotron for optimum plasma ECRH. *IEEE Trans. Plasma Science*, **20**, 452-457.
- [58] Dumbrajs, O., Thumm, M., Pretterebner, J., Wagner, D., 1992, A cavity with reduced mode conversion for gyrotrons. *Int. J. Infrared and Millimeter Waves*, **13**, 825-840.
- [59] Denisov, G.G., Kuftin, A.N., Malygin, V.I., Venediktov, N.P., Vinogradov, D.V., Zapevalov, V.E., 1992, 110 GHz gyrotron with a built-in high-efficiency converter. *Int. J. Electronics*, **72**, 1079-1091.
- [60] Hargreaves, T.A., Fliflet, A.W., Fischer, R.P., Barsanti, M.L., 1990, Depressed collector performance on the NRL quasi-optical gyrotron. *Conf. Digest 15th Int. Conf on Infrared and Millimeter Waves, Orlando, Proc., SPIE 1514*, 330-332.
- [61] Häfner, H.E., Bojarsky, E., Norajitra, P., Reiser, H., 1992, Cryocooled windows for high frequency plasma heating. *Fusion Technology 1992*, eds. C. Ferro, M. Gasparotto, H. Knoepfel (Elsevier Science Publishers B.V. 1992), pp.520-523.
- [62] Häfner, H.E., Bojarsky, E., Heckert, K., Norajitra, P., Reiser, H., 1994, Liquid nitrogen cooled window for high frequency plasma heating. *Journal of Nuclear Materials*, **212-215**, 1035-1038.
- [63] Häfner, H.E., Heckert, K., Norajitra, P., Vouriot, R., Hofmann, A., Münch, N., Nickel, H.-U., Thumm, M., Erckmann, V., 1994, Investigations of liquid nitrogen cooled windows for high power millimeter wave transmission. *Conf. Digest 19th Int. Conf. on Infrared and Millimeter Waves, Sendai, JSAP Catalog No.: AP 941228*, 281-282.
- [64] Saitoh, Y., Itoh, K., Yoshiyuki, T., Ebisawa, K., Yokokura, K., Nagashima, T., Yamamoto, T., 1992, Cryogenic window for millimeter-wave transmission. *Fusion Technology 1992*, eds. C. Ferro, M. Gasparotto, H. Knoepfel (Elsevier Science Publishers B.V. 1992), pp. 632-636.
- [65] Kasugai, A., Yokokura, K., Sakamoto, K., Tsuneoka, M., Yamamoto, T., Imai, T., Saito, Y., Ito, K., Yoshiyuki, T., Ebisawa, K., 1994, High power tests of the cryogenic window for millimeter wave. *Conf. Digest 19th Int. Conf. on Infrared and Millimeter Waves, Sendai, JSAP Catalog No.: AP 941228*, 295-296.
- [66] Pain, M., Berger-By, G., Capitain, J.J., Crenn, J.P., Smits, F., Tonon, G., 1992, The 110 GHz electron cyclotron heating and current drive system for Tore Supra. *Proc. 8th Joint Workshop on Electron Cyclotron Emission and Electron Cyclotron Resonance Heating (EC-8)*, Gut Ising, Germany, Vol II, pp. 523-530.

- [67] Fix, A.S., Sushilin, P.B., 1993, Calculation and experimental investigation of cryogenic window. Proc. 5th Russian-German Meeting on ECRH and Gyrotrons, Karlsruhe, pp. 389-392 and, 1994, Proc. 6th Russian-German Meeting on ECRH and Gyrotrons, Moscow, 1994, Vol. 2, pp. 244-247.
- [68] Moeller, C.P., Doane, J.L., DiMartino, M., 1994, A vacuum window for a 1 MW CW 110 GHz gyrotron. Conf. Digest 19th Int. Conf. on Infrared and Millimeter Waves, Sendai, Conf. Digest 19th Int. Conf. on Infrared and Millimeter Waves, Sendai, JSAP Catalog No.: AP 941228, 279-280.
- [69] Heidinger, R., 1994, Dielectric property measurements on CVD diamond grades for advanced gyrotron windows. Conf. Digest 19th Int. Conf. on Infrared and Millimeter Waves, Sendai, JSAP Catalog No.: AP 941228, 277-278.
- [70] Petelin, M.I., Kasperek, W., 1991, Surface corrugation for broadband matching of windows in powerful microwave generators. Int. J. Electronics, **71**, 871-873.
- [71] Nickel, H.-U., Ambrosy, U., Thumm, M., 1992, Vacuum windows for frequency-tunable high-power millimeter wave systems. Conf. Digest 17th Int. Conf. on Infrared and Millimeter Waves, Pasadena, Proc., SPIE **1929**, 462-463.
 Nickel, H.-U., Massler, H., Thumm, M., 1993, Development of broadband vacuum windows for high-power millimeter wave systems. Conf. Digest 18th Int. Conf. on Infrared and Millimeter Waves, Colchester (Essex, UK), Proc., SPIE **2104**, 172-173.
 Shang, C.C., Caplan, M., Nickel, H.-U., Thumm, M., 1993, Electrical analysis of wideband and distributed windows using time-dependent field codes. Conf. Digest 18th Int. Conf. on Infrared and Millimeter Waves, Colchester (Essex, UK), Proc., SPIE **2104**, 178-179.
- [72] Kreischer, K.E., Grimm, T.L., Guss, W.C., Temkin, R.J., Xu, K.Y., 1990, Research at MIT on high frequency gyrotrons for ECRH. Proc. Int. Workshop on Strong Microwaves in Plasmas, Suzdal, Inst. of Applied Physics, Nizhny Novgorod, 1991, 713-725.
- [73] Grimm, T.L., Borchard, P.M., Kreischer, K.E., Guss, W.C., Temkin, R.J., 1992, High power operation of a 200-300 GHz gyrotron oscillator and multimegawatt gyrotrons for ITER. Conf. Digest 17th Int. Conf. on Infrared and Millimeter Waves, Pasadena, Proc., SPIE **1929**, 190-191 and 194-195.
- [74] Zaytsev, N.I., Pankratova, T.P., Petelin, M.I., Flyagin, V.A., 1974, Millimeter- and submillimeter-wave gyrotrons. Radio Eng. and Electronic Phys., **19**, 103-107.
- [75] Idehara, T., Tatsukawa, T., Ogawa, I., Tanabe, H., Mori, T., Wada, S., Brand, G.F., Brennan, M.H., 1992, Development of a second cyclotron harmonic gyrotron operating at submillimeter wavelengths. Phys. Fluids **B4**, 267-273 and 1993, Phys. Fluids **B5**, 1377-1379.
- [76] Idehara, T., Tatsukawa, T., Ogawa, I., Shimizu, Y., Makino, S., Ichikawa, K., 1993, Development of medium power, submillimeter wave gyrotrons. Conf. Digest 18th Int. Conf. on Infrared and Millimeter Waves, Colchester (Essex, UK), Proc., SPIE **2104**, 533-534.
- [77] Idehara, T., Shimizu, Y., Ichikawa, K., Makino, S., Shibutani, K., Tatsukawa, T., Ogawa, I., Okazaki, Y., Okamoto, T., 1994, Development of a submillimeter wave gyrotron using a 17 T superconducting magnet. Conf. Digest 19th Int. Conf. on Infrared and Millimeter Waves, Sendai, JSAP Catalog No.: AP 941228, 218-219.
- [78] Brand, G.F., Fekete, P.W., Hong, K., Moore, K.J., Idehara, T., 1990, Operation of a tunable gyrotron at the second harmonic of the electron cyclotron frequency. Int. J. Electronics, **68**, 1099-1111.
- [79] Hong, K.D., Brand, G.F., 1993, A 150-600 GHz step-tunable gyrotron. J. Appl. Phys., **74**, 5250-5258.
- [80] Spira-Hakkarainen, S.E., Kreischer, K.E., Temkin, R.J., 1990, Submillimeter-wave harmonic gyrotron experiment. IEEE Trans. Plasma Science, **18**, 334-342.

- [81] Geist, T., Thumm, M., Wiesbeck, W., 1991, Linewidth measurement on a 140 GHz gyrotron. Conf. Digest 16th Int. Conf. on Infrared and Millimeter Waves, Lausanne, Proc., SPIE **1576**, 272-273.
- [82] Bratman, V.L., Ginzburg, N.S., Nusinovich, G.S., Petelin, M.I., Strelkov, P.S., 1981, Relativistic gyrotrons and cyclotron autoresonance masers. Int. J. Electronics, **51**, 541-567.
- [83] Granatstein, V.L., Herndon, M., Sprangle, P., Carmel, Y., Nation, J.A., 1975, Gigawatt microwave emission from an intense relativistic electron beam. Plasma Physics, **17**, 23-28.
- [84] Didenko, A.N., Zherlitsyn, A.G., Zelentsov, V.I., Sulakshin, A.S., Fomenko, G.P., Shtein, Yu.G., Yushkov, Yu.G., 1976, Generation of gigawatt microwave pulses in the nanosecond range. Sov. J. Plasma Phys., **2**, 283-285.
- [85] Kremontsov, V.I., Petelin, M.I., Rabinovich, M.S., Rukhadze, A.A., Strelkov, P.S., Shkvarunets, A.G., 1978, Plasma-filled gyrotron with a relativistic supervacuum electron beam, Sov. Phys. JETP, **48**, 1084.
- [86] Ginzburg, N.S., Kremontsov, V.I., Petelin, M.I., Strelkov, P.S., Shkvarunets, A.G., 1979, Experimental investigation on a high-current relativistic cyclotron maser. Sov. Phys. Tech. Phys., **24**, 218-222.
- [87] Voronkov, S.N., Kremontsov, V.I., Strelkov, P.S., Shkvarunets, A.G., 1982, Stimulated cyclotron radiation and millimeter wavelengths from high-power relativistic electron beams, Sov. Phys. Tech. Phys., **27**, 68-69.
- [88] Bratman, V.L., Denisov, G.G., Ofitserov, M.M., Korovin, S.D., Polevin, S.D., Rostov, V.V., 1987, Millimeter-wave HF relativistic electron oscillators. IEEE Trans. on Plasma Science, **15**, 2-15.
- [89] Gold, S.H., Fliflet, A.W., Manheimer, W.M., McCowan, R.B., Lee, R.C., Granatstein, V.L., Hardesty, D.L., Kinkead, A.K., Sucey, M., 1988, High peak power Ka-band gyrotron oscillator experiments with slotted and unslotted cavities, IEEE, Trans. Plasma Science, **16**, 142.
- [90] Black, W.M., Gold, S.H., Fliflet, A.W., Kirkpatrick, D.A., Manheimer, W.M., Lee, R.C., Granatstein, V.L., Hardesty, D.L., Kinkead, A.K., Sucey, M., 1990, Megavolt Multikiloamp Ka-band gyrotron oscillator experiment. Phys. Fluids, **B2**, 193.
- [91] Cross, A.W., Spark, S.N., Phelps, A.D.R., 1988, Gyrotron experiments using cavities of different ohmic Q. Conf. Digest 17th Int. Conf. on Infrared and Millimeter Waves, Pasadena, Proc., SPIE **1929**, 392-393.
- [92] Gilgenbach, R.M., Wang, J.G., Choi, J.J., Outten, C.A., Spencer, TA, 1988, Intense electron beam cyclotron masers with microsecond pulse lengths. Conf. Digest 13th Int. Conf. on Infrared and Millimeter Waves, Honolulu, Hawaii, Proc., SPIE **1039**, 362-363.
- [93] Fliflet, A.W., Hargreaves, T.A., Fischer, R.P., Manheimer, W.M., Sprangle, P., 1990, Review of quasi-optical gyrotron development. J. Fusion Energy, **9**, 31-58.
Fischer, R.P., Fliflet, A.W., Manheimer, W.M., Levush, B., Antonsen Jr., T.M., 1993, Mode priming an 85 GHz quasioptical gyrotron. Conf. Digest 18th Int. Conf. on Infrared and Millimeter Waves, Colchester (Essex, UK), Proc., SPIE **2104**, 330-331.
- [94] Hogge, J.P., Cao, H., Kasperek, W., Tran, T.M., Tran, M.Q., Paris, P.J., 1991, Ellipsoidal diffraction grating as output coupler for quasi-optical gyrotrons. Conf. Digest 16th Int. Conf. on Infrared and Millimeter Waves, Lausanne, Proc., SPIE **1576**, 540-541.
- [95] Bratman, V.L., Denisov, G.G., 1992, Cyclotron autoresonance masers - recent experiments and prospects. Int. J. Electronics, **72**, 969-981.
- [96] Bratman, V.L., Denisov, G.G., Ofitserov, M.M., Samsonov, S.V., Arkhipov, O.V., Kazacha, V.I., Krasnykh, A.K., Perelstein, E.A., Zamrij, A.V., 1992, Cyclotron autoresonance maser with high Doppler frequency up-conversion. Int. J. Infrared and Millimeter Waves, **13**, 1857-1873.

- [97] Bratman, V.L., Denisov, G.G., Samsonov, S.V., 1993, Cyclotron autoresonance masers: achievements and prospects of advance to the submillimeter wavelength range. Proc. 2nd Int. Workshop on Strong Microwaves in Plasmas, Moscow - Nizhny Novgorod -Moscow, Inst. of Applied Physics, Nizhny Novgorod, 1994, Vol. 2, 690-711.
- [98] Caplan, M., Kulke, B., Westenskow, G.A.; McDermott, D.B., Luhmann, Jr., N.C., 1992, Induction-linac-driven, millimeter-wave CARM oscillator. Exploratory Research and Development, FY 90, 146-147.
- [99] Danly, B.G., Hartemann, F.V., Chu, T.S., Legorburn, P., Menninger, W.L, Temkin, R.J., 1992, Long-pulse millimeter-wave free-electron laser and cyclotron autoresonance maser experiments. Phys. Fluids, B4, 2307-2314.
- [100] Wang, J.G., Gilgenbach, R.M., Choi, J.J., Outten, C.A., Spencer, T.A., 1989, Frequency-tunable, high-power microwave emission from cyclotron autoresonance maser oscillation and gyrotron interactions. IEEE Trans. Plasma Science, 17, 906-908.
Choi, J.J., Gilgenbach, R.M., Spencer, T.A., 1992, Mode competition in Bragg resonator cyclotron resonance maser experiments driven by a microsecond intense electron beam. Int. J. Electronics, 72, 1045-1066.
- [101] Burke, J.M., Czarnaski, M.A., Fischer, R.P., Giangrave, M., Fliflet, A.W., Manheimer, W.M., 1991, 85 GHz TE₁₃ phase-locked gyrokystron oscillator experiment. Conf. Digest 16th Int. Conf. on Infrared and Millimeter Waves, Lausanne, Proc., SPIE 1576, 228-229.
- [102] Fischer, R.P., Fliflet, A.W., Manheimer, W.M., 1992, The NRL 85 GHz quasioptical gyrokystron experiment. Conf. Digest 17th Int. Conf. on Infrared and Millimeter Waves, Pasadena, Proc., SPIE 1929, 254-255.
- [103] Tantawi, S.G., Main, W.T., Latham, P.E., Nusinovich, G.S., Lawson, W.G., Striffler, C.D., Granatstein, V.L., 1992, High-power X-band amplification from an overmoded three-cavity gyrokystron with a tunable penultimate cavity. IEEE Trans. Plasma Science, 20, 205-215.
- [104] Lawson, W., Calame, J.P., Hogan, P., Skopec, M., Striffler, C.D., Granatstein, V.L., 1992, Performance characteristics of a high-power X-band two-cavity gyrokystron. IEEE Trans. Plasma Science, 20, 216-223.
Matthews, H.W., Lawson, W., Calame, J.P., Flaherty, M.K.E., Hogan, B., Cheng, J., Latham, P.E., 1994, Experimental studies of stability and amplification in a two-cavity second harmonic gyrokystron. IEEE Trans. Plasma Science, 22, 825-833.
Lawson, W., Hogan, B., Calame, J.P., Cheng, J., Latham, P.E., Granatstein, V.L., 1994, Experimental studies of 30 MW fundamental mode and harmonic gyro-amplifiers. Conf. Digest 19th Int. Conf. on Infrared and Millimeter Waves, Sendai, JSAP Catalog No.: AP 941228, 421-422.
- [105] Park, G.-S., Granatstein, V.L., Park, S.Y., Armstrong, C.M., Ganguly, A.K., 1992, Experimental study of efficiency optimization in a three-cavity gyrokystron amplifier. IEEE Trans. on Plasma Science, 20, 224-231.
- [106] Antakov, I.I., Aksenova, L.A., Zasytkin, E.V., Moiseev, M.A., Popov, L.G., Sokolov, E.V., Yulpatov, V.K., 1990, Multicavity phase-locked gyrotrons for lower-hybrid heating in toroidal plasmas. Proc. Int. Workshop on Strong Microwaves in Plasmas, Suzdal, Inst. of Applied Physics, Nizhny Novgorod, 1991, 773-782.
- [107] Antakov, I.I., Moiseev, M.A., Sokolov, E.V., Zasytkin, E.V., 1993, Theoretical and experimental investigation of X-band two-cavity gyrokystron. Conf. Digest 18th Int. Conf. on Infrared and Millimeter Waves, Colchester (Essex, UK), Proc., SPIE 2104, 336-337.
Antakov, I.I., Zasytkin, E.V., Sokolov, E.V., Yulpatov, V.K., Keyer, A.P., Musatov, V.S., Myasnikov, V.E., 1993, 35 GHz radar gyrokystrons. Conf. Digest 18th Int. Conf. on Infrared and Millimeter Waves, Colchester (Essex, UK), Proc., SPIE 2104, 338-339.

- [108] Antakov, I.I., Gaponov, A.V., Zasytkin, E.V., Sokolov, E.V., Yulpatov, V.K., Aksenova, L.A., Keyer, A.P., Musatov, V.S., Myasnikov, V.E., Popov, L.G., Levitan, B.A., Tolkachev, A.A., 1993, Gyroklystrons: millimeter wave amplifiers of the highest power. Proc. 2nd Int. Workshop on Strong Microwaves in Plasmas, Moscow - Nizhny Novgorod - Moscow, ed. A.G. Litvak, Inst. of Applied Physics, Nizhny Novgorod, 1994, Vol. 2, 587-596.
- [109] Anatokov, I.I., Zasytkin, E.V., Sokolov, E.V., 1993, Design and performance of 94 GHz high power multicavity gyrokystron amplifier. Conf. Digest 18th Int. Conf. on Infrared and Millimeter Waves, Colchester (Essex, UK), Proc., SPIE 2104, 466-467 and Proc. 2nd Int. Workshop on Strong Microwaves in Plasmas, Moscow - Nizhny Novgorod - Moscow, ed. A.G. Litvak, Inst. of Applied Physics, Nizhny Novgorod, 1994, Vol. 2, 754-758.
- [110] Leou, K.C., McDermott, D.B., Luhmann, Jr., N.C., 1992, Design of experimental dielectric loaded wideband Gyro-TWT. Conf. Digest 17th Conf. on Infrared and Millimeter Waves, Pasadena, Proc., SPIE 1929, 326-327.
Leou, K.C., Wang, Q.S., Chong, C.K., Balkcum, A.J., Fochs, S.N., Garland, E.S., Pretterebner, J., Lin, A.T., McDermott, D.B., Hartemann, F., Luhmann, Jr., N.C., 1993, Gyro-TWT amplifiers at UCLA, Conf. Digest 18th Int. Conf. on Infrared and Millimeter Waves, Colchester (Essex, UK), Proc., SPIE 2104, 531-532.
Wang, Q.S., Leou, K.C., Chong, C.K., Balkeum, A.J., McDermott, D.B., Luhmann, Jr., N.C., 1994, Gyro-TWT amplifier development at UCD, Conf. Digest 19th Int. Conf. on Infrared and Millimeter Waves, Sendai, JSAP Catalog No.: AP 941228, 415-416.
- [111] Chu, K.R., Barnett, L.R., Lau, W.K., Chang, L.H., Chen H.Y., 1990, A wide-band millimeter-wave gyrotron traveling-wave amplifier experiment. IEEE Trans. Electron Devices, 37, 1557-1560.
- [112] Park, G.S., Park, S.Y., Kyser, R.H., Armstrong, C.M., Ganguly, A.K., Parker, R.K., 1994, Broadband operation of a Ka-band tapered gyro-traveling wave amplifier. IEEE Trans. Plasma Science, 22, 536-543.
- [113] Park, S.Y., Kyser, R.H., Armstrong, C.M., Parker, R.K., Granatstein, V.L., 1990, Experimental Study of a Ka-band gyrotron backward-wave oscillator. IEEE Trans. on Plasma Science, 18, 321-325.
- [114] Kou, C.S., Chen, S.H., Barnett, L.R., Chu, K.R., 1993, Experimental study of an injection locked gyrotron backward wave oscillator. Phys. Rev. Lett., 70, 924-927.
- [115] Guss, W.C., Basten, M.A., Kreisler, K.E., Temkin, R.J., Caplan, M., Kulke, B., 1989, Operation of a 140 GHz tunable backward-wave gyrotron oscillator. Conf. Digest 14th Int. Conf. on Infrared and Millimeter Waves, Würzburg, SPIE 1240, p. 83.
- [116] Gold, S.H., Fliflet, A.W., Kirkpatrick, D.A., 1989, High-power millimeter-wave gyro-traveling-wave amplifier. Conf. Digest 14th Int. Conf. on Infrared and Millimeter Waves, Würzburg, SPIE 1240, 332-333.
- [117] Walter, M.T., Gilgenbach, R.M., Menge, P.R., Spencer, T.A., 1994, Effects of tapered tubes on long-pulse microwave emission from intense e-beam gyrotron-backward-wave oscillators. IEEE Trans. Plasma Sciences, 22, 578-584.
- [118] Ono, S., Yamanouchi, K., Shibata, Y., Koike, Y., 1962, Cyclotron fast-wave tube using spatial harmonic interaction- the traveling wave peniotron. Proc. 4th Int. Congress Microwave Tubes, Scheveningen, 355-363.
- [119] Ganguly, A.K., Ahn, S., Park, S.Y., 1988, Three dimensional nonlinear theory of the gyropeniotron amplifier. Int. J. Electronics, 65, 597-618.
- [120] Ono, S., Tsutaki, K., Kageyama, T., 1984, Proposal of a high efficiency tube for high power millimetre or submillimetre wave generation: The gyro-peniotron. Int. J. Electronics, 56, 507-519.

- [121] Yokoo, K., Razeghi, M., Sato, N., Ono, S., 1988, High efficiency operation of the modified peniotron using TE₁₁ rectangular waveguide cavity. Conf. Digest, 13th Int. Conf. on Infrared and Millimeter Waves, Honolulu, Hawaii, Proc., SPIE **1039**, 135-136
- [122] Yokoo, K., Musyoki, S., Nakazato, Y., Sato, N., Ono, S., 1990, Design and experiments of auto-resonant peniotron oscillator. Conf. Digest 15th Int. Conf on Infrared and Millimeter Waves, Orlando, Proc., SPIE **1514**, 10-12.
- [123] Yokoo, K., Shimawaki, H., Tadano, H., Ishihara, T., Sagae, N., Sato, N., Ono, S., 1992, Design and experiments of higher cyclotron harmonic peniotron oscillators. Conf. Digest 17th Int. Conf. on Infrared and Millimeter Waves, Pasadena, Proc., SPIE **1929**, 498-499.
- Musyoki, S., Sagae, K., Yokoo, K., Sato, N., Ono, S., 1992, Experiments on highly efficient operation of the auto-resonant peniotron oscillator. Int. J. Electronics, **72**, 1067-1077.
- [124] Ono, S., Ansai, H., Sato, N., Yokoo, K., Henmi, K., Idehara, T., Tachikawa, T., Okazaki, I., Okamoto, T., 1986, Experimental study of the 3rd harmonic operation of gyro-peniotron at 70 GHz. Conf. Digest 11th Int. Conf. on Infrared and Millimeter Waves, Pisa, 37-39, and Okazaki, Y., 1994, private communication, Toshiba, Nasushiobara, Japan.
- [125] Marshall, T.C., 1985, Free electron lasers, MacMillan, New York.
- [126] Sprangle, P., Coffey, T., 1985, New high power coherent radiation sources, in Infrared and Millimeter Waves, Vol. 13, ed. K.J. Button, Academic Press, New York, 19-44.
- [127] Gallerano, G.P., 1994, The free electron laser: state of the art, developments and applications. Nucl. Instr. Meth., **A340**, 11-16.
- [128] Phillips, R.M., 1960, The ubitron, a high-power traveling-wave tube based on a periodic beam interaction in unloaded waveguide., IRE Trans. Electron. Dev., **ED-7**, 231-241 and, 1988, History of the ubitron. Nucl. Instr. and Methods, **A272**, 1-9.
- [129] Verhoeven, A.G.A., Bongers, W.A., Best, R.W.B., van Ingen, A.M., Manintveld, P., Urbanus, W.H., van der Wiel, M.J., Bratman, V.L., Denisov, G.G., Shmelyov, M.Yu., Nickel, H.-U., Thumm, M., Müller, G., Kasperek, W., Pretterebner, J., Wagner, D., Caplan, M., 1992, The 1 MW, 200 GHz FOM-Fusion-FEM, Conf. Digest 17th Int. Conf. on Infrared and Millimeter Waves, Pasadena (Los Angeles), Proc., SPIE **1929**, 126-127.
- Urbanus, W.H., Best, R.W.B., Bongers, W.A., van Ingen, A.M., Manintveld, P., Sterk, A.B., Verhoeven, A.G.A., van der Wiel, M.J., Caplan, M., Bratman, V.L., Denisov, G.G., Varfolomeev, A.A., Khlebnikov, A.S., 1993, Design of the 1 MW, 200 GHz, FOM fusion FEM, Nucl. Inst. and Methods, **A 331**, 235-240.
- [130] Bottolier-Curtet, H., Gardelle, J., Bardy, J., Bonnafond, C., Devin, A., Gardent, D., Germain, G., Gouard, Ph., Labrousche, J., Launspach, J., Le Taillandier, P., de Mascureau, J., 1992, Progress in free electron maser experiments at CESTA, Nucl. Instr. Meth., **A318**, 131-134.
- [131] Marshall, T.C., Cecere, M.A., 1994, A measurement of space-charge fields in a microwave free electron laser, Physica Scripta, **T52**, 58-60.
- [132] Cecere, M., Marshall, T.C., 1994, A free electron laser experiment on angular steering. IEEE Trans. Plasma Science, **22**, 654-658.
- [133] Ciocci, F., Bartolini, R., Doria, A., Gallerano, G.P., Giovenale, E., Kimmitt, M.F., Messina, G., Renieri, A., 1993, Operation of a compact free-electron laser in the millimeter-wave region with a bunched electron beam. Phys. Rev. Lett., **70**, 928-931.
- [134] Hartemann, F., Buzzi, J.M., 1988, Experimental studies of a millimeter-wave free-electron laser. Proc. 7th Int. Conf. on High-Power Particle Beams, Karlsruhe 1988, eds., Bauer, W., Schmidt, W., Vol. II, 1278-1292.

- [135] Bratman, V.L., Denisov, G.G., Ofitserov, M.M., Korovin, S.D., Polevin, S.D., Rostov, V.V., 1987, Millimeter-wave hf relativistic electron oscillators. *IEEE Trans. Plasma Science*, **15**, 2-15
- [136] Akiba, T., Tanaka, K., Mokuno, M., Miyamoto, S., Mima, K., Nakai, S., Kuruma, S., Imasaki, K., Yamanaka, C., Fukuda, M., Ohigashi, N., Tsunawaki, Y., 1990, Helical distributed feedback free-electron laser. *Appl. Phys.Lett.*, **56**, 503-505.
- [137] Sakamoto, K., Kishimoto, Y., Watanabe, A., Kobayashi, T., Musyoki, S., Oda, H., Tokuda, S., Nakamura, Y., Kawasaki, S., Ishizuka, H., Sato, M., Nagashima, T., Shiho, M., 1992, MM wave FEL experiment with focusing wiggler, Course and Workshop on High Power Microwave Generation and Applications. *Int. School of Plasma Physics, Varenna, 1991*, eds., D. Akulina, E. Sindoni, C. Wharton, Editrice Compositori Bologna, 597-604.
- Sakamoto, K., Shiho, M., Musyoki, S., Watanabe, A., Kishimoto, Y., Kawasaki, S., Ishizuka, H., 1993, Study of waveguide mode identification in FEL experiment. *Proc. 15th Int. Free Electron Laser Conference, The Hague, The Netherlands, Paper Mo 4-16.*
- [138] Ozaki, T., Ebihara, K., Hiramatsu, S., Kimura, Y., Kishiro, J., Monaka, T., Takayama, K., Whittum, D.H., 1992, First result of the KEK X-band free electron laser in the ion channel guiding regime. *Nucl. Instr. Meth.*, **A318**, 101-104.
- Takayama, K., Kishiro, J., Ebihara, K., Ozaki, T., Hiramatsu, S., Katoh, H., 1994, 1.5 MeV ion-channel guided X-band free-electron laser amplifier. *Conf. Digest 19th Int. Conf. on Infrared and Millimeter Waves, Sendai, JSAP Catalog No.: AP 941228, 3-4.*
- [139] Orzechowski, T.J., Anderson, B.R., Clark, J.G., Fawley, W.M., Paul, A.C., Prosnitz, D., Scharlemann, E.T., Yarema, S.M., Hopkins, D.B., Sessler, A.M., Wurtele, J.S., 1986, High-efficiency extraction of microwave radiation from a tapered-wiggler free-electron laser. *Phys. Rev. Lett.*, **57**, 2172-2175.
- [140] Allen, S.L., Casper, T.A., Fenstermacher, M.E., Foote, J.H., Hooper, E.B., Hoshino, K., Lasnier, C.J., Lopez, P., Makowski, M.A., Marinak, M.M., Meyer, W.H., Moller, J.M., Oasa, K., Oda, T., Odajima, K., Ogawa, T., Ogo, T., Rice, B.W., Rognlien, T., Stallard, B.W., Thomassen, K.I., Wood, R.D., 1992, Electron cyclotron resonance heating in the microwave tokamak experiment. *Proc. 14th Int. Conf. on Plasma Physics and Controlled Nuclear Fusion Research, Würzburg, Vol. 1, 617-625, (IAEA-CN-56/E-1-4).*
- [141] Hartemann, F., Legorburu, P.P., Chu, T.S., Danly, B.G., Temkin, R.J., Faillon, G., Mourier, G., Trémeau, T., Bres, M., 1992, Long pulse high gain 35 GHz free-electron maser amplifier experiments. *Nucl. Instr. Meth.*, **A318**, 87-93.
- Chu, T.S., Hartemann, F., Legorburu, P.P., Danly, B.G., Temkin, R.J., Faillon, G., Mourier, G., Trémeau, T., Bres, M., 1992, High-power millimeter-wave Bragg free-electron maser oscillator experiments. *Nucl. Instr. Meth.*, **A318**, 94-100.
- Conde, M.E., Bekefi, G., 1992, Amplification and superradiant emission from a 33.3 GHz free electron laser with a reversed axial guide magnetic field. *IEEE Trans. Plasma Science*, **20**, 240-244 and *Nucl. Instr. Meth.*, **A318**, 109-113.
- Volfbeyn, P., Ricci, K., Chen, B., Bekefi, G., 1994, Measurement of the temporal and spatial phase variations of a pulsed free electron laser amplifier. *IEEE Trans. Plasma Science*, **22**, 659-665.
- [142] Pasour, J.A., Gold, S.H., 1985, Free electron laser experiments with and without a guide magnetic field: a review of millimeter-wave free electron laser research at the NRL. *IEEE J. Quantum Electronics*, **21**, 845-858.
- [143] Karbushev, N.I., Mirnov, P.V., Sazhin, V.D., Shatkus, A.D., 1992, Generation of microwave radiation by an intense microsecond electron beam in an axisymmetric wiggler. *Nucl. Instr. Meth.*, **A318**, 117-119.

- [144] Liu, S., 1992, Recent development of FEL research activities in P.R. China. Conf. Digest 17th Int. Conf. on Infrared and Millimeter Waves, Pasadena, Proc., SPIE **1929**, 441 and private communication.
- [145] Chen, J., Wang, M.C., Wang, Z., Lu, Z., Zhang, L., Feng, B., 1991, Study of a Raman free-electron laser oscillator with Bragg reflection resonators. IEEE J. Quantum Electron., **27**, 477-495.
- [146] Feng, B., Lu, Z., Zhang, L., Wang, M., 1994, Investigation of Raman free-electron lasers with a bifilar helical small-period wiggler. IEEE J. Quantum Electron., **30**, 2682-2687.
- [147] Boehmer, H., Christensen, T., Camponi, M.Z., Hauss, B., 1990, A long-pulse millimeter-wave free electron maser experiment. IEEE Trans. Plasma Science, **18**, 392-398.
- [148] Elias, L.R., Ramian, G., Hu, J., Amir, A., 1986, Observation of single mode operation of a free electron laser. Phys. Rev. Lett., **57**, 424-427.
- Ramian, G., 1992, The new UCSB free-electron lasers. Nucl. Instr. Meth., **A318**, 225-229.